Synaptic transmission and plasticity in major excitatory hippocampal synapses of L1 conditional and CHL1 constitutive knockout mice *(Mus musculus* L., 1758*)*

Dissertation

zur Erlangung des Doktorgrades des Departments Biologie der Fakultät für Mathematik, Informatik und Naturwissenschaften an der Universität Hamburg

vorgelegt von Eka Lepsveridze

Hamburg, 2006

Name:	Eka Lepsveridze
Titel der Dissertation:	Synaptic transmission and plasticity in major excitatory hippocampal synapses of L1 conditional and CHL1 constitutive knockout mice *(Mus musculus* L., 1758*)*
Gutachter:	Herr Prof. Dr. K. Wiese Frau Prof. Dr. M. Schachner

Genehmigt vom Department Biologie
der Fakultät für Mathematik, Informatik und Naturwissenschaften
an der Universität Hamburg
auf Antrag von Frau Professor Dr. M. SCHACHNER
Weiterer Gutachter der Dissertation:
Herr Professor Dr. K. WIESE
Tag der Disputation: 23. Juni 2006

Hamburg, den 06. Juni 2006

Professor Dr. Reinhard Lieberei
Leiter des Departments Biologie

Table of contents

TABLE OF CONTENTS

TABLE OF CONTENTS

TABLE OF CONTENTS

TABLE OF CONTENTS

I. Abstract

The hippocampal formation is a group of structures within the limbic system, which includes the hippocampus, dentate gyrus, subiculum, presubiculum, parasubiculum and the entorhinal cortex. It plays an important role in processing of multimodal sensory information, novelty detection, emotions, learning and memory.

Cell adhesion molecules are implicated in cell interactions during nervous system development and they are also recognized as important mediators of synaptic plasticity in the hippocampal formation. Among cell adhesion molecules, L1 has received a lot of attention since it was discovered as a transmembrane glycoprotein in the mouse. It subserves neuron-neuron adhesion via homophilic and heterophilic interactions with other adhesion and extracellular matrix molecules and mediates numerous neural functions. In humans, mutations in the L1 gene result in mental retardation, aphasia, shuffling gate, adducted thumbs, hydrocephalus as a result of stenosis of the aqueduct of Sylvius, spastic paraplegia and agenesis of the corpus callosum. Mouse mutants constitutively deficient in L1 (L1-/-) also show severe abnormalities in the development of the central and peripheral nervous systems. Conditional mutant (L1fy+) with ablation of L1 in the adult brain does not show any of the abnormalities in gross morphology described for the L1-/- mutant. Another interesting cell adhesion molecule is CHL1, which is a newly identified member of the L1 family. It is expressed in subpopulations of developing neurons in the central and peripheral nervous systems and persists at low levels in the mature brain in areas of high plasticity. The CALL gene, the human homologue of the mouse CHL1 gene, is linked to mental retardation and schizophrenia.

The aim of our study was to identify excitatory synapses in the hippocampus and dentate gyrus, in which basal synaptic transmission and/or synaptic plasticity depend on expression of cell adhesion molecules L1 and CHL1, and to investigate the underlying mechanisms.

To reach this aim, I have taken an advantage of availability of L1 conditional (L1fy+) and CHL1 constitutive knockout mice and performed extracellular recordings in acute hippocampal slices prepared from these animals and corresponding wild-type control mice to reveal genotype-specific changes in physiological parameters (amplitude of field excitatory postsynaptic potentials or currents, paired-pulse facilitation, post-tetanic or short-term potentiation, and LTP). Field potentials and synaptic currents have been recorded from synapses formed by (1) Schaffer collateral projections to the CA1 field; (2) lateral perforant path (LPP) and (3) medial perforant path (MPP) projections to the dentate gyrus; (4) direct perforant path projections to the CA3 and (5) CA1 fields; and (6) associational/commissural and (7) mossy fiber projections to the CA3

field. In addition, to investigate the influence of L1 molecule on L-type voltage-dependent Ca^{2+} channels, patch-clamp recordings of Ca^{2+} channel-transfected CHO cells have been used.

Analysis of basal synaptic transmission and synaptic plasticity at above described major hippocampal excitatory synapses of L1 deficient mice and corresponding wild-type control animals revealed that LTP is specifically impaired in synapses formed by perforant path fibers on apical distal dendrites of CA1 and CA3 pyramidal neurons in L1fy+ mice. In light of impaired associative memory in the L1 mutant, our findings provide first evidence for importance of CA1 and CA3 perforant path projections for this kind of memory.

Investigation of mechanisms underlying these abnormalities in LTP at the perforant path synapses in the CA3 region, by checking cholinergic modulation of perforant path and associational/commissural synapses in the CA3 field, uncovered that this system works normally in L1 conditional mutant animals. Examination of the role of NMDA receptors and L-type Ca^{2+} channels in induction and maintenance of LTP at perforant path projections to the CA3 field showed, that both are involved in this process and abnormal function of L-type Ca^{2+} channels may account for the difference in LTP between wild-type and knockout mice. Though pharmacological manipulations with L-type Ca^{2+} channels abolished differences between genotypes, the patch-clamp recording of CHO cells could not reveal direct influences of extracellular L1 on one subtype of neuronal VDCCs, suggesting that either other subtypes are affected or the influence of L1 on L-type Ca^{2+} channels is indirect.

Analysis of CHL1 constitutive knockout mice revealed that deficiency in CHL1 molecule has a different impact on the synaptic plasticity at CA3-CA1 connections in animals of different ages, being normal in 2-month-old CHL1-deficient mice and reduced in 1-month-old and 9-month-old mutants. Investigation of mechanisms underlying impaired short- and long-term potentiation in 1 month-old mice revealed that increased activation of inhibitory interneurons might be responsible for this phenomenon. Apart from that, 2-month-old CHL1 deficient mice exhibit elevated levels of basal synaptic transmission in the dentate gyrus, which correlate with reduced behavioral response of these mutants to novel environmental stimuli.

In summary, these results provide a new insight into synaptic functions of two cell adhesion molecules, demonstrating a synapse type- and Ca^{2+} channel-dependent impairment of synaptic plasticity in L1 deficient mice, and age- and GABAergic transmission-dependent deficit in synaptic plasticity in CHL1 deficient mutants.

II. Zusammenfassung

Die Hippocampale Formation ist eine Gruppe von Strukturen im Limbischen System des Gehirns, die Hippocampus, Gyrus Dentatus, Subikulum, Presubikulum, Parasubikulum und Entorhinal Cortex umfasst. Sie spielt unter anderem eine wichtige Rolle bei der Verarbeitung verschiedener sensorischer Informationen sowie in Lernprozessen und Gedächtnis.

Verschiedene Zelladhäsionsmoleküle sind an Interaktionen zwischen Zellen während der Entwicklung des Nervensystems beteiligt und dienen außerdem als wichtige Mediatoren synaptischer Plastizität in der Hippocampalen Formation. Unter diesen Zelladhäsionsmolekülen hat L1, ein in der Maus entdecktes membrandurchspannendes Glycoprotein, viel Aufmerksamkeit erlangt. Es vermittelt Zelladhäsion zwischen Neuronen durch entweder homophile Bindung oder heterophile Interaktion mit anderen Adhäsionsmolekülen. Außerdem interagiert es mit Molekülen der extrazellulären Matrix und ist an vielen neuronalen Prozessen beteiligt. Beim Menschen zeigt sich eine Mutation des L1-Gens unter anderem in mentaler Retardation, Aphasie, Hydrocephalus als Auswirkung des HSAS-Syndroms, spastischer Paraplegie und fehlerhafter Entwicklung des Corpus' Callosum. Konstitutive L1-Mausmutanten (L1-/-) zeigen starke Abnormalitäten in der Entwicklung von zentralem und peripherem Nervensystem. Konditionelle Mutanten (L1fy+), bei denen L1 nur im erwachsenen Gehirn fehlt, zeigen keine der morphologischen Abnormalitäten, die für die L-/- -Mutante nachgewiesen wurden.

CHL1 ist ein anderes interessantes Mitglied der L1-Familie, das in Neuron-Subpopulationen des sich entwickelnden zentralen und peripheren Nervensystem exprimiert wird, aber auch in geringen Konzentrationen in Bereichen des erwachsenen Gehirns, die hohe synaptische Plastizität aufweisen, nachweisbar ist. Eine Mutation des CALL-Gens, des CHL1-Gen-Homologs im Menschen, führt zu mentaler Retardation und Schizophrenie.

Das Ziel dieser Arbeit war, excitatorische Synapsen im Hippocampus und Gyrus Dentatus von Mäusen zu identifizieren, in denen die basale synaptische Transmission und/oder synaptische Plastizität auf der Expression der Zelladhäsionsmoleküle L1 und CHL1 beruht, und eventuell zugrunde liegende Mechanismen zu untersuchen.

Zu diesem Zweck wurden extrazelluläre Messungen an hippocampalen Schnitten von L1fy+ - und CHL1-/- -Mäusen sowie von entsprechenden Wildtyp-Kontrollen durchgeführt, die Genotyp-spezifische Änderungen in physiologischen Parametern (Amplitude der excitatorischen Feld-Potentiale oder –Ströme, Bahnung, post-tetanische Potenzierung, LTP) aufzeigen sollten. Feldpotentiale und synaptische Ströme wurden an Synapsen von (1) Schaffer-Collateralen in der CA1-Region, (2) Lateral Perforant Path (LPP) und (3) Medial Perforant Path (MPP) im Gyrus

Dentatus, direkten Perforant Path-Projektionen in der (4) CA3-Region oder (5) CA1-Region sowie von (6) Associational/Commissural-Projektionen und (7) Moosfasern in der CA3-Region gemessen. Zusätzlich wurde mit Hilfe von Patch-Clamp-Messungen an transfizierten CHO-Zellen der Einfluss von L1 auf die Eigenschaften eines neuronalen L-Typ Calcium-Kanals untersucht.

Analyse der Messungen zur Transmission und Plastizität an den oben erwähnten Synapsen in L1fy+ -/CHL1-/- - und entsprechenden Wildtyp-Mäusen hat ergeben, dass in konditionellen L1-Mutanten die Langzeitpotenzierung von Synapsen des Perforant Path an apical distalen Dendriten von Pyramidenzellen in der CA1- und CA3-Region des Hippocampus vermindert ist. Diese Ergebnisse geben erste Hinweise auf die Bedeutung dieser Projektionen für das autoassoziative Gedächtnis, das in L1-Mutanten gestört ist.

Pharmakologische Untersuchungen zu den Mechanismen, die der Störung des LTP zugrunde liegen könnten, ergaben, dass die cholinerge Modulation der Synapsen von Perforant Path und Associational/Commissural-Projektionen in der CA3-Region in L1fy+ -Mäusen normal ist. Allerdings zeigte sich, dass sowohl NMDA-Rezeptoren als auch L-Typ Calcium-Kanäle an der Induktion und der Aufrechterhaltung des LTP an Synapsen des Perforant Path in der CA3-Region beteiligt sind, und dass eine beeinträchtigte Funktion der L-Typ Calcium-Kanäle für den Unterschied in der Langzeitpotenzierung zwischen Wildtypen und Mutanten verantwortlich sein könnte. In Patch-Clamp-Messungen an transfizierten CHO-Zellen konnte ein direkter Einfluss von extrazellulärem L1 auf einen Subtyp neuronaler L-Typ Calcium-Kanäle nicht nachgewiesen werden, was darauf hinweist, dass entweder andere Subtypen beteiligt sind oder die Interaktion von L1 mit L-Typ Calcium-Kanälen indirekt erfolgt.

Analyse der Messungen an konstitutiven CHL1-Mutanten zeigte, dass das Fehlen von CHL1 unterschiedliche Auswirkungen auf die synaptische Plastizität von CA3-CA1-Verbindungen, abhängig von Alter der Tiere, hat. In einem Monat und in neun Monate alten Mäusen ist sie reduziert, während sie in zwei Monate alten Tieren normal erscheint. Untersuchungen zu den Mechanismen, die der verminderten Kurz- und Langzeitpotenzierung in einem Monat alten CHL1-/- -Mäusen zugrunde liegen könnten, zeigten eine erhöhte Aktivität inhibitorischer Interneurone. In zwei Monate alten CHL1-/- -Mutanten war die basale synaptische Transmission im Gyrus Dentatus erhöht, was mit der verminderten Reaktion dieser Mäuse auf eine neue Umgebung korreliert.

Zusammenfassend geben die Ergebnisse dieser Arbeit neue Einblicke in die synaptischen Funktionen zweier Zelladhäsionsmoleküle: Sie demonstrieren erstens eine L-Typ Calcium-Kanal-abhängige Verminderung der Plastizität spezifischer Synapsen in L1-defizienten Mäusen und zweitens eine altersabhängige Verminderung der synaptischen Plastizität in CHL1

defizienten Mäusen, die mit den Eigenschaften der GABAergen Transmission in den jeweiligen Altersstufen zusammenhängt.

III. Abbreviations

A/C - associational/commissural

ACSF - artificial cerebrospinal fluid

AMPA - α- amino-3-hydroxy-5-methyl-4-isoxazolepropionate

APV - 2-D,L-aminophosphonovaleric acid

CAM - Cell adhesion molecules

CaMK - Ca^{2+}/calmodulin kinase

cAMP - cyclic adenosine mono phosphate

CHL1- close homologue of L1

DCGIV - 2, 3-dicarboxycyclopropyl-glycine IV

DG - dentate gyrus

DMEM - Dulbeco's modified Eagle's medium

DNA - deoxyribonucleic acid

ECM - extracellular matrix

EDTA - ethylenediaminetetraacetic acid

EGTA - ethyleneglycoltetraacetic acid

E-LTP - early phase long-term potentiation

EPSCs - excitatory postsynaptic currents

ERK - extracellular signal-regulated kinase

FCS - fetal bovine serum

fEPSP - field excitatory post-synaptic potentials

FGF-R - fibroblast growth factor-receptor

FNIII - fibronectin repeat of the subtype III

GABA - γ-aminobutyric acid

GFP - green fluorescence protein

GluR - glutamate receptor

GPI - glycosylphosphatidylinositol

GTPases - guanosine triphosphatases

HFS - high frequency stimulation

HVA - high voltage-activated

Ig - immunoglobulin

IP - inositol phosphates

L-LTP - long-lasting LTP

LPP - lateral perforant path

ABBREVIATIONS

LTD - long-term depression

LTP - long-term potentiation

LVA - low voltage-activated

MAPK - mitogen-activated protein kinase

mGluR -metabotropic glutamatergic receptor

MPP - medial perforant path

MR- mental retardation

mRNA - messenger ribonucleic acid

NCAM - neural cell adhesion molecule

Ng-CAM - neuron-glia cell adhesion molecule

NMDA - N-methyl-D-aspartatic acid

PDZ - postsynaptic density-95/Discs large/zona occludens-1

PI - protease inhibitor

PIP - phosphatidylinositol 4,5-bisphosphate

PKA - protain kinase A

PKC - protein kinase C

PLC - phospholipase C

PP - perforant path

PPD - paired-pulse depression

PPF - paired-pulse facilitation

PTP - post-tetanic potentiation

S/C - Schaffer collateral/commissural

SEM - standard error of mean

STP - short-term potentiation

TA - temporo-ammonic

TAG - transient axonal glycoprotein

TBS - theta-burst stimulation

TEA - tetraethylammonium chloride

VDCC - voltage-dependent Ca^{2+} channels

IV. Review of the literature

1. Hippocampal formation

The hippocampus is one of the most thoroughly studied areas of the mammalian central nervous system. There are at least two main reasons for this. First, it has a distinctive and readily identifiable structure at both the gross and histological levels. The second, since the early 1950s, it has been recognized to play the fundamental role in some forms of learning and memory (Scoville and Milner, 1957). The hippocampal formation, a group of structures within the limbic system that includes the dentate gyrus, hippocampus, subiculum, presubiculum, parasubiculum, and entorhinal cortex (Johnston and Amaral, 2004) is also of a great interest because of its high seizure susceptibility. It has the lowest seizure threshold of any brain region (Green, 1964). Furthermore, portions of the hippocampal formation, particularly the entorhinal cortex, appear to be prime targets for the pathology associated with Alzheimer's disease, and the hippocampus is very vulnerable to the effects of ischemia and anoxia.

1.1. Morphology of the rat hippocampus

The rat hippocampus is elongated, banana-shaped structure with its long axis extended in a 'C'- shaped fashion from the septal nuclei rostrally, over and behind the diencephalons, into the temporal lobe caudally and ventrally. The long axis of the hippocampus is referred to as septotemporal axis, and the orthogonal one as the transversal axis (Johnston and Amaral, 2004).

The dentate gyrus consists of three layers: the principal or granule cell layer; the large acellular molecular layer that is located above the granule cell layer; and the diffusely populated polymorphic cell layer (also called the hilus) that is located below the granule cell layer (Figure 1).

The principal neurons of the hippocampus are pyramidal neurons. The cell bodies of the hippocampal pyramidal neurons are arranged, three to six cells deep, in an orderly layer called the pyramidal cell layer. These neurons have elaborate dendritic trees extending perpendicularly to the cell layer in both directions and are thus considered to be multipolar. The apical dendrites are longer than the basal and extend from the apex of the pyramidal cell body toward the center of the hippocampus, i.e., toward the dentate gyrus. The apical dendrites traverse three strata: stratum lucidum, strata radiatum and stratum lacunosum-moleculare (Figure 1). The basal dendrites extend from the base of the pyramidal cell body into stratum oriens.

The pyramidal cell layer of the hippocampus has been divided into four regions designated CA1, CA2 CA3 and CA4, based on the size and appearance of the neurons (Lorente de No,

1934). The hippocampus can also be divided into two major regions: a large-celled region closer to the dentate gyrus and a smaller-celled distal region. Ramon y Cajal called these regions *regio inferior* and *regio superior*. CA3 and CA2 fields are equivalent to the large-celled *regio inferior* and CA1 is equivalent to *regio superior* (Johnston and Amaral, 2004). Since CA4 referred to the region occupied by the polymorphic layer of the dentate gyrus this term is no longer used. *Regio inferior* and *regio superior* also have a clear-cut connectional difference, namely the CA3 pyramidal cells receive a mossy fiber input from the dentate gyrus and the CA2 and CA1 pyramidal cells do not.

The CA2 field has been a matter of some controversy. As originally defined by Lorente de No, it was a narrow zone of cells interposed between CA3 and CA1, which had large cell bodies like CA3 but, did not receive mossy fiber innervation like CA1 cells. The bulk of available evidence indicates that there is indeed a narrow CA2 that has both connectional and perhaps even functional differences with the other hippocampal fields. CA2, for example, appears to be more resistant to epileptic cell death than CA3 or CA1 and is sometimes referred to as the resistant sector (Corsellis and Bruton, 1983).

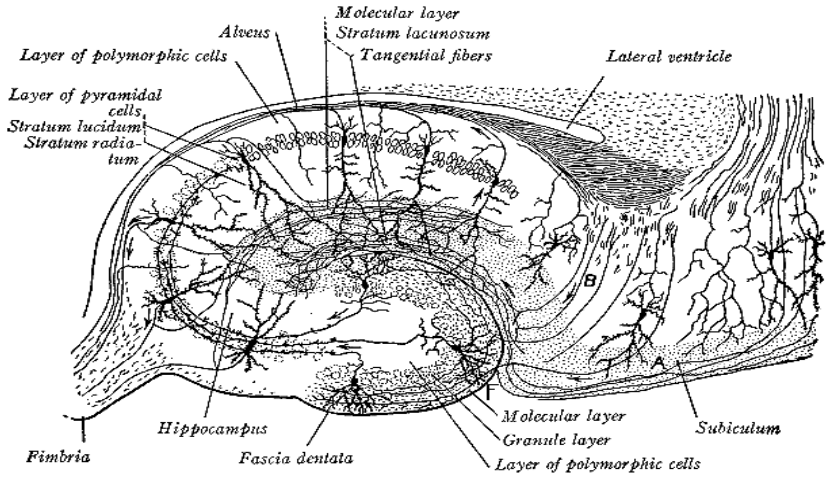

Figure 1. Diagram of the structure and connections of the Hippocampus. The arrows show the direction of conduction; A, molecular layer, and B, pyramidal cell layer of the subiculum; F, Hippocampal fissure (Cajal).

1.2. The basic circuitry of the hippocampal formation

The basic circuitry of the hippocampal formation has been known since the time of Ramon y Cajal (1911), although details worked out by modern anatomists have contributed to our current understanding, which is illustrated schematically on Figure 2. (Johnston and Amaral, 2004).

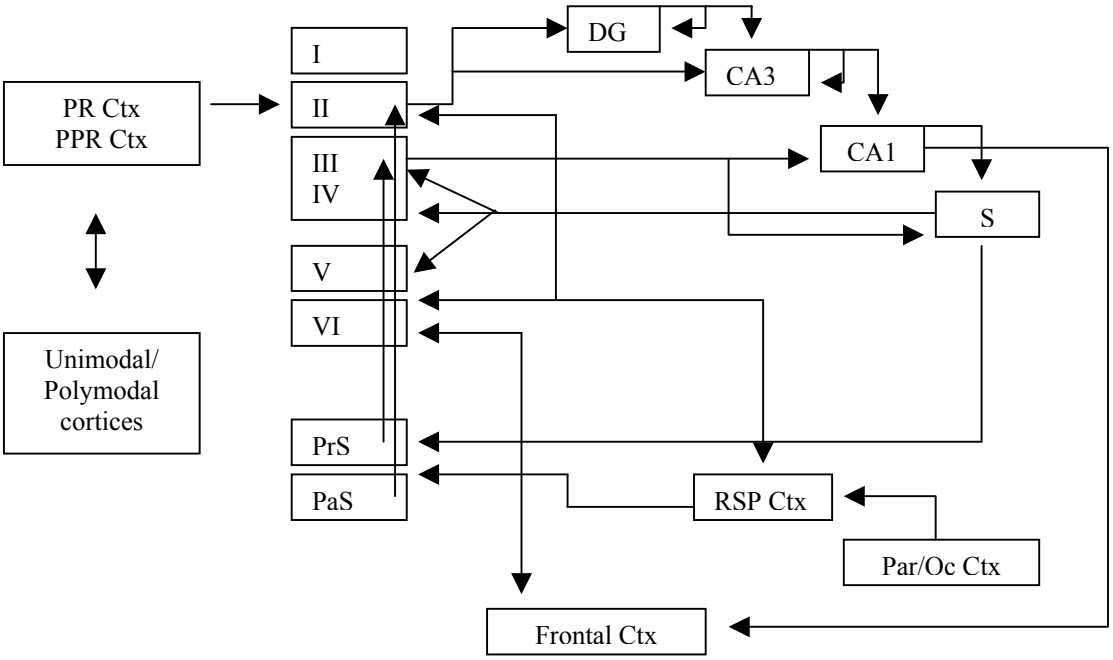

Figure 2. Summary diagram of the major intrinsic connections of the rat hippocampal formation and several of the extrinsic cortical inputs. This diagram emphasizes the serial and parallel aspects of the intrinsic hippocampal circuitry. Abbreviations: DG, dentate gyrus; CA3, CA1 fields of the hippocampus; PR, perirhinal; POR, postrhinal; PrS, presubiculum; PaS, parasubiculum; Par/Oc Ctx, parietal occipital cortices; RSP Ctx, retrosplenial cortex; I, II, III, IV, V, VI, layers of the entorhinal cortex.

Andersen and colleagues emphasized the unique unidirectional progression of excitatory pathways that linked each region of the hippocampal formation and coined the term trisynaptic circuit (Andersen and Bliss, 1971). For simplicity, the entorhinal cortex is considered to be the starting point of the circuit because much of the sensory information that reaches hippocampus enters through the entorhinal cortex. Most of the sensory information to the hippocampal formation arises in two adjacent cortical areas: the perirhinal and postrhinal (parahippocampal in the primate) cortices. These relay high level polysensory information to the entorhinal cortex (Burwell, 2000). These inputs to the entorhinal cortex are generally excitatory (Martina et al., 2001). The other major source of sensory information is the retrosplenial cortex (van Groen and Wyss, 1992).

Neurons located in layer II of the entorhinal cortex give rise to a pathway, the perforant path, that projects through (perforates) the subiculum and terminates both in the dentate gyrus and in the CA3 field of the hippocampus. Cells in the medial entorhinal cortex contribute axons that terminate in a highly restricted fashion within the middle portion of the molecular layer of the dentate gyrus, and those from the lateral entorhinal cortex terminate in the outer third of the molecular layer. These two components of the perforant path also end in a laminar pattern in the stratum lacunosum-moleculare of CA2 and CA3. Neurons located in layer III of the entorhinal cortex do not project to the dentate gyrus or CA3 but do project to CA1 and the subiculum. In this case the projection is not organized in a laminar fashion but rather in a topographic manner.

Axons originating from neurons in the lateral entorhinal cortex terminate in that portion of stratum lacunosum-moleculare which is located at the border of CA1 with the subiculum. Projections arising from the medial entorhinal cortex terminate in that portion of stratum lacunosum-moleculare of CA1 that is located close to CA3 and in the molecular layer of the subiculum located close to the presubiculum.

The dentate gyrus is the next structure in the progression of connections, and it gives rise to the mossy fibers that terminate on the proximal dendrites of the CA3 pyramidal cells. The granule cells also synapse on cells of the polymorphic layer, the mossy cells, which provides associational connections to other levels of the dentate gyrus. The CA3 pyramidal cells, in turn, project heavily to other levels of CA3 as well as to CA1. The projection to CA1 is typically called Schaffer collateral projection. CA1 pyramidal cells give rise to connections both to the subiculum and to the deep layers of the entorhinal cortex. The subiculum also originates a projection to the deep layers of the entorhinal cortex. The deep layers of the entorhinal cortex, in turn, originate projections to many of the same cortical areas that originally project to the entorhinal cortex. Thus information entering the entorhinal cortex from a particular cortical area can traverse the entire hippocampal circuit through the excitatory pathways, just described above, and ultimately be returned to the cortical area from which it originated. The transformations that take place through this traversal are presumably essential for enabling the information to be stored as long-term memories.

1.3. Characterization of main excitatory hippocampal synapses and LTP in them

1.3.1. Perforant path projections to the dentate gyrus

Perforant pathway projecting to the dentate gyrus originates from layer II of the entorhinal cortex and consists of two groups of fibers which according to their origin are called lateral and medial projections. Lateral perforant path fibers project to outer part of molecular layer of the dentate gyrus and medial fibers to the inner part. These projections differ in physiological characteristics that are important for their discrimination. Medial perforant path projections reveal paired-pulse depression, while lateral ones show facilitation (McNaughton, 1980).

In terms of LTP these two groups of fibers do not show any strong differences (Hanse and Gustafsson, 1992). Experiments have revealed that in untreated slices, magnitude of LTP at the perforant path synapses depends on the protocol of repetitive stimulation. Bursts of brief high-frequency trains (Greenstein et al., 1988), or tetanization at higher frequencies (400 Hz) rather than lower ones (50 and 100 Hz) (Winson and Dahl, 1986), constitute a very efficient production of LTP. But in slices, where $GABA_A$–mediated inhibition is blocked, 400 Hz tetanization

producing potentiation is no more stable than that following 100 Hz trains (Hanse and Gustafsson, 1992).

1.3.2. Mossy fiber projections to the CA3 field

Granule cells of the dentate gyrus send signal to the CA3 pyramidal neurons with help of mossy fibers which project to stratum lucidum of the CA3 field. Each CA3 pyramidal neuron receives approximately 15000 excitatory inputs and only about 50 of them are mossy fibers (Claiborne et al., 1986). In a transverse hippocampal slice, the number of intact and healthy mossy fiber inputs to any given pyramidal cell is even smaller, because the course of the mossy fiber axons is not perpendicular to the long axis of the hippocampus. In addition the fiber trajectories slant toward the temporal pole of the hippocampus at an angle that varies from 15^0 to 20^0, depending on the location along the septotemporal axis (Gaarskjaer, 1986).

Mossy fiber synapses on the CA3 neurons exhibit robust short- and long-term presynaptic plasticity (Henze et al., 2000;Kobayashi et al., 1996;Zalutsky and Nicoll, 1990), which is independent of activation of NMDA receptors (Harris and Cotman, 1986). Mossy fiber synapses have several unusual structural features, including large terminals, multiple release sites and a proximal termination zone along the apical dendrites of CA3 neurons (Chicurel and Harris, 1992;Claiborne et al., 1986). The induction of mossy fiber LTP appears to be insensitive – or at least less sensitive – to buffering of postsynaptic calcium (Williams and Johnston, 1989). Finally, mossy fiber LTP expression clearly interacts with paired-pulse facilitation (PPF), a presynaptic process (Son and Carpenter, 1996).

Since LTP at the mossy fiber synapses does not require activation of NMDA receptors, one might expect that it has non-Hebbian character. As it is known, LTP requiring coincident activation of pre- and postsynaptic elements is called ‘Hebbian’, whereas LTP requiring activation of either pre- or postsynapse is referred to as ‘non-Hebbian’ (Morris, 1999), and postsynaptic NMDA receptors serve as the primary integration site of pre- and postsynaptic activity.

Some groups have showed that blockade of postsynaptic activation by hyperpolarization and buffering of cytosolic calcium does not prevent induction of mossy fiber LTP (Castillo et al., 1994;Katsuki et al., 1991;Langdon et al., 1995), while others showed that mossy fiber LTP required both pre- and postsynaptic activation (Derrick and Martinez, Jr., 1994;Jaffe and Johnston, 1990). Subsequently, Urban and co-workers found out, that different patterns of high-frequency stimulation may induce either ‘Hebbian’, or ‘non-Hebbian’ LTP at mossy fiber-CA3 synapses (Urban and Barrionuevo, 1996).

The simple view of LTP in this system is that high-frequency firing of presynaptic afferent fibers triggers a rise in cAMP and activation of protein kinase A (PKA) in presynaptic terminals, which leads to a persistent enhancement of transmitter release probability (Nicoll and Malenka, 1995).

As mentioned above, mossy fiber LTP does not depend on the activation of NMDA receptors, but studies have shown that there are quite a few NMDA receptors in this system. Experiments dedicated to the investigation of mossy fiber NMDA receptors function revealed that these receptors can trigger non-Hebbian heterosynaptic LTP at entorhino-CA3 synapses (Tsukamoto et al., 2003).

1.3.3. Associational-commissural projections to the CA3 pyramidal neurons

CA3 pyramidal cells synapse not only onto CA1 neurons via Schaffer collateral pathway, but also onto other CA3 pyramidal neurons via fibers known as associational-commissural pathway or recurrent collaterals (Johnston and Amaral, 2004). These fibers make the most abundant projections in the strata radiatum and oriens of the CA3 field.

During development associational-commissural projections undergo certain changes. Comparison of CA3 pyramidal neurons of the second postnatal week with the mature neurons, revealed that in the adult brain recurrent axon arbors had the same length, although the adult arbor had half as many branches. Consequently, each of the remaining adult branches increased in length, thereby offsetting the loss of branches. Both arbors have the same density of varicosities, even though varicosities have been lost on the eliminated branches after the second postnatal week. However, other varicosities have been added on the remaining, but longer, axons of the adult (Moody et al., 1998).

Studies of LTP at associational-commissural synapses have showed that in common to the Schaffer collateral projections to CA1 field, this pathway also exhibits NMDA dependent LTP (Collingridge et al., 1983;Gereau and Conn, 1994). In spite of similarities, processes at these synapses are not identical. It has been shown that 5-Hz stimulation is able to induce LTP at Schaffer collateral-CA1 synapses and this LTP is highly activity dependent in that while 15- to 30s long trains of 5-Hz stimulation is sufficient for LTP induction, longer trains (> 1 min in duration) have short-lasting effect on synaptic strength. Moreover, induction of LTP by 5-Hz stimulation is modulated by noradrenergic receptor activation. In contrast, associational-commissural fiber synapses onto CA3 pyramidal cells do not undergo LTP during 5-Hz stimulation, and activation of adrenergic system by agonists of β-adrenergic receptors has no effect on this process (Moody et al., 1998).

Since associational-commissural pathway is not the only one which projects onto the CA3 pyramidal neurons, it is likely that activity of these projections are under influence of other pathways, which exist in this area. Indeed, investigations have shown, that recurrent collaterals can be modified by mossy fibers, in spike train timing-dependent manner (Kobayashi and Poo, 2004).

1.3.4. Direct perforant path projections to the CA3 pyramidal neurons

In addition to mossy fibers that bring information from the dentate gyrus, CA3 field receives direct monosynaptic input from the entorhinal cortex, via the perforant path projections located in stratum lacunosum-moleculare. Because an almost equal number of synapses are formed by perforant path fibers in CA3 and in the dentate gyrus the perforant path projection to the CA3 could be as strong as perforant path projections to the dentate gyrus. Findings from electrophysiological experiments in vitro (Doller and Weight, 1982) and in anesthetized animals in vivo (Yeckel and Berger, 1990) suggest that the monosynaptic input from the entorhinal cortex to CA3 and CA1 is sufficiently strong enough to excite pyramidal cells in these areas to the level of action potential generation. These data suggest that the direct perforant path input to areas CA1 and CA3 play a significant role in hippocampal function.

The heterogeneity of the perforant path input to the hippocampus adds another dimension to the characterization of this projection. Specifically, the perforant path synapses in the CA3 similarly to the dentate gyrus, consist of lateral and medial fibers and distribution of these fibers in CA3 area also reminds their distribution in the dentate gyrus. Namely, lateral perforant path synapses are located more distally on the dendritic tree whereas medial perforant path synapses are located more proximally (Witter, 1993).

Perforant path (PP) projections to both dentate gyrus and CA3 field are thought to arise from the same cell population in the entorhinal cortex (Witter et al., 1989) and thus may show the same presynaptic properties. With low intensity of stimulation (which resulted in response of <15% of maximal amplitude) it is possible to observe responses that exhibit either paired-pulse facilitation (PPF) or paired-pulse depression (PPD), which means it is possible to distinguish lateral and medial perforant path evoked postsynaptic potentials, but higher intensity of stimulation usually causes simultaneous activation of both types of fibers (Berzhanskaya et al., 1998).

LTP of the perforant path synapses to CA3 is both cooperative (in that recruitment of a suprathreshold number of afferents is necessary to induce potentiation) and associative (in that afferent fibers of different orders are capable of contributing to potentiation). Perforant path LTP under both conditions was found to be NMDA receptor dependent (McMahon and Barrionuevo,

2002). Although it is likely that strong high frequency stimulation during the cooperative induction of LTP also recruits recurrent collateral axons to some extent, it would only do so at stimulation intensity high enough to induce spiking in the postsynaptic cell. In *in vivo* experiments it has been shown that lateral perforant pathway exhibits NMDA receptor-dependent LTP, whereas medial one is NMDA receptor independent (Do et al., 2002).

Perforant path LTP is not readily inducible *in vitro* without blockade of inhibition (Colbert and Levy, 1993). One probable cause of the susceptibility of PP LTP to GABAergic suppression is the fact that bulk stimulation in the lacunosum-moleculare in slices recruits both perforant path fibers and axons of inhibitory interneurons (Freund and Buzsaki, 1996). It is likely that transmission through perforant path in the intact brain is ordinarily under strong inhibitory control. Given that perforant path LTP is readily inducible in area CA3 in vivo (Breindl et al., 1994) inhibitory suppression of perforant path LTP can be disengaged in the intact brain.

Since CA3 pyramidal neurons receive three different excitatory inputs, (mossy fibers from dentate gyrus, direct perforant pathway from entorhinal cortex and recurrent collaterals from other CA3 neurons) there should be a possibility of induction of associative LTP among these projections. Indeed, *in vivo* recordings have shown that associative LTP can be induced between extrinsic afferents of the hippocampal CA3 field, such as perforant path and associational-commissural projections (Martinez et al., 2002).

1.3.5. Direct perforant path projections to the CA1 pyramidal neurons

Entorhinal cortex sends direct projections to the CA1 field too. In contrast to direct projections to the CA3 region, these fibers originate from layer III of the entorhinal cortex, but similarly to the CA3 field they are located in stratum lacunosum-moleculare.

Direct perforant path evoked excitatory postsynaptic currents are accompanied by inhibitory potentials (Colbert and Levy, 1993;Empson and Heinemann, 1995), which are thought to be disynaptic. Anatomic data also suggest that hippocampal interneurons receiving direct perforant path input mediate this disynaptic inhibition.

Perforant path projections to the CA1 field sometimes are called as temporo-ammonic pathway (TA). Scientists have shown that TA-CA1 synapses undergo both early and late phase LTP in rat hippocampal slices. LTP at TA projections to the CA1 field requires NMDA receptors and voltage-dependent Ca^{2+} channels, is insensitive to the blockade of fast $GABA_A$ mediated inhibitory transmission (Chapman et al., 1998) and interestingly, depends also on $GABA_B$-dependent slow inhibitory transmission (Remondes and Schuman, 2003).

1.3.6. Schaffer collateral projections to the CA1 pyramidal neurons

The final step of information flow along the trisynaptic pathway is Schaffer collateral synapse onto the CA1 pyramidal neurons. These projections originate from CA3 pyramidal cells and project in the stratum radiatum and stratum oriens of CA1 region.

Since it is very easy to find responses and induce long-term potentiation at this synapse, it has been widely used as a main target for investigation of characteristics of synaptic plasticity. Therefore most of the information related to these projections will be discussed in the chapter of LTP and memory.

2. Cell adhesion molecules

One of the major challenges in developmental neurobiology is a full understanding of the molecular mechanisms that allow for the formation of specific synaptic connections in the central and peripheral nervous system. The mammalian brain contains over 10^{12} neurons, and many of these receive synaptic inputs from thousands of other neurons.

Cell adhesion molecules (CAMs) are integral membrane proteins, which play important role in interactions between cells or/and cells and extracellular matrix (ECM) elements (Gordon-Weeks and Fischer, 2000;Kater and Rehder, 1995). Among these molecules are the cadherins (Fannon and Colman, 1996;Tang et al., 1998), integrins (Staubli et al., 1998) and members of the immunoglobulin superfamily, such as the neural cell adhesion molecule NCAM (Dityatev et al., 2000;Luthi et al., 1994) and its associated polysialic acid (Eckhardt et al., 2000;Muller et al., 1996), F3/F11/contactin (Perrin et al., 2001), and L1 (Luthi et al., 1994).

2.1. The immunoglobulin (Ig) superfamily of cell adhesion molecules

Members of the Ig superfamily of cell adhesion molecules are characterized by the presence of one or more Ig-like modules. In the nervous system many cell adhesion molecules combine their Ig-like modules with other repeated structures such as the fibronectin repeat of the subtype III (FNIII domain). Functional analysis of fibronectin revealed that FNIII domains are involved in interactions of cells with the ECM (Ruoslahti and Pierschbacher, 1987). Members of this family often have a single transmembrane region or a GPI anchor and, in most cases, an intracellular domain.

The Ig superfamily is composed of several subgroups according to the number of Ig-domains, the presence of a catalytic cytoplasmic domain, the mode of attachment to the cell membrane and the presence and number of FNIII-domains, (Cunningham, 1995). Neural cell adhesion molecule NCAM (Thiery et al., 1977) and L1 (Rathjen and Schachner, 1984;Salton et

al., 1983), representative molecules of two different subfamilies, were the first isolated and characterized Ig-like CAMs. F3 (mouse F3/chicken F11/human contactin), DCC (deleted in colonrectal carcinoma), MAG (myelin associated glycoprotein), and FGF-R (fibroblast growth factor-receptor) are additional subgroups present in the brain.

2.1.1. The L1 family

The L1 family consists of six members, among which four are found in vertebrates: L1, CHL1 (close homologue of L1), Nr-CAM (Ng-CAM related CAM) and neurofascin, and two in invertebrates: neuroglian and tractin (Brummendorf and Rathjen, 1995;Hortsch, 2000;Kenwrick et al., 2000). All members of the L1 family display high similarity in the composition and conformation of their modules and are composed of six amino-terminal Ig-domains, four to five FNIII-repeats, a single hydrophobic membrane-spanning region and a short, phylogenetically highly conserved cytoplasmic tail at the carboxyl terminus (Brummendorf and Rathjen, 1995). These molecules are widespread throughout the developing nervous system from postmitotic stage on and involved in a variety of morphogenetic processes, such as cell migration, axon outgrowth, myelination, pathfinding, fasciculation and synaptic plasticity. Members of the L1 family are mainly found on the surface of axons and at sites of cell-cell contact and are expressed by neurons and glial cells (Hortsch M, 1996).

2.1.1.1. The neural cell adhesion molecule L1

L1 is one of the first isolated and characterized cell adhesion molecules, and it has been found in variety of species. In humans, it's called L1CAM or L1, in chicks - Ng-CAM (neuron-glia CAM), in rats - NILE (nerve growth factor-inducible large external glycoprotein), in drosophila – neuroglian, in mice - L1, in goldfish - E587, and in zebrafish - L1.1 and L1.2. There is a quite high sequence similarity among species homologous that ranges between 30 to 60 % and the intracellular domain shows the highest degree of interspecies homology, reaching even complete identity in human, rat and mouse. The presence of homologues across diverse species and the high degree of conservation in the course of evolution speaks for the key role of L1. (Hortsch M, 1996;Hortsch, 2000).

Characteristics of L1

Mammalian L1 consists of six Ig-domains of the C2-type, which are folded into a horseshoe shaped conformation rather than an extended one (Schurmann et al., 2001), five FNIII repeats, a single membrane-spanning region followed by a short cytoplasmic tail. The size of full

length L1 is approximately 200 kD. Proteolytic cleavage gives rise to smaller forms with a molecular weight of 180, 140, 80 and 50 kD (Sadoul et al., 1988). Twenty one putative sites for asparagine-(N-) linked glycosylation are distributed over the extracellular domain of L1 (Figure 3). Since deglycosylation produces molecular mass of about 150 kD, glycans should be about 25% of the total molecular mass of L1, (Lindner et al., 1983;Rathjen and Schachner, 1984). A substantial portion of the glycans are O-linked which is indicated by tunicamycin inhibition of cotranslational N-glycosylation (Faissner et al., 1985).

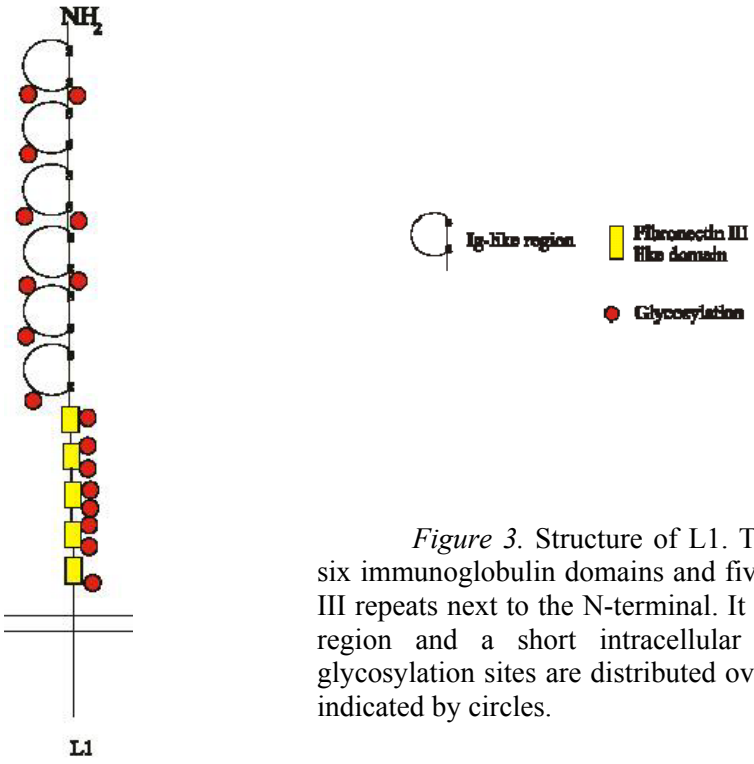

Figure 3. Structure of L1. The L1 molecule consists of six immunoglobulin domains and five complete fibronectin type III repeats next to the N-terminal. It also has the transmembrane region and a short intracellular domain. 21 putative N-glycosylation sites are distributed over the extracellular part and indicated by circles.

Two tissue and cell specific isoforms are known for L1, resulting from alternative splicing, which are expressed in a tissue- and cell type-specific pattern. The L1 protein is encoded by a single gene, which is located on the X-chromosome and contains 29 exons, 28 exons encode the protein (designated 1b-28) while one exon contains 5´untranslated sequences (exon 1a) (Kallunki et al., 1997;Kohl et al., 1992). The mRNA provides an open reading frame of 3783 nucleotides. The encoded 1260 amino acids comprise a 19 amino acid signal peptide and a mature protein of 1241 amino acids (Moos et al., 1988). Neurons usually have the entire 28 exon coding sequence of L1 (Takeda et al., 1996). A shorter isoform which lacks exons 2 and 27, is expressed only in non-neuronal cells, such as cells of the epidermis and kidney (Debiec et al., 1998;Nolte et al., 1999), hematopoetic origin, intestinal crypt and the male urogenital tract (Kowitz et al.,

1992;Kujat et al., 1995). More recently oligodendrocytes were also found to express short L1, regulated in a maturation-dependent manner (Itoh et al., 2000).

Expression and function of L1 in the nervous system

The cellular expression pattern of L1 exhibits a dependency on the state of differentiation and is consistent with its functions. L1 expression is detectable early in neural development. Analysis of 1, 8 and 21-day-old mouse hippocampus revealed that L1 was present only on fasciculating axons. It was not detectable on dendrites and cell bodies of pyramidal cells, granule cells and interneurons in any of the hippocampal regions and was never seen at contacts between astrocytes and axons. In adult nervous system L1 was expressed only at the surface membranes of unmyelinated axons, such as the molecular layers of the cerebellum or the hippocampus (Persohn and Schachner, 1990). In the peripherial nervous system, L1 was also expressed by nonmyelinated Schwann cells (Martini and Schachner, 1986), but it has never been detected in synapses (Schuster et al., 2001).

During the development of the nervous system, L1 plays a role in adhesion between neurons and between neurons and Schwann cells (Persohn and Schachner, 1987;Rathjen and Schachner, 1984), axon outgrowth, pathfinding and fasciculation (Chang et al., 1987;Fischer et al., 1986;Kunz et al., 1996;Lagenaur and Lemmon, 1987), migration of postmitotic neurons (Asou et al., 1992;Lindner et al., 1983), myelination (Seilheimer et al., 1989;Wood et al., 1990a;Wood et al., 1990b), growth cone morphology (Burden-Gulley et al., 1995;Payne et al., 1992). Axonal regeneration (Martini and Schachner, 1988), learning and memory formation (Rose, 1995), and the establishment of long-term potentiation in the hippocampus (Luthi et al., 1996;Luthi et al., 1994). It has been shown that Y1176 of the YRSL motif within L1 cytoplasmic domain is dephosphorylated in LTP-induced hippocampus and clathrin-mediated recycling of L1 at presynaptic sites is important for maintenance of LTP-induced synaptic changes (Itoh et al., 2005). L1 deficient mice show reduced GABAergic transmission and number of hippocampal perisomatic inhibitory synapses (Saghatelyan et al., 2004). Conditional ablation of L1 brings about decreased anxiety, altered place learning, and increased CA1 basal excitatory synaptic transmission (Law et al., 2003). L1 was shown to be involved in spinal cord regeneration in zebra fish (Becker et al., 2004).

Homophilic and heterophilic adhesion

Most of L1 functions depend on its interaction with diverse binding partners and posttranslational modification as a trigger for signalling cascades. Cytoplasmic and extracellular parts, *cis* and *trans* interactions, homophilic and heterophilic bindings are involved factors.

It has been shown that L1 is capable of both, homo and heterophilic interaction. Most of its functions L1 performs via homophilic interactions (Hankin and Lagenaur, 1994;Lemmon et al., 1989;Miura et al., 1992). Different studies, dedicated to map the regions needed for homophilic binding and optimal levels of neurite outgrowth, achieved various conclusions. Some studies (Appel et al., 1993;Holm et al., 1995) found that several extracellular domains were required for homophilic interactions, while Zhao and colleagues (Zhao et al., 1998;Zhao and Siu, 1995) suggested that the second Ig-domain, and more specifically a 14 amino acid peptide within this Ig-domain, was sufficient for homophilic binding. The shedded L1 fragment is suggested to abrogate homophilic L1-L1-mediated aggregation (Nayeem et al., 1999). L1 shedding results from cleavage near the membrane, by a disintegrin and metalloproteinase family and leads to an amino-terminal 180 kD and a membrane associated 30 kD fragment (Gutwein et al., 2000;Mechtersheimer et al., 2001).

L1 and its species homologues are also able to interact in *cis* or *trans* manner with a variety of ligands such as laminin (Grumet et al., 1993), DM-GRASP (DeBernardo and Chang, 1996), F3/F11/contactin (Brummendorf et al., 1993), axonin-1/TAG-1 (Kuhn et al., 1991), and CD24 or nectadrin (Kadmon G, 1995;Kalus et al., (in press);Sammar et al., 1997). Furthermore, the Arg-Gly-Asp (RGD) site within Ig-domain 6 supports binding with subsets of integrins such as α5β1, αVβ1 or αVβ3 (Felding-Habermann et al., 1997;Montgomery et al., 1996). It has been suggested that L1 serves as a co-receptor with neuropilin for Sema3A signal transduction (Castellani et al., 2000). L1 can also interact with the ECM, namely by binding to the chondroitin sulfate proteoglycans neurocan and phosphacan, major constituents of the ECM (Milev et al., 1994;Rauch et al., 1991).

Intracellular events mediated by L1

Numerous studies suggest that CAMs function by activating second messenger cascades. It has been shown that antibodies directed against L1 and NCAM reduce intracellular levels of the inositol phosphates IP_2 and IP_3, while intracellular levels of cAMP are unaffected. They also reduce intracellular pH and increase intracellular Ca^{2+} by opening Ca^{2+} channels in a pertussis toxin-inhibitable manner, suggesting the involvement of a G protein in the signal transduction process (Schuch et al., 1989).

Axon extension and guidance during development of the nervous system is defined by many factors and the signaling mechanisms responsible for triggering this extension is of a great interest. Investigations have revealed that the Rho family small guanosine triphosphatases (GTPases) is involved in this process by diffusible factors and asymmetry in Rho kinase or filopodial initiation across the growth cone is sufficient to trigger the turning response (Yuan et

al., 2003). Axonal growth in response to homophilic L1-L1 interactions *in trans* is triggered by an activation of the FGF-R (a receptor tyrosine kinase) after *in cis* interactions between the extracellular domains of L1 and FGF-R, leading to an autophosphorylation of the receptor (Lom et al., 1998;Meiri et al., 1998;Ronn et al., 2000). There could also be some other signaling cascade for L1. It has been shown that L1 can be phoshorylated by Cek5 (chicken embryo kinase 5 /EphB2) a receptor-type tyrosine kinase of the ephrin (Eph) kinase family (Zisch et al., 1997;Zisch and Pasquale, 1997) and two serine/threonine protein kinases, such as casein kinase II and p90rsk (Kunz et al., 1996;Wong et al., 1996a;Wong et al., 1996b). Clustering of L1 at the neural surface is reported to transiently activate the MAP kinase (mitogen-activated protein kinase) and ERK2 (extracellular signal-regulated kinase) (Schmid et al., 1999;Schmid et al., 2000). A role of the non-receptor type tyrosine kinase src in L1-dependent neurite outgrowth is indicated by the fact that neurite outgrowth from src-deficient nerve cells is impaired on an L1 substrate (Ignelzi MA, 1994). An example for influences of heterophilic binding on such signaling cascades is the finding that dimerization of L1 with TAG1/axonin-1 is associated with non-receptor tyrosine kinase activation (Kunz et al., 1996).

All members of the L1-subgroup are able to interact with the spectrin-based membrane skeleton by binding to the adaptor protein ankyrin (Davis and Bennett, 1993;Davis and Bennett, 1994;Hortsch, 2000). Interactions between L1 and ankyrin might be a mechanism by which interactions with the substrate are linked to the cytoskeleton and lead to ankyrin-dependent alterations in the cellular organization or in the targeting of proteins to specific membrane compartments (Bennett and Chen, 2001). L1 has also been shown to colocalize with filamentous actin in the filopodia and lamellipodia of growth cones of cultured chick dorsal root ganglion neurons (Letourneau and Shattuck, 1989). The molecular mechanisms by which L1 could be involved in growth cone migration were uncovered by recent studies. Clathrin-mediated endocytosis of L1 occurs preferentially in the central domain of growth cones followed by centrifugal transport of vesicles into the peripheral domains and reinsertion into the membrane at the leading edge which could be responsible for producing polarized adhesion and directed migration of the growth cone (Kamiguchi et al., 1998;Kamiguchi and Lemmon, 2000;Kamiguchi and Yoshihara, 2001).

Neurological disorders caused by mutations in the L1 gene

It has been known that the human gene encoding L1 is located near the long arm of the X-chromosome (Djabali et al., 1990) in Xq28 (Chapman et al., 1990). A lot of different pathogenic mutations have been identified in virtually all regions of the gene. All types of mutations were

found in human patients including missense, nonsense, and frame shift mutations, deletions, duplication, insertion, and splice site mutations.

Since different X-linked mental retardation syndromes have been related to Xq28 and the morphological abnormalities of these syndromes might result from deficits in cell migration, axonal pathfinding and fasciculation, L1 is considered to be a candidate gene causing these syndromes.

Among syndromes related to abnormal L1 expression one should mention HSAS syndrome - hydrocephalus due to stenosis of the aqueduct of Sylvius (Bickers D, 1949;Rosenthal et al., 1992), MASA syndrome - mental retardation, aphasia, shuffling gait and adducted thumbs (Bianchine JW, Jr., 1974), X-linked complicated SP-1 - spastic paraplegia (Kenwrick et al., 1986) or ACC - agenesis of the corpus callosum (Fransen et al., 1994;Jouet et al., 1994;Kaplan, 1983;Vits et al., 1994). The fact that all of these conditions are allelic disorders proved that HSAS, MASA, SP-1, and ACC represent overlapping clinical spectra of the same disease, and therefore now are summarized under the term ´L1 spectrum` (Moya et al., 2002). This term might be more widely acceptable than the previously proposed term CRASH - corpus callosum agenesis, retardation, adducted thumbs, shuffling gait, and hydrocephalus (Fransen et al., 1995).

2.1.1.2. The close homologue of L1 (CHL1)

CHL1 is also a member of immunoglobulin superfamily of cell adhesion molecules. Structure of the CHL1 is very close to L1 molecule and therefore it is called a close homologue of L1. Evaluation of structural homologies of CHL1 with other L1-related molecules revealed that CHL1 is most similar to chicken NgCAM in the extracellular domain (37% identity) and to mouse NrCAM in the intracellular domain (64% identity). Since the degree of identity is not sufficient to consider these proteins as species homologues, CHL1 was defined as a new, the fourth member of the L1 family in mouse with L1, NrCAM and neurofascin (Holm et al., 1996).

Characteristics of CHL1

CHL1 is composed of a single transmembrane segment with 23 amino acids, an intracellular portion of 105 amino acids and the extracellular domain which comprises two structural motifs characteristic for L1-subfamily, such as: a stretch of 585 amino acids which displays homology with Ig-like domains and a region composed of 472 amino acids that shows homology with FNIII-like domains (Figure 4). Since a fifth FNIII-like motif is only partially expressed in the CHL1 sequence, this new member of L1-subfamily introduces a new structural feature to the subclass of L1-related molecules. CHL1 also contains a DGEA sequence, a

potential integrin interaction motif, in the β-strand C of the sixth Ig-like domain that is not found in other members of the L1-subfamily (Staatz et al., 1991).

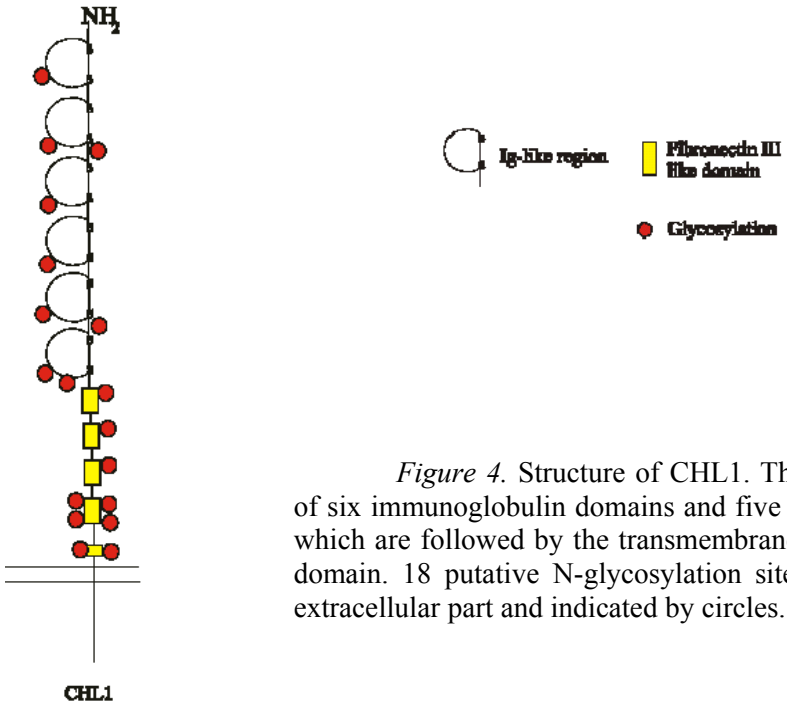

Figure 4. Structure of CHL1. The CHL1 molecule consists of six immunoglobulin domains and five fibronectin type III repeats which are followed by the transmembrane region and a intracellular domain. 18 putative N-glycosylation sites are distributed over the extracellular part and indicated by circles.

CHL1 has been identified in mice, rats (Holm et al., 1996), and humans (Wei et al., 1998). The CHL1 gene, also referred to as CALL, is located in a short (p) arm of chromosome 3 and may be associated with intelligence (Angeloni et al., 1999b).

Budding yeast CHL1 was identified by virtue of decreased chromosome transmission fidelity or chromosome loss screens and in this organisms mutations in CHL1 result in increased chromosome loss, sister-chromatid nondisjunction, and a variety of phenotypes, including bisexual mating of diploids, donor locus selection defects in *MAT*a cells, and increased mitotic recombination (Spencer et al., 1990;Weiler et al., 1995). In combination, these findings suggested that Chl1p is critical for higher-order chromatin conformations that, in addition to blocking inappropriate recombination, are central to chromosome segregation (Weiler et al., 1995). Chl1p exhibits significant homology to Rad3p, a DNA helicase that exhibits nucleotide excision repair activity (Gerring et al., 1990). Human CHLR1 (CHL1-related mRNA) protein exhibits DNA helicase activity, binding both single- and double-stranded DNA (Amann et al., 1997;Hirota and Lahti, 2000). Also it has been found that budding yeast Chl1p physically associates with Ctf7p and it is critical for sister-chromatid cohesion (Skibbens, 2004).

Expression and function of CHL1 in the nervous system

Expression of CHL1 appears to be restricted to the nervous system (Hillenbrand et al., 1999;Holm et al., 1996). In mice, CHL1 expression is first detectable in the brain at embryonic

day 13, reaches peak levels from embryonic day 18 to postnatal day 7, and subsequently declines to lower levels in the adult brain (Hillenbrand et al., 1999). Neurons in most brain areas express CHL1 mRNA, but its expression is often restricted to particular subsets of neurons, e.g., in the hippocampal formation, where CHL1 shows a stronger expression in the CA1 field and the dentate gyrus than in the CA2, CA3, and CA4 fields (Hillenbrand et al., 1999). CHL1 is expressed in pyramidal neurons in a high-caudal to low-rostral gradient within the developing cortex and it has been shown that CHL1 modulates area-specific neuronal positioning and dendrite orientation in the cerebral cortex (Demyanenko et al., 2004). CHL1 is also expressed by subpopulations of astrocytes and oligodendrocyte precursors in the central nervous system and by nonmyelinated Schwann cells and some neurons in the peripheral nervous system (Hillenbrand et al., 1999;Zhang et al., 2000), where prolonged upregulation of CHL1 mRNA by neuronal and glial cells during regeneration has been described (Chaisuksunt et al., 2000b;Chaisuksunt et al., 2000a;Zhang et al., 2000).

In vitro, CHL1 strongly promotes neurite outgrowth by hippocampal and cerebellar neurons via an as yet unidentified receptor or receptors on the neuronal surface (Hillenbrand et al., 1999). Chen et al. investigated the effect of CHL1-Fc fusion protein on the survival of cultured murine cerebellar granule and hippocampal neurons of rat embryos. Serum deprivation induces apoptosis that can be prevented by either soluble or substrate-coated CHL1 fusion protein. Addition of CHL1 increased the number of surviving neurons by about 45 % (Chen et al., 1999). It has been shown that L1 and CHL1 are also important survival factors for motoneurons (Nishimune et al., 2005) and mice deficient in the L1 or CHL1 exhibit impaired sensorymotor gating (Irintchev et al., 2004). CHL1 deficiency also seems to cause alterations of hippocampal mossy fiber organization and of olfactory axon projections (Montag-Sallaz et al., 2002).

Motor and cognitive phenotype analyses revealed that mice deficient in CHL1 displayed signs of decreased stress and a modification of exploratory behavior. The mice also showed motor impairments on the Rotarod, but they were able to move as fast as controls in the alleys of a T-maze. The observed changes were assumed to be related to a deficit in attention. Also, gender differences have been found, that can be discussed in view of a possible interaction with other cell adhesion molecules during development (Pratte et al., 2003).

Homophilic and heterophilic adhesion

It has been known that several cell adhesion molecules like L1, neuroglian or TAG-1 are able of homophilic interaction (Hortsch M, 1996;Kadmon and Altevogt, 1997;Malhotra et al., 1998), therefore the question was addressed whether CHL1 was also able to interact in a

homophilic manner or not. However, cell aggregation assays could demonstrate neither a homophilic interaction between CHL1-CHL1 molecules nor a heterophilic interaction between CHL1 and L1. Recently it has been shown that CHL1 is an enhancer of integrin-mediated cell migration (Buhusi et al., 2003). Enhancement of migration was disrupted by mutation of a potential integrin interaction motif Asp-Gly-Glu-Ala (DGEA) in the sixth immunoglobulin domain of CHL1, suggesting that CHL1 functionally interacts with beta1 integrins through this domain. CHL1 was shown to associate with beta1 integrins on the cell surface by antibody-induced co-capping. Through a cytoplasmic domain sequence containing a conserved tyrosine residue, CHL1 recruited the actin cytoskeletal adapter protein ankyrin to the plasma membrane, and this sequence was necessary for promoting integrin-dependent migration to extracellular matrix proteins. These results support a role for CHL1 in integrin-dependent cell migration that may be physiologically important in regulating cell migration in nerve regeneration and cortical development.

Neurological disorders caused by mutations in the CHL1 gene

Cloning and chromosomal localization of the human CHL1 homologue CALL (Wei et al., 1998) suggested an important role of CHL1 in neurological disorders since the CALL gene was mapped to the chromosome 3p26 locus, a region that is associated with mental retardation in 3p-syndrome. More than 70 patients with 3p- syndrome (Conte et al., 1995;Drumheller et al., 1996) or partial 3p trisomies (Reiss et al., 1986) have been reported. Molecular analysis showed that the deleted or duplicated regions vary in size (Drumheller et al., 1996).

Mental retardation (MR) can be classified as either syndromic or non-specific. In patients with syndromic forms of MR, the clinical manifestations include MR associated with other physical features (such as neurological symptoms, skeletal defects or facial dysmorphism), whereas in patients with non-specific MR no distinctive clinical or biochemical manifestations occur, apart from the cognitive impairment. The CALL gene has been reported as a candidate for autosomal-recessive non-specific MR (Higgins et al., 2000) and moreover, it is proposed as a gene which may be associated with schizophrenia (Chen et al., 2005;Sakurai et al., 2002).

3. Long-term potentiation, learning and memory

Learning may be described as the mechanism by which new information about the world is acquired, and memory as the mechanism by which that knowledge is retained (Lynch, 2004). For convenience, learning can be categorized as being explicit, which is defined as that involved in the conscious recall of information about people, places, and things, or implicit, which is

characterized by the unconscious recall of tasks such as motor skills. Explicit memory depends on the integrity of temporal lobe and diencephalic structures such as the hippocampus, subiculum, and entorhinal cortex. Implicit memory includes simple associative forms of memory, for instance classical conditioning, and non-associative forms, such as habituation, and relies on the integrity of the cerebellum and basal ganglia (Lynch, 2004).

At least two components of memory can be discerned: short-term memory, which endures for a few hours, and long-term memory, which persists for several days and often much longer. At the cellular level, the storage of long-term memory is associated with gene expression, *de novo* protein synthesis, and formation of new synaptic connections. Consistently, protein synthesis inhibitors can block persistent memory but leave short-term memory unaffected, suggesting that stable, long-lasting memories rely on gene activation that is triggered at, or close to, the time of the experience. One of the most compelling problems in neuroscience is to identify the mechanisms underlying memory, and although a great deal of progress has been made in the past few decades, it remains a significant challenge.

Activity-dependent synaptic plasticity plays a vital role in sculpting synaptic connections during development and has been identified in several synaptic pathways. Although it occurs, in particular, during critical periods of early development, it is also a feature of the adult brain. For example, it is widely accepted that memory formation is dependent on changes in synaptic efficiency that permit strengthening of associations between neurons.

Hebb on the basis of Cajal's hypotheses proposed that if two neurons are active at the same time, the synaptic efficiency of the appropriate synapse will be strengthened. An enormous effort has been channeled into understanding the mechanism by which strengthening of synaptic connections can be achieved and, in this effort, the importance of one model, above all others, cannot be overestimated; this model is long-term potentiation (LTP).

There are multiple forms of LTP induced by different paradigms in different synaptic connections and under different experimental conditions, and consequently, LTP can not be considered as a unified construct, without specifying precise experimental conditions (Lynch, 2004).

3.1. Hippocampus, learning and memory

The hippocampus has been recognized as playing a vital role in formation of declarative memory in particular, which describes the synthesis of episodic and semantic memories. Bilateral hippocampal removal as a treatment for epilepsy suffered by patient H.M., resulted in anterograde amnesia (Lynch, 2004). This indicates the importance of the role of the hippocampus and temporal lobe structures in memory.

Hippocampus-neocortical connections are crucial for the processing of information in the brain, therefore it has been studied with great interest. It is known that the subiculum receives positional, directional, sensory, and contextual information. Studies have shown that lesions of this area lead to deficits in certain forms of learning. Current evidence suggests that positional information relies on hippocampal-subicular interaction, directional information on the interaction between postsubiculum and subiculum, and sensory information on the interaction between entorhinal cortex and subiculum (Lynch, 2004).

While recognizing the primary role of the hippocampus in memory formation, the interaction with cortical structures, particularly in the context of long-term storage of memories, remains an issue of debate, and it has been proposed that sequential activation of the hippocampus and neocortex may be involved in consolidation of memory. One proposal is that although the hippocampus may be largely responsible for recall of recent memories, the neocortex is primarily concerned with recall of more remote memories (Lynch, 2004). This idea is linked with the view that the hippocampus allows for rapid learning, permitting the neocortex to undergo synaptic changes required for slow learning. One prediction emanating from the hypothesis that hippocampus and cortex are responsible for maintenance of short- and long-term storage of memory, respectively, is that recall of distant memories would be independent of the hippocampus and, consistent with this, it has been reported that remote childhood memories and general knowledge were not affected in individuals with hippocampal damage. However, data from a recent systematic study on individuals with lesions of the hippocampus, in some cases extending to the temporal cortex, revealed that the extent of the lesion (from that affecting only the CA1, CA3, and dentate gyrus to that involving the entire hippocampal complex and temporal lobe) dictated the degree of impairment in recall and, to some extent, the remoteness of the memory. The development of neuroimaging techniques has allowed further assessment of the role of the hippocampal complex in retrieval of distant memories, and the evidence suggests that activation of hippocampal circuits occurs even when very remote memories are elicited (Scoville and Milner, 2000).

Analysis of this question in animals has revealed that sectioning the fornix, or damaging the hippocampus or entorhinal cortex, typically impaired very recent memory, but generally spared more remote memory. This suggests that the hippocampus is necessary for memory storage and retrieval for only a limited time after learning and that time-related modification of cortical connections allows for memory retrieval independent of the hippocampus (Schenk and Morris, 1985). However, it has been pointed out that this might also be explained if representation of older memories was more diffusely distributed in hippocampus. In this case, temporally graded retrograde amnesia could be explained because a partial lesion of the hippocampus will spare a

remote memory more than a recent memory, whereas complete hippocampal lesions will affect recent and remote memories equally (O'Mara et al., 2000).

It is appropriate to state that while great emphasis has been placed on the role of the hippocampus in spatial memory, a number of studies have identified its importance in nonspatial memory tasks. For instance, using social transmission of food preference, Clark and colleagues (Squire, 1992) reported the lesions of the hippocampus and subiculum resulted in anterograde amnesia and temporally graded retrograde amnesia.

3.2. Long-term potentiation as a possible model of learning and memory

The first full description of LTP by Bliss and Lomo in 1973 (Nadel et al., 2000) reported that trains of high-frequency stimulation to the rabbit perforant path caused a sustained increase in efficiency of synaptic transmission in the granule cells of the dentate gyrus. This report, and others which followed during the 1970s, confirmed the Hebbian nature of this form of synaptic plasticity, and it was immediately recognized that the synaptic changes that underpin certain forms of learning and memory might be similar to those upon which expression of LTP relied.

The four well-described characteristics of LTP, cooperativity, associativity, input specificity (Squire and Alvarez, 1995), and the durability (Nadel and Moscovitch, 1997), have been identified as solid arguments that support the hypothesis that LTP may be a biological substrate for at least some forms of memory. Several other pieces of evidence have consolidated this view. *1*) LTP is most easily demonstrable in the hippocampus, an area of the brain known to be fundamentally important in memory acquisition. *2*) Rhythmic bursts of activity that induce LTP mimic naturally occurring theta rhythm recorded in the hippocampus during exploratory behavior (Diamond et al., 1988;Greenstein et al., 1988;Rose and Dunwiddie, 1986). *3*) Inhibitors of hippocampal LTP also block hippocampal learning and retention of tasks (Rose and Dunwiddie, 1986). *4*) Several biochemical changes that occur after induction of LTP also occur during memory acquisition. However, a definitive demonstration indicating that memory consolidation requires induction of changes that resemble those necessary for induction of LTP remains elusive. Similarly, it remains to be clearly shown that induction of LTP will result in some form of memory consolidation.

It has been established that the majority of synapses, which support LTP, in hippocampus and elsewhere, do so in an NMDA receptor-dependent fashion. Indeed LTP, that has been most extensively studied in CA1 region of the hippocamal formation and in dentate gyrus is in both regions believed to be induced by Ca^{2+} influx through postsynaptic NMDA channels (Errington et al., 1987;Malenka et al., 1989). But while the resultant increase in postsynaptic calcium concentration was both necessary and sufficient for expression of LTP, NMDA receptor

activation, although required in many cases, was not sufficient to result in its induction (Errington et al., 1987).

There is an interesting parallel between memory and LTP, since it has been revealed that LTP consists of distinct phases involving different molecular mechanisms. The early phase (E-LTP), which lasts 2–3 h, is independent of protein synthesis, while more persistent long-lasting LTP (L-LTP), which lasts several hours in vitro and weeks in vivo, requires synthesis of new proteins (Lynch, 2004).

3.3. Mechanisms underlying long-term potentiation

The critical event leading to induction of LTP appears to be the influx of calcium ions into the postsynaptic spine and therefore, it is agreed that elevation of postsynaptic calcium concentration is both, necessary and sufficient for the induction of hippocampal LTP (Lynch, 2004). With the exception of mossy fiber-CA3 synapses, induction of LTP in all major excitatory connections on principal neurons of the hippocampus is NMDA dependent, although it has been shown that LTP in CA1 can be induced without the participation of NMDA receptors; in this case, the increase in postsynaptic calcium concentration is a consequence of activation of voltage-operated calcium channels, and therefore, calcium channel inhibitors suppress this form of LTP (Grover and Teyler, 1990).

NMDA activation alone does not induce LTP (Kauer et al., 1988). This observation, together with the demonstration that thapsigargin, which depletes intracellular calcium stores, inhibits LTP (Bortolotto and Collingridge, 1993), suggests that calcium release from intracellular stores augments NMDA receptor-mediated calcium influx.

A lot of work has been done to identify the signalling pathways involved in LTP. For several years a great debate continued about whether changes occurred presynaptically, postsynaptically, or both. Most likely, the changes occur on both sides of the synapse and the proportion of pre- versus postsynaptic changes depends on the type of the synapse and LTP induction protocol. Among those events, that take place presynaptically one should mention increased CaMKII phosphorylation of synapsin I (Fukunaga et al., 1996;Nayak et al., 1996) and MAP2 (Fukunaga et al., 1996); presynaptic activation of PKA (Tong et al., 1996), increased phosphorylation of synaptophisin, PLC-γ, TrkA, TrkB (Gooney and Lynch, 2001;McGahon and Lynch, 1998;Mullany and Lynch, 1998); presynaptic activation of ERK (Gooney et al., 2002;McGahon et al., 1999a) which also modulates LTP-associated transmitter release (Casey et al., 2002;Gooney and Lynch, 2001); presynaptic activation of CREB (Gooney and Lynch, 2001); activation of PI 3-K (Kelly and Lynch, 2000); phosphorylation of PKC substrates (Meberg et al., 1995;Ramakers et al., 1997); synthesis of different presynaptic proteins including

synaptic vesicle proteins (Casey et al., 2002;Kelly et al., 2000b;Lynch et al., 1994), and presynaptic morphological changes (Applegate et al., 1987;Buchs and Muller, 1996;Meshul and Hopkins, 1990).

At the postsynaptic part mostly the same substrates are involved in induction and maintenance of LTP and similarly to the presynaptic area LTP induces postsynaptic protein synthesis (Nayak et al., 1998;Ouyang et al., 1999) and postsynaptic morphological changes (Buchs and Muller, 1996;Desmond and Levy, 1988;Fifkova and Van Harreveld, 1977;Schuster et al., 1990).

3.3.1. NMDA receptors and long-term potentiation

Since many studies showed the importance of NMDA receptors for LTP, a lot of groups have started detailed analyses of the function of NMDA receptors regarding synaptic plasticity. Analysis of the subunit composition of the NMDA receptor has revealed differential expression of NR1 and NR2 with brain area, development, and activity (Seeburg, 1993;Watanabe et al., 1992), and gene targeting has allowed examination of some of the physiological roles of the different subunits. Both hippocampal LTP and spatial learning rely on expression of NR2A, disruption of this subunit is associated with deficits in both (Kiyama et al., 1998;Sakimura et al., 1995). Deletion of the gene encoding NR2B also resulted in impairment of LTP in hippocampus as well as impairment in development of the barrel organ in the trigeminal complex (Kutsuwada et al., 1996;Li et al., 1994). In addition to the effects of disruption of NR2 subunits, genetic disruption of the NR1 subunit also leads to impairments in LTP and spatial learning (Tsien et al., 1996a;Tsien et al., 1996b). Conversely, overexpression of the NR2B subunit was found to be associated with enhanced LTP and enhanced learning and memory (Tang et al., 1999). Analysis of the dynamics of different NMDA receptor subunits has revealed that visual experience results in insertion of new receptors with a higher proportion of NR2A subunits, resulting in an increase in the ratio between NR2A and NR2B (Quinlan et al., 1999). One consequence of this is that NMDA receptor-associated currents are shortened and, therefore, conditions will favour induction of LTD rather than LTP; this is consistent with the idea that an LTD-LTP modification threshold monitors plasticity and that this threshold alters with maturity (Bear, 1996).

Signaling events following NMDA receptor activation

When it was established that increased calcium concentration in the postsynaptic cell, as a consequence of NMDA receptor activation, was a critical factor in the induction of LTP, attention turned to analysis of the downstream cellular consequences of this increase. Among the early findings was that postsynaptic entry of calcium led to activation of calmodulin kinase II

(CaMKII); this observation turned out to be a finding of major importance. CaMKII is one of the most abundant proteins in neurons comprising 1–2% of the total. Although it is expressed presynaptically and postsynaptically, its expression is particularly high in the postsynaptic density, where it is ideally located to respond to changes in calcium concentration. There are more than 30 isoforms of CaMKII and numerous substrates, many of which are located in the postsynaptic density (Fink and Meyer, 2002). CaMKII appears likely to be a mediator of primary importance in linking transient calcium signals to neuronal plasticity (Malenka et al., 1989;Malinow et al., 1989).

Among the consequence of the increase in intracellular Ca^{2+} concentration ($[Ca^{2+}]_i$) is increased CaMKII activity which exerts multiple actions. One significant effect is increased AMPA conductance as a result of AMPA receptor (AMPA-R) phosphorylation and increased recycling of AMPA-R, which is due to CaMKII-induced changes in cytoskeletal proteins (Lynch, 2004).

3.3.2. Metabotropic glutamatergic receptors and LTP

The first indication of a possible role for metabotropic glutamate receptors in LTP was in 1991 with the observation that the nonselective mGluR agonist 1-amino-1,3-cyclopentanedicarboxylic acid (ACPD) enhanced LTP (McGuinness et al., 1991) these findings were subsequently replicated by other groups too. ACPD was later shown to induce a long-lasting potentiation of the synaptic response in CA1 (Bortolotto et al., 1994;Bortolotto and Collingridge, 1993;Chinestra et al., 1993;Manahan-Vaughan, 1997) and in the dentate gyrus (O'Connor et al., 1995), and the effect was shown to rely on calcium-dependent changes and on activation of protein kinase C (PKC), since it was prevented by thapsigargin and staurosporine (Bortolotto and Collingridge, 1998). mGluR activation has a modulatory effect on LTP, since mutant mice lacking mGluR5 have been reported to show attenuated LTP induction in CA1 and dentate gyrus, but at the same time LTP in mossy fiber-CA3 synapses was spared (Lu et al., 1997). It was subsequently shown that potentiation of the NMDA response was absent in mGluR5 mutant mice but that potentiation of the AMPA response was preserved (Jia et al., 1998). These findings led the authors to conclude that activation of mGluR5 plays a pivotal role in expression of NMDA receptor-dependent LTP.

3.3.3. Voltage-dependent Ca^{2+} channels and LTP

There are two major routes of Ca^{2+} influx that can induce LTP on principal neurons, one via NMDA receptors and the other through voltage-dependent Ca^{2+} channels (VDCC).

VDCCs are divided in two main groups, high voltage-activated (HVA) and low voltage-activated (LVA) channels. Among HVA channels are L, P/Q (which at one time was proposed to be distinct entities, but now they appear to be extremes of continuum, resulting from alternative splicing of a single gene), N and R and LVA includes T channels (Jones, 2003). L-VDCCs are composed of three to four subunits: the pore-forming $\alpha 1$ subunit and auxiliary ß, $\alpha 2\delta$ and γ subunits (Figure 5).

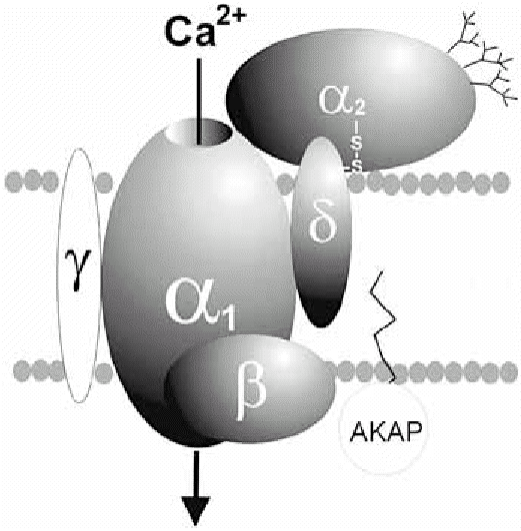

Figure 5. Subunit composition of VDCCs and functions of subunits.

$\alpha 1$ *(ten genes)*
pore formation and voltage sensor;
binding site for the most agonists/antagonists
ß *(four genes, two are expressed in the brain)*
cell surface delivery of the channel;
setting of proper kinetics of activation/inactivation; improved voltage dependence of pore opening
$\alpha 2$, δ *(four genes, disulfide linked, glycosylated)*
functional channel assembly; cell surface delivery of the channel; voltage dependence and kinetics; current amplitude
γ *(eight genes, four of them stargazin-isoforms)*
stabilizes inactivated state

It has been shown that K^+ channel blocker tetraethilammonium chloride (TEA) is able to induce LTP that according to some studies does not depend on the NMDA receptor activation (Aniksztejn and Ben Ari, 1991) and is blocked by L-type voltage-dependent Ca^{2+} channel (VDCC) antagonist or postsynaptic injection of a Ca^{2+} chelator (Aniksztejn and Ben Ari, 1991;Huang and Malenka, 1993).

High frequency stimulation at 100 Hz of CA3-CA1 synapses induces LTP, which is related to postsynaptic Ca^{2+} increase by the activation of NMDA receptors (Collingridge et al., 1983), but 200 Hz stimulation causes long-term potentiation that is based on voltage-dependent Ca^{2+} channels (Grover and Teyler, 1990).

Some time ago it was thought that, in contrast to NMDA receptor mediated Ca^{2+} increase that is localized in dendritic spines, VDCCs were mostly concentrated on the soma and proximal dendrites and mediated Ca^{2+} increase in dendritic shafts (Muller and Connor, 1991). More recent studies showed that they are present in dendritic spines as well (Carter et al., 2004; Lee et al., 2002).

3.3.4. AMPA receptors and LTP

AMPA receptors are supposed to play an important role in synaptic plasticity. The importance of AMPA receptors in fast excitatory synaptic transmission has been acknowledged for decades, and because of this, it has been recognized that modulation of AMPA receptor activity could significantly contribute to expression of LTP. The production of mutant mice expressing different receptor subunits provided some insight into the role of AMPA receptors, particularly in relation to control of calcium fluxes and induction of LTP. Calcium entry is modulated by the GluR2 subunit of the AMPA receptor; specifically, high expression of GluR2 mRNA has been correlated with low calcium entry (Gashler and Sukhatme, 1995). Predictably, AMPA receptors assembled from GluR2 subunits, in contrast to those assembled from GluR1, GluR3, or GluR4 subunits, are impermeable to calcium ions (Gashler and Sukhatme, 1995). Thus, AMPA receptor-associated calcium permeability is low in pyramidal and granule cells of the hippocampus where there is a relatively high expression of GluR2-containing AMPA receptors. LTP was found to be enhanced in GluR2 mutant mice (Jia et al., 1996), whereas it was markedly attenuated in mice lacking the GluR1 subunit (Morales and Goda, 1999).

A great deal of evidence has suggested that increased expression of AMPA receptors on the postsynaptic membrane is likely to be the important requirement for expression of LTP. The primary work leading to the development of the so-called silent synapse theory of LTP was initiated with the recognition that certain synapses were functionally silent because of a lack of AMPA receptors, although NMDA receptors were present (Isaac et al., 1995;Liao et al., 1995). Thus, when single connections between CA3 axons and CA1 pyramidal cells were assessed, only NMDA receptor-generated excitatory postsynaptic currents (EPSCs) could be elicited in a proportion of CA1 pyramidal cells; however, stimulus paradigms that induced LTP resulted in the recruitment of AMPA receptor-generated responses (Isaac et al., 1995;Liao et al., 1995). This was interpreted as evidence that AMPA receptors were inserted into the postsynaptic membrane after induction of LTP. Since then, a great deal of evidence has been accumulated indicating that AMPA receptor expression on cells is a dynamic process and is controlled by a cycle of exocytosis and endocytosis (Luscher and Frerking, 2001;Malinow and Malenka, 2002).

Recently it has been shown that GluR2/GluR3 heteromeric receptors are inserted at the synapse during basal synaptic activity where they can interact with either GRIP/ABP (glutamate receptor-interacting protein/AMPA-binding protein), which stabilizes them at the synaptic surface for some time, or with PICK1 (PKC-interacting protein 1), which primes them for endocytosis. The equilibrium between GluR2-GRIP/ABP and GluR2-PICK1 binding primarily determines the steady-state number of synaptic AMPA-Rs. GluR2S880 (The glutamate receptor

subunit 2 PDZ ligand domain serine 880 (S880)) phosphorylation (P) prevents interaction of the receptor with GRIP/ABP, so that the formation of GluR2-PICK1 complexes is facilitated and endocytosis of the receptor is accelerated. As a result, the number of synaptic AMPA-Rs and synaptic transmission is depressed. Maintenance of the depression may be mediated by removal of GRIP/ABP anchoring sites from the synapse. Phosphorylated receptors could also be sorted into a nonrecycling compartment and/or degraded (Figure 6) (Seidenman et al., 2003).

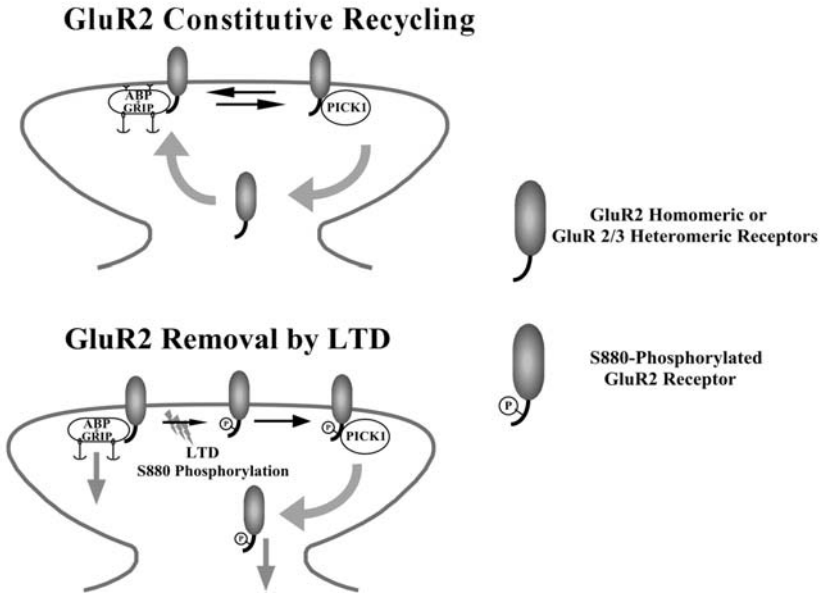

Figure 6. Model of GluR2/GluR3 heteromeric receptor trafficking during basal synaptic activity and after LTD induction. ABP, AMPA-binding protein; GRIP, glutamate receptor-interacting protein; PICK1, PKC-interacting protein 1.

3.4. Age and long-term potentiation

Among those factors that show some correlation with LTP one should mention age (Barnes, 1979;Barnes and McNaughton, 1985;Landfield et al., 1978b;Landfield et al., 1978a;Lynch and Voss, 1994;McGahon et al., 1997;Murray and Lynch, 1998a;Murray and Lynch, 1998b;Toledo-Morrell and Morrell, 1985). Several groups have reported that induction of LTP is dependent on development. Neonatal rats, up to postnatal day 8, are incapable of sustaining LTP, but this inability disappears shortly afterwards (Baudry et al., 1981;Bronzino et al., 1994;Durand et al., 1996). In an interesting parallel it has been established that silent synapses demonstrate a developmental profile; thus the number of synapses expressing NMDA, but not AMPA, receptors in the hippocampus decreases with age (Liao et al., 1999). During the so-called critical period, many thalamocortical synapses exhibit NMDA-, but no detectable

AMPA-generated, receptor currents, suggesting the presence of functionally silent receptors. It has been proposed that LTP may lead to conversion of thalamocortical synapses from silent to functional and that is fundamental in modulation of experience-dependent changes in thalamocortical circuits (Feldman et al., 1999;Isaac et al., 1997).

Clearly, one of the major goals in neuroscience is to identify the underlying cause of the age-related deficit in LTP, but this is not trivial given the array of changes that have been documented in the aged brain. Data from several experiments have indicated that the age-related decrease in LTP is coupled with a decrease in depolarization-induced glutamate release, which is mainly related to increase in Ca^{2+} currents and activation of Ca^{2+} dependent K^{+} channels (Lynch and Voss, 1994;McGahon et al., 1997;McGahon et al., 1999a;McGahon et al., 1999b; McGahon et al., 1999c; McGahon et al., 1999d).

Because the more persistent components of LTP rely on protein synthesis and probably morphological changes, it is significant that an age-related decrease in protein synthesis has been reported (Goldspink, 1988;Kelly et al., 2000a;Mullany and Lynch, 1997) and this has been identified as a possible factor that contributes to the decrease in neuronal density (McLay et al., 1999). In addition, while LTP has been associated with an increase in the number of non-perforated synapses (Geinisman et al., 1991), aging is associated with a reduced number of such connections (Geinisman et al., 1986). The number of synaptic contacts per neuron is reduced in aged, compared with young, animals (Geinisman et al., 1993), also a decrease in synapses with multiple, completely partitioned, transmission zones was observed in aged rats that exhibited impaired LTP (Geinisman et al., 1994).

V. The aim of the study

The aim of the study is to identify excitatory synapses in the hippocampus and dentate gyrus, in which expression of cell adhesion molecules L1 and CHL1 influences basal synaptic transmission and/or synaptic plasticity and investigate the underlying mechanisms.

To reach this aim, extracellular recordings in acute hippocampal slices prepared from L1 conditional and CHL1 constitutive knockout mice and corresponding wild-types have been performed in order to reveal genotype-specific changes in physiological parameters, such as amplitude of field excitatory postsynaptic potentials, paired-pulse facilitation, post-tetanic or short-term potentiation, and LTP. Field potentials and synaptic currents have been recorded from synapses formed by (1) Schaffer collateral projections to the CA1 field; (2) lateral perforant path (LPP) and (3) medial perforant path (MPP) projections to the dentate gyrus; (4) direct perforant path projections to the CA3 and (5) CA1 fields; and (6) associational/commissural and (7) mossy fiber projections to the CA3 field. In addition, to investigate the influence of L1 on L-type voltage-dependent Ca^{2+} channels, patch-clamp recordings of Ca^{2+} channel transfected CHO cells have been used.

VI. Materials and methods

1. Animals

To investigate the influence of L1 and CHL1 on synaptic transmission and plasticity in major excitatory hippocampal pathways, we used L1 conditional and CHL1 constitutive knockout mice *(Mus musculus* L., 1758*)* and corresponding wild types. Animals were bred in the specific pathogen-free utility. All treatments were performed in accordance to the German law for protection of experimental animals.

CHL1-deficient (CHL1-/-) and corresponding wild type (CHL1+/+) mice (129Ola-C57BL/6J genetic background (Montag-Sallaz et al. 2002) were used at ages of 1, 2, 3 and 9 months.

L1 conditional knockouts and corresponding wild types were studied at the age of 3-4 months. To generate conditional L1 deficient mice (Law et al., 2003), homozygous L1-floxed females were crossed with transgenic males (on the C57BL/6J genotype backgound) that express cre-recombinase under the control of the calcium/calmodulin-dependent kinase II subunit of the CaMKII promoter (kindly provided by Dr. Günther Schütz, German Cancer Research Center, Heidelberg, Germany). All resulting male progeny were homozygous for the L1-floxed allele, among which 50% carried the CAMKII-cre transgene (designated L1fy+) and 50% did not (designated L1fy-). These mice have a mixed 129/Sv and C57BL/6J genetic background (four back crossings into the C57BL/6J strain). Specificity and efficiency of cre-mediated L1 disruption were assayed by Western blot analysis of homogenates isolated from different parts of the brain, including hippocampus. At postnatal day (P) 7, there was no difference between the genotypes in L1 expression in hippocampus, but significant reduction was observed at P22. A further reduction of L1 expression to undetectable levels was found in the hippocampus of L1fy+ mice at P49 and P126. No L1 immunoreactivity was observed that could represent truncated L1 protein fragments, indicating a complete inactivation of the L1 gene in the hippocampus of L1fy+ mutant mice. L1 levels were also examined immunohistochemicaly in 6-month-old mice. Coronal sections of the whole brain stained with two different polyclonal antibodies against L1 showed a strong reduction in the amount of L1 immunoreactivity in the hippocampus, cerebral cortex and striatum. L1fy+ mice are normal in body weight and gross behavior and reproduce according to Mendelian ratios (Law et al., 2003).

2. *Preparation of hippocampal slices*

Hippocampal slices were prepared from mice, which have been anesthetized by CO_2 and fast decapitated in ice-cold dissection artificial cerebrospinal fluid (composition of all artificial cerebrospinal fluids used are shown in tables bellow). After decapitation, brain was removed and cut in two hemispheres. Depending on the projections, which were supposed to be investigated, hemispheres were cut with a Vibroslice (Leica, Germany) either transversally, for CA3-CA1; commissural/associational-CA3 and perforant path-dentate gyrus synapses or horizontally for perforant path projections to the CA1 and CA3 fields. Based on the characteristics of mossy fiber projections, horizontal slices for mossy fiber-CA3 recordings were cut with an angle of $15\text{-}30^0$ (Eckhardt et al., 2000). All procedures during slice preparations took place in ice-cold dissection artificial cerebrospinal fluid, which in case of mossy fibers contained less Ca^{2+} to reduce excitotoxicity.

After 350μm slices were cut, they were kept at room temperature in a large chamber (500 ml) filled with carbogen-bubbled artificial cerebrospinal fluid (ACSF). Recording of field excitatory post-synaptic potentials (fEPSP) were started two hours after slice preparations. In the recording chamber, slices were continuously superfused with carbogen-bubbled ACSF (2-3 ml/min). Chamber and recording solutions in contrast to dissection one, contained 125 mM NaCl instead of 250 mM sucrose.

Table 1. *Composition of dissection ACSF*

Compound	Concentration (g/l)	Molarity (mM)
KCl	0.186	2.5
NaH_2PO_4	0.173	1.25
$NaHCO_3$	2.016	24.0
$MgSO_4$	0.370	1.5
$CaCl_2$	0.294	2.0
Glucose	4.505	2.5
Sucrose	85.575	250

Table 2. *Composition of recording ACSF*

Compound	Concentration (g/l)	Molarity (mM)
NaCl	7.013	120
KCl	0.186	2.5
NaH_2PO_4	0.172	1.25
$NaHCO_3$	2.016	24.0
$MgCl_2$	0.305	1.5
$CaCl_2$	0.294	2.0
Glucose	4.955	27.5

Table 3. *Dissection ACSF for mossy fibers*

Compound	Concentration (g/l)	Molarity (mM)
KCl	0.186	2.5
NaH_2PO_4	0.173	1.25
$NaHCO_3$	2.185	26.0
$MgSO_4$	2.465	10.0
$CaCl_2$	0.074	0.5
Glucose	1.802	10.0
Sucrose	78.729	230

Table 4. *Recording ACSF for mossy fibers*

Compound	Concentration (g/l)	Molarity (mM)
NaCl	7.013	120
KCl	0.186	2.5
NaH_2PO_4	0.172	1.25
$NaHCO_3$	2.016	24.0
$MgCl_2$	0.305	1.5
$CaCl_2$	0.441	2.5
Glucose	4.955	27.5

pH was adjusted to 7.3 with HCl.

3. Recording of field excitatory post-synaptic potentials

Field EPSPs were recorded by glass pipettes filled with ASCF having a resistance of 2-3 MΩ. Stimulation was applied via monopolar stimulating glass electrode with a broken tip and resistance less then 1 MΩ. Basal synaptic transmission was monitored at 0.033 Hz. Responses were amplified and filtered at 1 kHz using CyberAmp 320 (Axon Instruments, Foster City, CA). Data acquisition and analysis were performed using the Pulse program (Heka Electronik, Lambrecht/Pfalz, Germany).

Amplitude of responses was measured as a function of intensity of stimulation and stimulus-response curves in individual experiments were determined with an accuracy of 10 or 20 μA.

Paired-pulse facilitation (PPF) was defined as A2/A1x100%, where A1 and A2 are the amplitudes of the fEPSPs evoked by the first and second pulses, respectively. For most of projections we checked PPF with 10, 20, 50, 100 and 200 ms interstimulus intervals. Examples of PPF with different interstimulus intervals are shown on Figure 7.

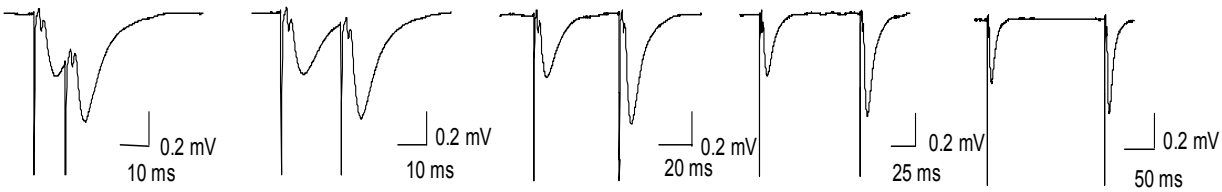

Figure 7. Paired-pulse facilitation of CA3-CA1 responses with 10, 20, 50, 100 and 200 ms interstimulus intervals.

Long-term potentiation was induced by different numbers of trains of either high frequency stimulation (HFS), which included 100 pulses delivered at 100 Hz, or theta-burst stimulation (TBS) consisting of 10 bursts delivered at 5 Hz. Each burst was composed of four stimuli delivered at 100 Hz. Duration of pulses was 0.2 ms. Patterns of fEPSPs elicited by HFS and TBS are shown bellow.

The mean amplitude of fEPSPs recorded 0-10 min before TBS or HFS was taken as 100 %. The values of LTP were calculated as increase in the mean amplitudes of fEPSPs measured 50-60 min after tetanic stimulation.

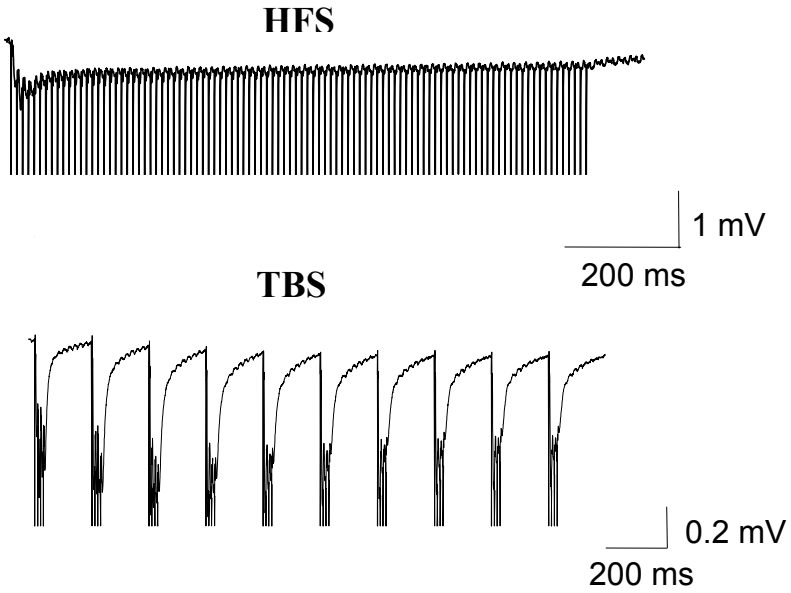

Figure 8. Field EPSPs elicited by high frequency (above) and theta-burst (below) stimulations.

3.1. Field EPSPs at lateral and medial perforant path (LPP and MPP) projections to the dentate gyrus

For recording of LPP-DG responses stimulating and recording electrodes were placed in outer part of molecular layer of the dentate gyrus (Figure 9A). Responses were identified by application of paired-pulse stimulation with 50 ms interstimulus intervals, and those fEPSPs were recorded further, which showed facilitation under such conditions.

In case of MPP-DG fEPSPs, stimulating and recording electrodes were placed in inner part of molecular layer (Figure 9B) and only those responses were recorded further, which exhibited paired-pulse depression.

LTP was induced by 5 trains of HFS with intertrain interval of 20 sec and 100% of stimulation intensity in disinhibited slices (Evers et al., 2002). Disinhibition, which is required to induce LTP in perforant path synapses (Hanse and Gustafsson, 1992) was achieved by application of 100 μM picrotoxin 10 minutes before and during HFS.

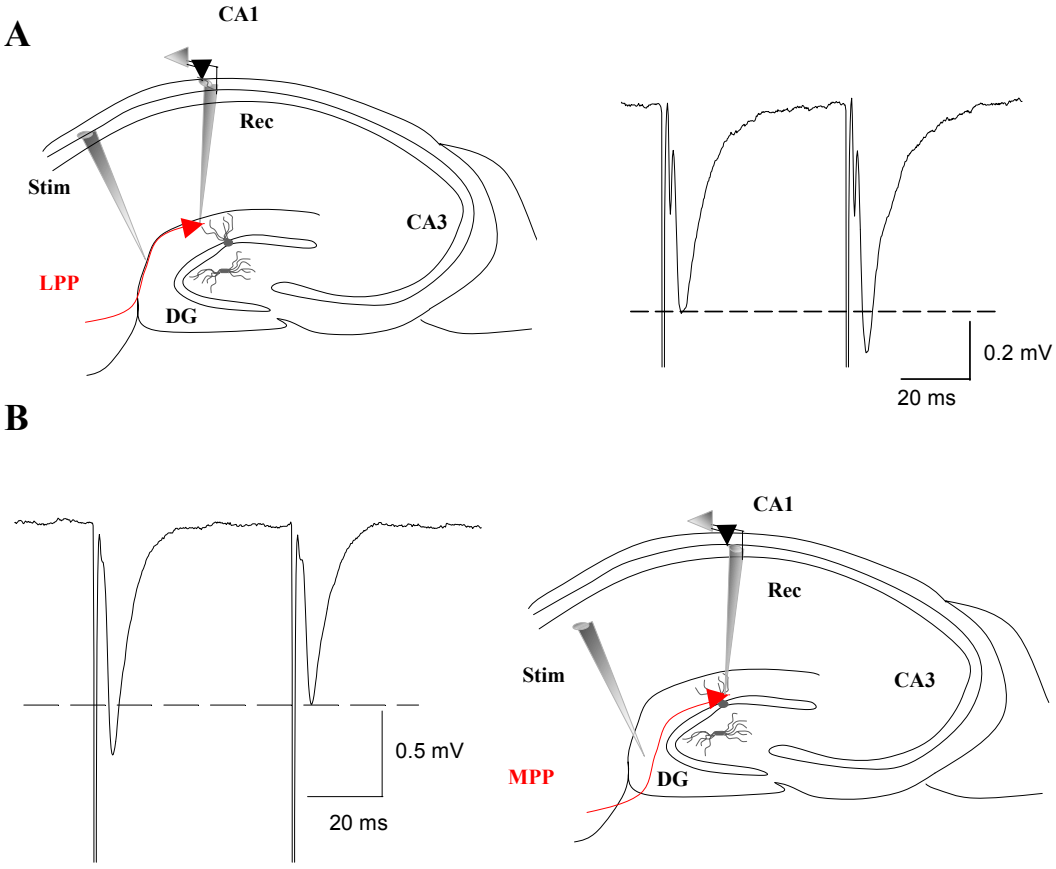

Figure 9. A) Scheme of the hippocampal slice showing location of stimulating and recording electrodes for registration of LPP-DG fEPSPs (left) and paired-pulse facilitation of these responses (right).

B) Scheme of the hippocampal slice showing location of stimulating and recording electrodes for registration of MPP-DG fEPSPs (right) and paired-pulse depression of these responses (left).

3.2. Field EPSPs at mossy fiber projections to the CA3 field

To record mossy fiber responses, we put stimulating electrode in the dentate gyrus near to the internal side of granule cell layer and recording electrode in the str. lucidum of the CA3 field (Figure 10).

Responses were identified by delivering of 0.33 Hz stimulation. Since mossy-fiber responses exhibit facilitation to this stimulation, only those fEPSPs were recorded further which showed frequency-dependent facilitation >150%.

Two trains of HFS were used for induction of LTP, interval between trains was 20 sec (Eckhardt et al., 2000). LTP at this synapse is known to be NMDA receptor-independent, therefore 50 μM APV was applied 15 min before and during HFS. To confirm that the recorded field EPSPs were evoked by the stimulation of mossy fibers and were not contaminated by the associational/commissural pathway, an agonist of metabotropic glutamate receptors, 2 μM DCGIV was applied at the end of each experiment and only responses inhibited by > 80% were assumed to be elicited by mossy fiber stimulation (Cremer et al., 1998).

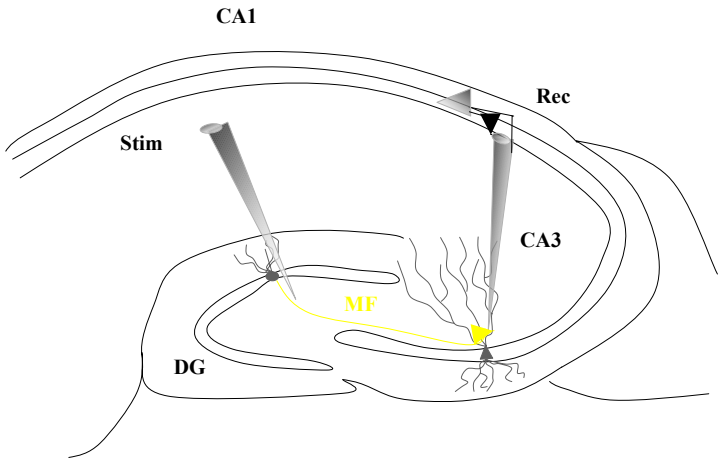

Figure 10. Scheme of the hippocampal slice showing location of stimulating and recording electrodes for registration of mossy fiber-CA3 responses.

3.3. Field EPSPs at associational/commissural projections to the CA3 field

To record associational/commissural-CA3 responses one can put stimulating electrode either in str. radiatum of the CA3 field and thus activate associational fibers directly, or in str. radiatum of the CA1 field and activate Schaffer collaterals, which generate antidromically propagating action potential toward the CA3 region and activate associational projections. In our experiments we used the second approach to avoid direct activation of the local CA3 interneurons. Since associational/commissural-CA3 synapses are located in str. radiatum of the CA3 field, recording electrode was placed in this area (Figure 11).

LTP was induced by two trains of HFS delivered with 20 sec intertrain interval with the stimulation strength being 50% from the supramaximal one (Ito et al., 1997).

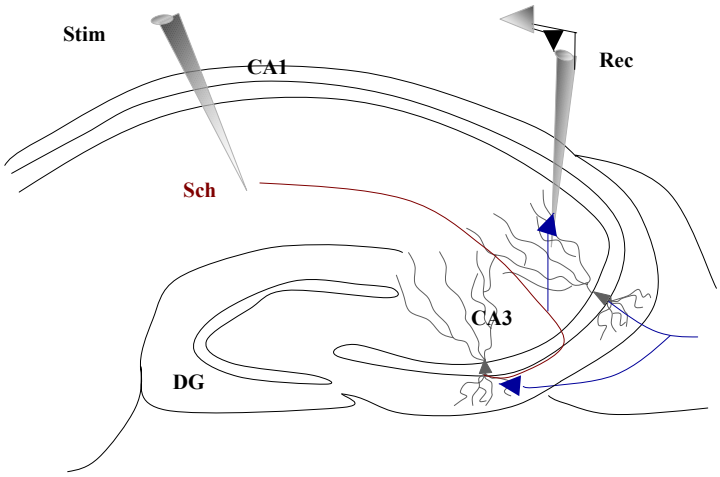

Figure 11. Scheme of the hippocampal slice showing location of stimulating and recording electrodes for registration of associational/commissural-CA3 responses.

3.4. Field EPSPs at Schaffer collateral/commissural projections to the CA1 field

CA3 neurons project to the CA1 area ipsilaterally via Schaffer collaterals and contralaterally via commissural projections. For recording of CA3-CA1 responses we put stimulating and recording electrodes in stratum radiatum of the CA1 region (Figure 12).

For LTP induction we used two patterns of tetanic stimulation. In all 3 month-old animals we used two trains of HFS with 50% of supramaximal stimulation strength (Pozzo-Miller et al., 1999) and in 1, 2 and 9 month-old CHL1 constitutive knockouts and corresponding wild-types we applied five times TBS with the stimulation strength being 50% from the supramaximal one (Muller at al., 1996; Eckhardt et al., 2000).

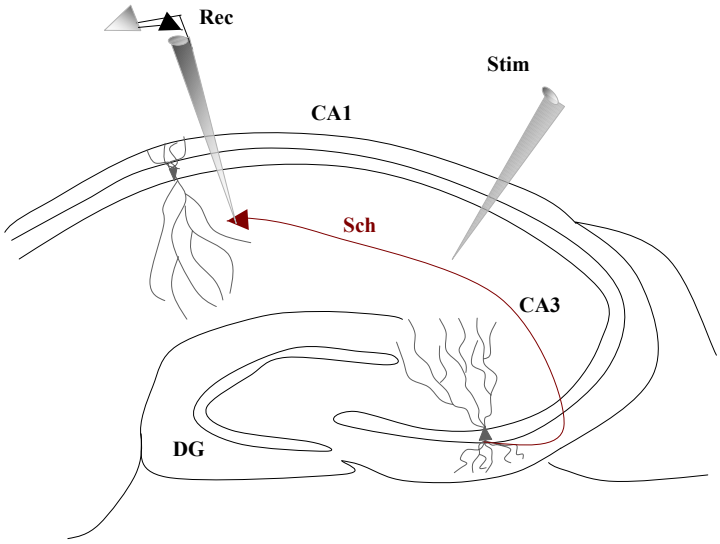

Figure 12. Scheme of the hippocampal slice showing location of stimulating and recording electrodes for registration of CA3-CA1 responses.

3.5. Field EPSPs at direct perforant path projections to the CA1 field

To record fEPSP at direct perforant path-CA1 synapses we put stimulating and recording electrodes in stratum lacunosum-moleculare of the CA1 field. Stimulating electrode was as close as possible to the subiculum. Since there is a high possibility to activate perforant path fibers projecting to the dentate gyrus, and therefore cause polysynaptic activation of CA1 neurons, we cut slices with help of glass pipette through the dentate gyrus and along the border between the CA1 and CA3 regions (Fugure 13) (Remondes and Schuman 2003).

LTP was induced by two trains of the HFS delivered with 100% stimulation intensity in disinhibited slices. For disinhibition, 100μM picrotoxin was washed in the slice 10 min before and during HFS.

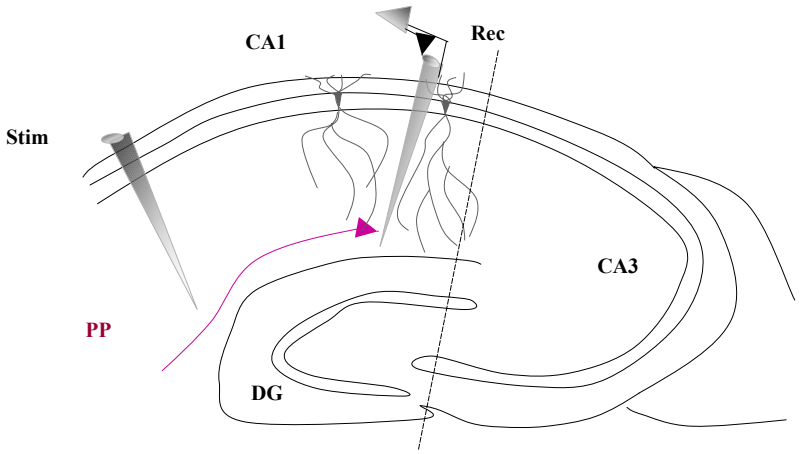

Figure 13. Scheme of the hippocampal slice showing location of stimulating and recording electrodes for registration of direct perforant path responses in the CA1 field. Dashed line shows the area of cutting.

3.6. Field EPSPs at direct perforant path projections to the CA3 field

For recording of direct perforant path-CA3 responses stimulating electrode was placed in str. lacunosum-moleculare of the CA1 field near to the subiculum and recording electrode in the str. lacunosum-moleculare of the CA3. To avoid disynaptic activation of the CA3 pyramidal neurons slices were cut with glass electrode through the dentate gyrus (Figure 14) (Berzhanskaya et al., 1998).

Long-term potentiation was induced by two trains of the HFS delivered with 100% of stimulation intensity. Slices were disinhibited with 100μM picrotoxin.

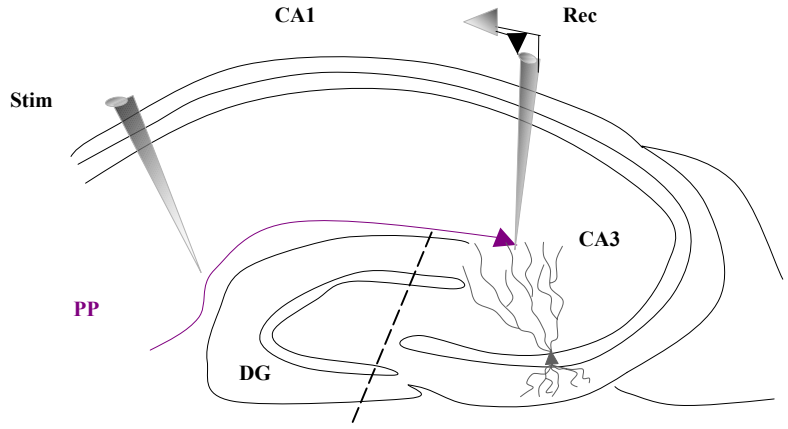

Figure 14. Scheme of the hippocampal slice showing location of stimulating and recording electrodes for registration of direct perforant path responses to the CA3 field. Dashed line shows the area of cutting.

Table 5. *The protocols used for induction of LTP in different synapses.*

Axonal Projections	Postsynaptic area	Pattern of stimulation	Stimulation strength	Pharmacology
Perforant path	DG,	5xHFS	100%	Picrotoxin
Perforant path	CA1, CA3	2 xHFS	100%	Picrotoxin
Mossy fibers	CA3	2xHFS	To elicit 40-60 μV responses	APV
CA3	CA1	5xTBS 2xHFS	50% 50%	No
CA3	CA3	2xHFS	50%	No

4. Patch-Clamp recording of L-VDCC currents

A standard patch-clamp technique (Hamill et al., 1981) was used to record macroscopic L-VDCC currents from transfected CHO cells. Whole-cell voltage clamp recordings were performed using an EPC-8 amplifier (Heka Electronik, Lambrecht Germany). Data acquisition and analysis were performed using the Pulse program (Heka Electronik, Lambrecht/Pfalz, Germany).

The measurements were carried out at room temperature, in extracellular solution, composition of which is shown in Table 6. Cells were clamped under upright microscope OLYMPUS BX50WI. Glass pipettes were filled with intracellular solution (see Table 7) and had a resistance of 3-5 MΩ. The voltage of the cell membrane was clamped at -60 mV (holding potential). Capacitive transients were compensated electronically and leak current was subtracted

using the Pulse software. Membrane capacitance was 10-25 pF and the series resistance at the range between 5 and 20 MΩ.

To activate L-VDCCs a series of voltage steps from -50 to +70mV was applied every 2 seconds. The peak (at 15-80 ms time interval) and steady state (at 195-215 ms time interval) current amplitudes were plotted against the voltage of the pulse.

Table 6. *Composition of extracellular solution*

Compound	Concentration (g/l)	Molarity (mM)
HEPES	2.383	10
NaCl	7.012	120
$BaCl_2$	2.638	10.8
$MgCl_2$	0.203	1
CsCl	0.909	5.4
glucose	1.80	10

pH was adjusted to 7.4 with CsOH

Table 7. *Composition of intracellular solution*

Compound	Concentration (mg/ml)	Molarity (mM)
CsCl	20.208	120
$MgCl_2$	0.61	3
HEPES	1.192	5
EGTA	3.804	10
MgATP	2.536	5

pH was adjusted to 7.4 with HCl

4.1. Transfection of CHO cells with L-VDCCs

CHO cells were cultured in Dulbeco's modified Eagle's medium (DMEM) with high glucose concentration (4.5 g/l), which was supplemented with 10% dialyzed fetal bovine serum (FCS), 1% nonessential amino acids (MEM) (100 fold), 1% Na pyruvate, 1% (100 mM), L-Glutamine (200 mM) and 2 % Penicilin/Streptomicin (100 fold) solutions.

Cell passaging was done before 80-90% confluence level was reached. Cells were washed by Hanks balanced salt solution and detached by addition of tripsin – EDTA solution. For electrophysiological recordings, CHO cells were plated onto 22 mm coverslips and used at about 50% confluence.

To study L-type voltage dependent Ca^{2+} channels (L-VDCC), CHO cells were transfected with a pore forming Cav1.2 channel subunit α_1 and two subunits β_1b and $\alpha_2\delta_1$, which are important for cell surface expression of the channel. These three subunits were expressed at the

ratio of 1:1.2:1.2. The vector for α_1 subunit expression was pcDNA3, and for β_1b and $\alpha_2\delta_1$ subunits PMT2 was used. Co-transfection with the green fluorescence protein (GFP) was used for identification of Ca^{2+} channel transfected cells.

The transfection procedure included following steps: 6µl Plus reagent, 0.1-0.5 µg α_1 and 0.12-0.6 µg β_1b and $\alpha_2\delta_1$ subunit DNA and 0.5-1µg GFP was added to 200 µl DMEM without FCS and left for incubation during 15 minutes. After this, the solution was added to 100 µl DMEM with 4 µl Lipofectamin and again left for incubation during 15 minutes. Then this solution was mixed with 700 µl fresh DMEM without FCS and applied to cells in 6-well dish. for 2-3 hours. Before adding the transfection solution to cells, they were washed by medium without FCS. At the end of incubation time, cells were washed and transferred to FCS containing DMEM and kept in incubator until recordings.

5. *Chemicals used*

α_1, β_1b, $\alpha_2\delta_1$, subunits of L-VDCC, a gift from Beth Scharp, Washington

BAY K 8644, L type voltage-gated Ca^{2+} channel agonist, Tocris

$BaCl_2$, Merk

$CaCl_2$, Merck

CsCl, Merk

DCG IV, group II mGluR agonist, Tocris

D/L-APV - D/L-2-Amino-phosphonovalerate, NMDA receptor antagonist, Tocris.

DMEM, Dulbeco's modified Eagle's medium, PAA

EGTA, Ca2+ chelator , PAA

FCS, fetal bovine serum, PAA

GFP , green fluorescence protein, Clontech

Glucose, Fluka

HEPES - N-2-hydroxyethylpiperazine-N'-2-ethanesulfonic acid, pH buffer, PAA

KCl, Merck

L-Glutamine, PAA

MEM, nonessential amino acids, PAA

MgATP, PAA

$MgCl_2$, Merck

$MgSO_4$, Merck

(+)-Muscarine cloride, muscarinic receptor agonist, Sigma

NaCl, Merck

$NaHCO_3$, Merck

NaH_2PO_4, Merck

Na pyruvate, PAA

Nifedipine, L-type voltage gated Ca^{2+} channel antagonist, Tocris

Penicilin/Streptomicin, antibiotics, PAA

Picrotoxin, $GABA_A$ receptor antagonist, Tocris

Sucrose, Fluka

trypsin – EDTA, PAA

6. Statistical analysis

All values are reported as mean ± SEM (standard error of mean). Student's *t* test was used to assess statistical significance using Sigma Plot 8.0 (SPSS, Chicago, IL). Two-way ANOVA (Systat, 9) was used to compare paired-pulse facilitation and stimulus-response curves between genotypes.

VII. Results

1. Analysis of L1 conditional knockout mice and corresponding wild-types

To study the role of conditional ablation of L1 in synaptic transmission and plasticity at major excitatory hippocampal pathways, we decided to investigate all major cortical and the intrinsic hippocampal projections in 3 month-old L1 conditional knockouts and corresponding wild type mice.

Since most of the sensory information which reaches hippocampus enters through the entorhinal cortex via perforant path projections, we started with perforant path synapses onto the dentate gyrus.

1.1. Analysis of perforant path projections to the dentate gyrus

As mentioned above, there are two separate groups of fibers projecting to the dentate gyrus. Lateral perforant pathway, which projects mostly to the distal dendrites of the granule cells, and medial one projecting to the proximal part of these dendrites. In our experiments we analyzed characteristics of basal synaptic transmission, short- and long-term potentiation in synapses formed by both projections.

1.1.1. Analysis of lateral perforant path projections to the dentate gyrus

Lateral perforant path responses in the dentate gyrus were recorded in the outer part of the molecular layer and exhibited paired-pulse facilitation (PPF) with 50 ms interstimulus intervals. It was 119.5±2.0 % for wild-types and 118.8±4.1 % for knockout mice. To evaluate properties of basal synaptic transmission, we analysed a relationship between the amplitude of responses versus intensity of stimulation. As shown on Figure 15A, there was no statistically significant difference between two genotypes in terms of maximal amplitude of responses, which was 1.01±0.03 mV in wild-type animals (L1fy-) and 0.92±0.08 mV in knockouts (L1fy+). Maximal intensity of stimulation required to evoke these responses in L1fy- mice was 96.7±6.9 μA and in L1fy+ animals it was 86.1±5.8 μA. Evaluation of data using ANOVA revealed that there was no statistically significant difference either in terms of amplitude of fEPSPs or intensity of stimulation.

To study characteristics of short and long-term plasticity, 5 trains of high frequency stimulation were applied to disinhibited slices, in which GABAergic transmission was blocked by 100 μM picrotoxin. Short-term potentiation (STP) was 128.06±5.2 % in L1fy- and

142.48±3.62 % in L1fy+ mice. Difference was statistically significant (P<0.05). Long-term potentiation profiles showed very high similarity for both genotypes: in L1fy- mice the mean level of LTP was 122.8±4.8 % and in L1fy+ mice it was 121.7±5.3 % (Figure 15B).

1.1.2. Analysis of medial perforant path projections to the dentate gyrus

Medial perforant path responses in the dentate gyrus were recorded in the inner molecular layer and exhibited paired-pulse depression (PPD) with 50 ms interstimulus intervals. The level of PPD was 80.03±2.3 % in L1fy- mice and 83.2±2.8 % in L1fy+ animals. At the beginning of each experiment we analyzed amplitude of responses as a function of stimulation intensity (Figure 16A). For L1fy- maximal amplitude of fEPSPs was 2.0±0.2 mV and for L1fy+ it was 2.3±0.2 mV. Maximal intensity of stimulation, inducing these fEPSPs was 63.3±6.6 μA in L1fy- and 61.7±4.8 μA in L1fy+ mice. All statistical evaluations showed that there was no difference between genotypes in terms of PPD and basal synaptic transmission.

Five trains of HFS delivered with 100 % of stimulation intensity to disinhibited slices induced similar levels of STP and LTP in both genotypes. For L1fy- mice, the mean value of STP was 129.1±6.8 % and for L1fy+ it was 134.08±5.3 %. The value of LTP for L1fy- was 127.9±5.04 % and for L1fy+ it was 130.7±5.6 % (Figure 16B). The profile of LTP was similar to previously published results in this synapse (Evers at al., 2002).

.

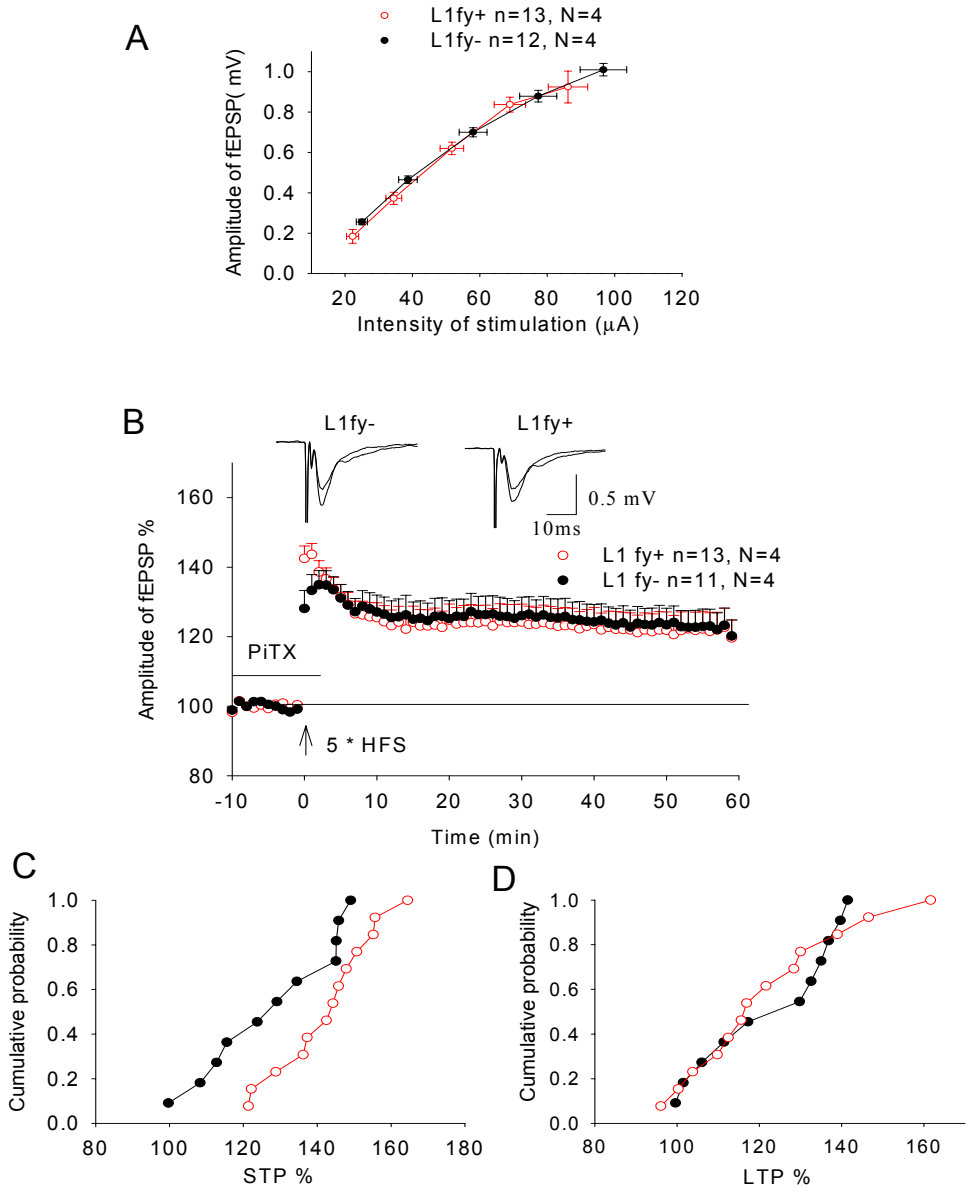

Figure 15. A) Input-output curves for amplitudes of fEPSPs evoked by stimulation of lateral perforant path projections to the dentate gyrus at different stimulation strengths. B) Short- and long-term potentiation induced by 5 trains of HFS. Upper panel shows fEPSPs recorded before and 50-60 min after HFS for both genotypes. C-D) Cumulative plots representing levels of short-term potentiation (STP) measured 1 min after HFS (C) and long-term potentiation (LTP) measured 50-60 min after HFS (D). Each symbol represents a single experiment. Cumulative probability at any given value x is the probability to observe potentiation less or equal to x. N represents the number of tested mice, n is the number of tested slices.

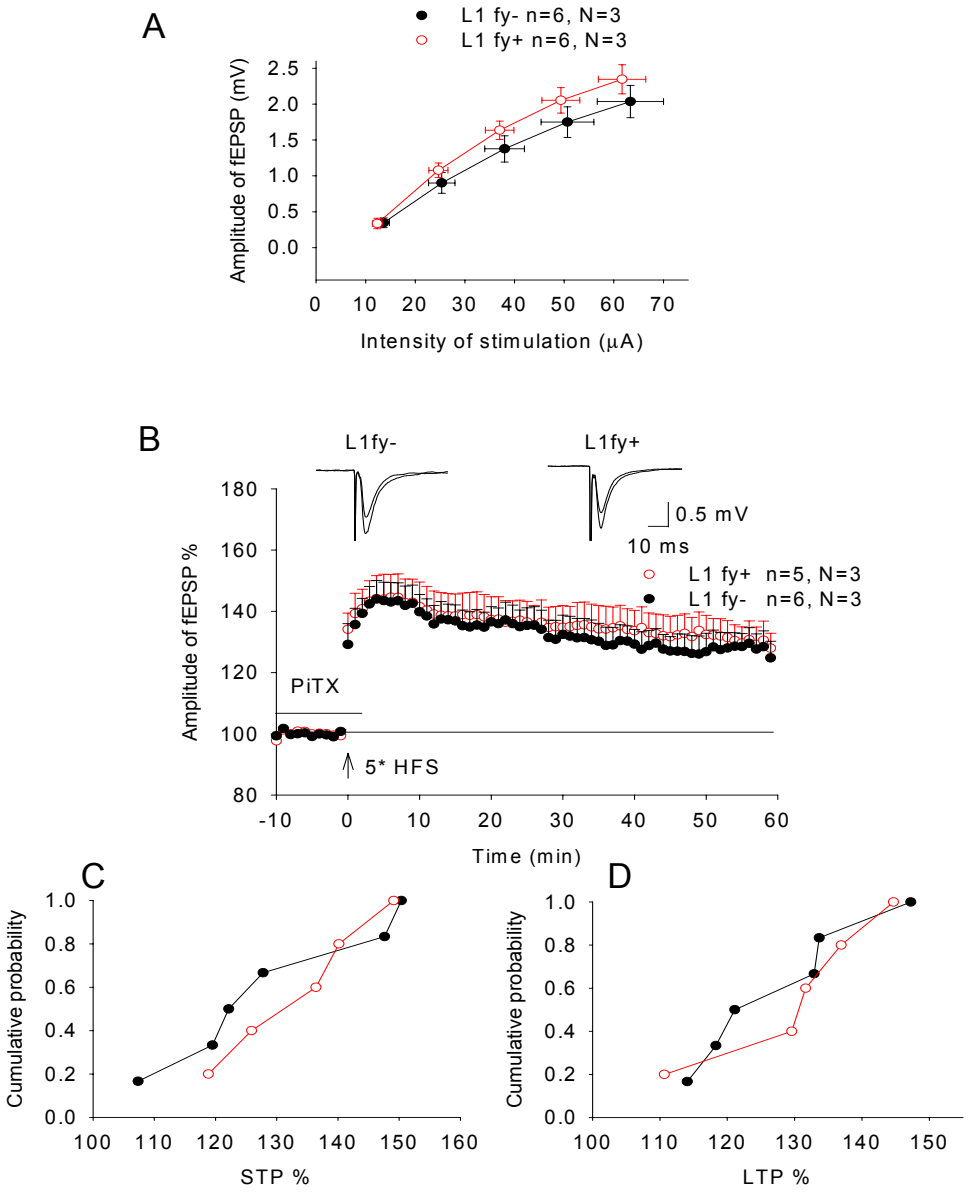

Figure 16. A) Input-output curves for amplitudes of fEPSPs evoked by stimulation of medial perforant path in the dentate gyrus at different stimulation strengths. B) Short- and long-term potentiation induced by 5 trains of HFS. Upper panel shows fEPSPs recorded before and 50-60 min after HFS in both genotypes. C-D) Cumulative plots representing levels of short-term potentiation (STP) measured 1 min after HFS (C) and long-term potentiation (LTP) measured 50-60 min after HFS (D). Each symbol represents a single experiment. Cumulative probability at any given value x is the probability to observe potentiation less or equal to x. N represents the number of tested mice, n is the number of tested slices

1.2. Analysis of mossy fiber projections to the CA3 field

Signal from the dentate gyrus is transferred to the CA3 field via mossy fibers. Mossy fiber responses have very small amplitudes and can be easily contaminated by associational/commissural fEPSPs, but there are certain features, by which rather pure mossy fiber responses can be identified. One of them is frequency-dependent facilitation (Salin et al., 1996) and therefore at the beginning of each experiment we always applied 0.33 Hz stimulation and only those fEPSPs were recorded further, which facilitated under such conditions (Figure 17A). To be sure about purity of recorded responses, at the end of each experiment we always applied 2 μM DCG IV and only those responses were taken into consideration, which were blocked at least by 70-80% (Figure 17B).

Mossy fiber LTP was induced by 2 trains of HFS delivered in the presence of 50 μM APV. Figure 17C shows that there was no statistically significant difference in terms of post-tetanic or long-term potentiation. Mean value of PTP was 792.4±153.2 % in L1fy- and 843.9±158.3 % in L1fy+ mice. The level of LTP in L1fy- animals was 172.8±13.4 % and in L1fy+ mice it was 188.7±10.6 %. The profile and level of LTP at this synapse was similar to that which had been published previously (Eckhardt et al., 2000).

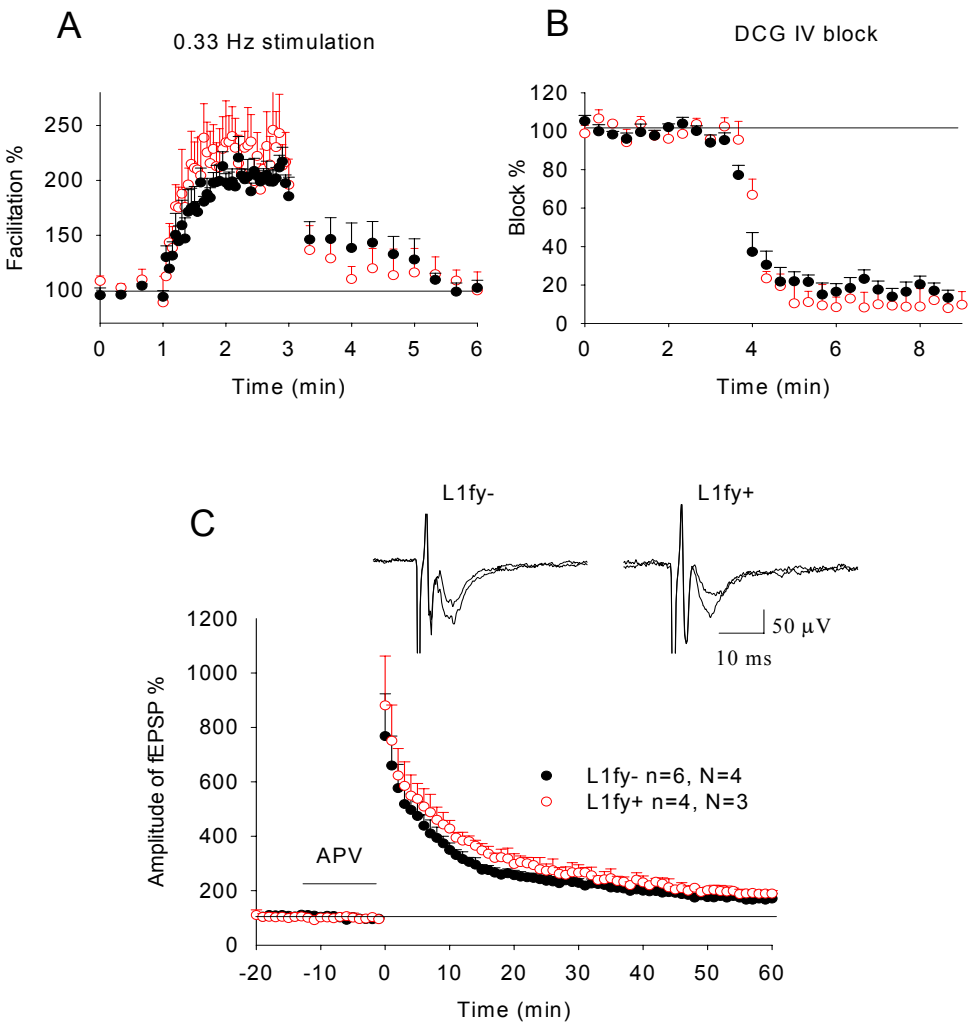

Figure 17. A) Frequency-dependent facilitation of mossy fiber responses by 0.33 Hz stimulation. B) Block of responses with group II mGluR agonist DCG IV. C) Post-tetanic and long-term potentiation induced by 2 trains of HFS in the presence of NMDA receptor antagonist APV. Upper panel shows fEPSPs recorded before and 50-60 min after HFS for both genotypes. N represents number of tested mice; n is number of tested slices.

1.3. Analysis of associational/commissural projections to the CA3 field

After signal enters CA3 field, on the one hand it is sent to the CA1 region via Schaffer collaterals and on the other hand it is additionally processed within the CA3 area by associational-commissural projections.

As Figure 18A shows there was no statistically significant difference in terms of maximal amplitude of fEPSPs between L1 conditional knockout mice and corresponding wild-types. In L1fy+ maximal amplitude of responses was 325.7± 27.1 μV and in L1fy- it was 326.2±28.8 μV. Maximal intensity of stimulation in L1fy+ was 172.2±7.4 μA and in L1fy- it was 194.5±6.3μA. ANOVA showed statistically significant difference in terms of stimulation intensity with $p<0.05$, also multiple comparisons t-test revealed that statistical significance was valid for all tested stimulation intensities with $P<0.05$.

No difference between genotypes was observed for paired-pulse facilitation with 10, 20, 50, 100 and 200 ms interstimulus intervals (Figure 18B).

Neither STP nor LTP showed any impairment in L1fy+ mice. STP in L1fy- animals was 188.1±7.3 % and in L1fy+ mice it was 203.0±13.8%. LTP in L1fy- was 132.7±4.2 % and in knockouts it was 133.5±7.4 % (Figure 18C).

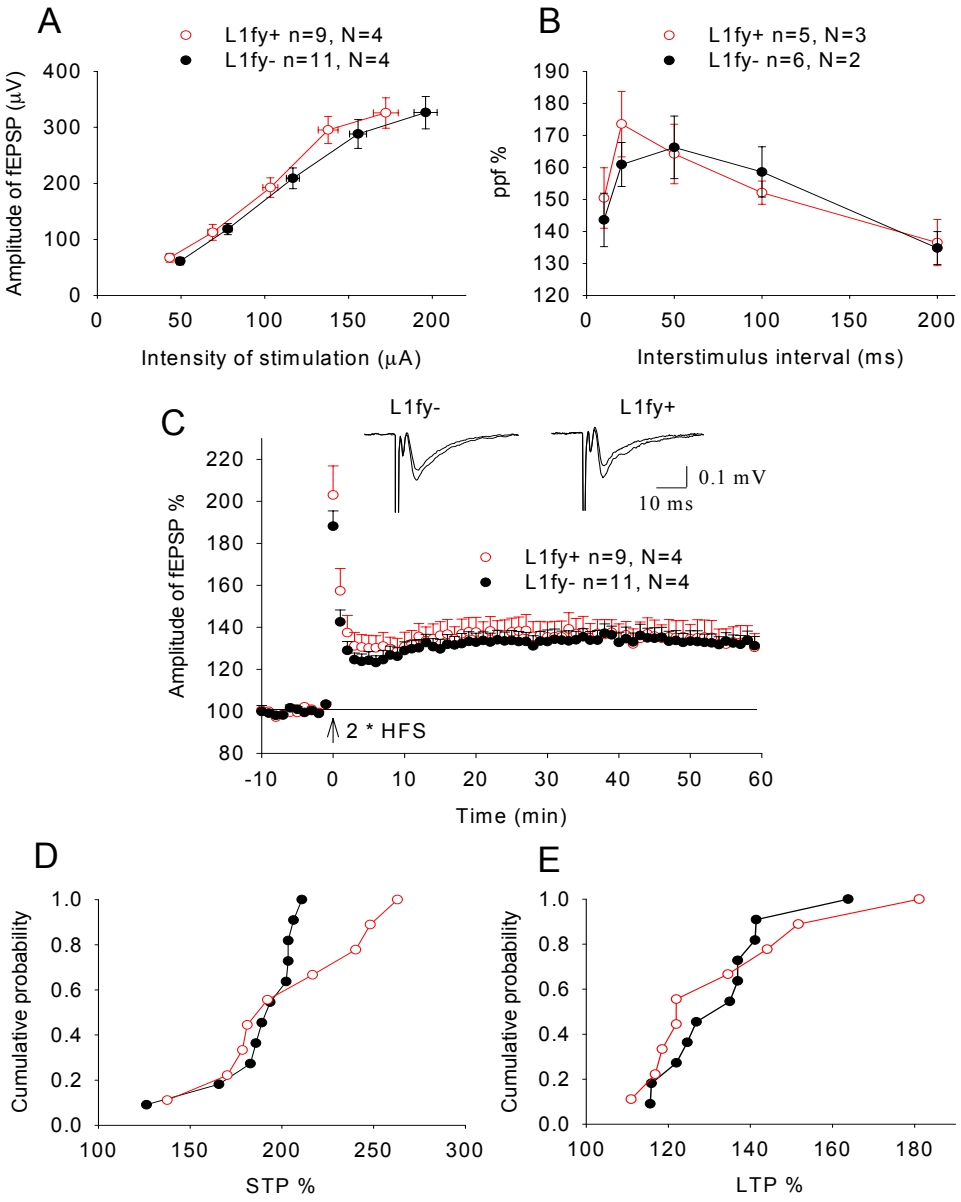

Figure 18. A) Input-output curves for amplitudes of fEPSPs evoked by stimulation of associational/commissural projections to the CA3 field at different stimulation strengths. B) Paired-pulse facilitation with 10, 20, 50, 100 and 200 ms interstimulus intervals. C) Short- and long-term potentiation induced by 2 trains of HFS. Upper panel shows fEPSPs recorded before and 50-60 min after HFS for both genotypes. D-E) Cumulative plots representing levels of short-term potentiation (STP) measured 1 min after HFS (D) and long-term potentiation (LTP) measured 50-60 min after HFS (E). Each symbol represents a single experiment. Cumulative probability at any given value x is the probability to observe potentiation less or equal to x. N represents the number of tested mice, n is the number of tested slices.

1.4. Analysis of direct perforant path projections to the CA1 field

CA1 pyramidal neurons receive signals on the one hand from CA3 field via Schaffer collateral/commissural fibers and on the other hand from the entorhinal cortex by direct perforant path projection, which originate from layer III of the entorhinal cortex. It means that CA1 neurons can be activated either trisynaptically, via consecutive activation of 1) perforant path synapses in the dentate gyrus, 2) mossy fiber synapses in the CA3 field and 3) Schaffer collateral synapses onto the CA1 pyramidal neurons, or disynaptically via activation of 1) CA3 neurons by direct perforant path projections and 2) Schaffer collateral synapses onto the CA1 field, or monosynaptically via direct perforant path fibers projecting to the CA1 pyramidal cells.

Figure 19A shows that there was no statistically significant difference between L1 conditional knockout mice and corresponding wild-types in terms of maximal amplitude of responses and maximal intensity of stimulation. In L1fy- mice, maximal amplitude of fEPSP was 0.79±0.04 mV and in L1fy+ it was 0.84±0.05 mV. The maximal intensity of stimulation which was required for induction of fEPSP was 170.7±8.0 μA in L1fy- mice and 172.3±8.2 μA in L1fy+ animals.

Paired-pulse facilitation analysis with ANOVA test revealed that there was no statistically significant difference between genotypes, also there was a tendency for L1fy+ mice to have small facilitation (P=0.052). Further analysis with multiple comparisons t-test revealed that no statistically significant difference could be detected for any interstimulus interval (Figure 19B).

Long-term potentiation was induced by 2 trains of HFS applied with 100% of stimulation intensity to slices disinhibited by 100 μM picrotoxin. The profile and level of LTP in wild-type mice was similar to previously published data (Remondes and Schuman, 2003). No statistically significant impairment of STP was observed in L1fy+, but LTP was significantly smaller than in L1fy- mice (Figure 19C). The level of STP was 174.3±6.9 % in L1fy- animals and 176.9±4.7 % in L1fy+ mice. LTP in L1fy- mice was 120.1±3.6 %, whereas in L1fy+ it was only 109.4±2.5 %. This difference was statistically significant ($P<0.05$). Also visual analysis of LTP values shows a shift of cumulative probability function in L1fy+ mice to the left (Figure 19E). Above described results show that there is a synapse-specific impairment of long-term potentiation in L1 conditional knockout mice.

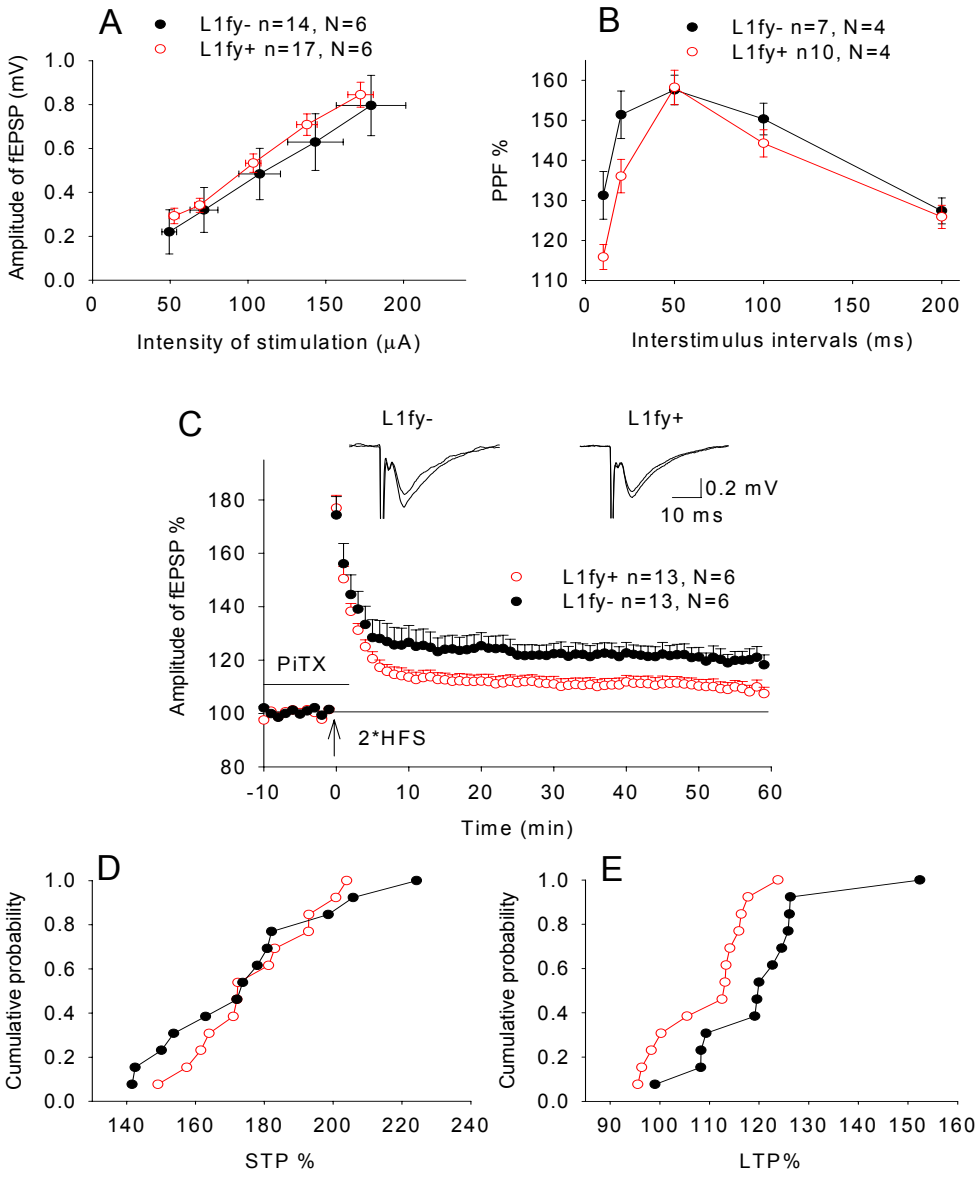

Figure 19. A) Input-output curves for amplitudes of fEPSPs evoked by stimulation of direct perforant path projections to the CA1 field at different stimulation strengths. B) Paired-pulse facilitation with 10, 20, 50, 100 and 200 ms interstimulus intervals. C) Short- and long-term potentiation induced by 2 trains of HFS. Upper panel shows fEPSPs recorded before and 50-60 min after HFS for both genotypes. D-E) Cumulative plots representing levels of STP measured 1 min after HFS (D) and levels of LTP measured 50-60 min after HFS (E). Each symbol represents a single experiment. Cumulative probability at any given value x is the probability to observe potentiation less or equal to x. N represents the number of tested mice, n is the number of tested slices.

1.5. Analysis of direct perforant path projections to the CA3 field

Neurons located in the entorhinal cortex send direct projections also to distal dendrites of CA3 pyramidal cells. However, unlike projections to CA1, perforant path fibers directed to CA3 originate from layer II rather than layer III of the entorhinal cortex.

As for the other pathways, the first step in our experiments was to measure the amplitudes of responses as a function of stimulation intensity. Figure 20A shows that there was no statistically significant difference in terms of maximal amplitude of fEPSPs, although statistical significance was achieved in maximal intensity of stimulation. Analysis showed that maximal amplitude of fEPSP in L1fy- mice was 0.79±0.05 mV and in L1fy+ mice it was 0.73±0.02 mV. The maximal intensity of stimulation in L1fy- animals was 191.5±2.2 μA and in L1fy+ mice it was 178.4±6.4 μA. Evaluation of stimulus-response curves using ANOVA did not reveal any statistically significant difference between genotypes.

Also no difference between genotypes was detected in paired-pulse facilitation with 10, 20, 50, 100 and 200 ms interstimulus intervals (Figure 20B).

Two trains of HFS applied to disinhibited slices caused much weaker LTP in knockouts than in wild-type animals, although no abnormalities were observed in terms of STP. Mean level of STP was 197.9±5.2 % in L1fy- mice and 189.2±5.4 % in L1fy+ animals. The level of LTP in L1fy- was 130.3±2.5 %, whereas in L1fy+ mice it was 117.8±3.0% ($P<0.01$; Figure 20C). Also there is an obvious shift of cumulative probability function for LTP values in L1fy+ mice to the left.

Thus, we found that cortical projections to CA1 and CA3 fields show reduced levels of LTP. Since different cortical layers project to CA1 versus CA3, the deficit appeared to be not specific to certain population of presynaptic cells. The only common feature of synapses with impaired LTP is that they are located on distal dendrites. Since lateral perforant path projections to dentate gyrus are also on distal dendrites, impaired LTP is specific for pyramidal cells but not granule ones.

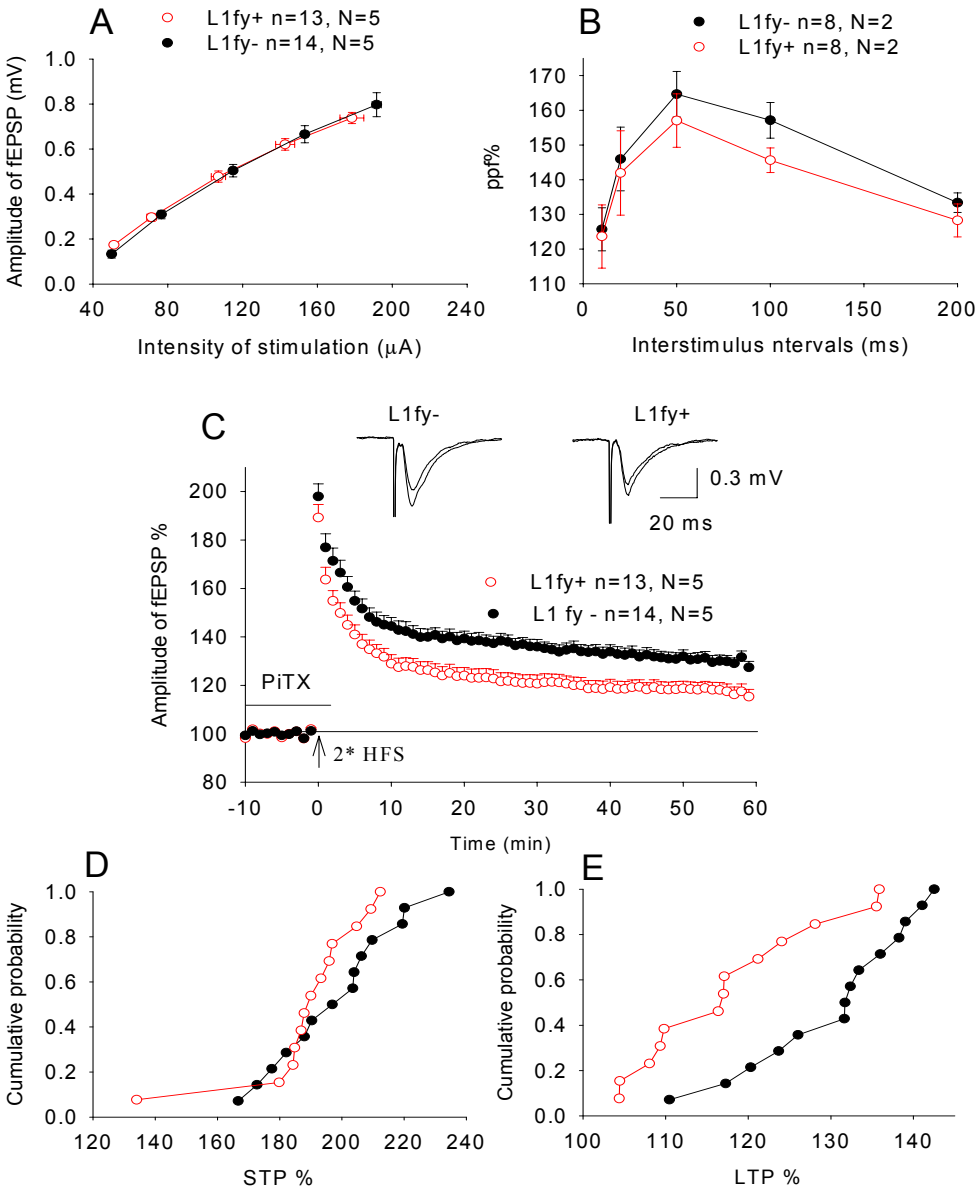

Figure 20. A) Input-output curves for amplitudes of fEPSPs evoked by stimulation of direct perforant path in the CA3 field at different stimulation strengths. B) Paired-pulse facilitation with 10, 20, 50, 100 and 200 ms interstimulus intervals. C) Short- and long-term potentiation induced by 2 trains of HFS. Upper panel shows fEPSPs recorded before and 50-60 min after HFS for both genotypes. D-E) Cumulative plots representing levels of STP measured 1 min after HFS (D) and LTP measured 50-60 min after HFS (E). Each symbol represents a single experiment. Cumulative probability at any given value x is the probability to observe potentiation less or equal to x. N represents the number of tested mice, n is the number of tested slices.

1.5.1. Mechanisms underlying impaired LTP in direct perforant path projections to the CA3 field

Since it is known that the influx of Ca^{2+} via both NMDA receptors and voltage-dependent Ca^{2+} channels is essential for induction and maintenance of some forms of LTP, we decided to check the role of these channels in long-term potentiation at direct perforant path projections to the CA3 field, which was strongly impaired in L1 conditional knockout mice.

To check the role of NMDA receptors in LTP at the above-described pathway, we applied 50 μM APV 15 minutes before and during delivering HFS. As shown on Figure 21A, APV blocked LTP in both L1 conditional knockouts and corresponding wild-type animals. The amplitude of fEPSPs after induction of LTP was just 102.1±2.2 % and 104.7±1.5 % for L1fy+ and L1fy- mice, respectively. Interestingly, STP in slices treated with APV was 164.0±5.8 % in L1fy+ and 177.11±9.07 % in L1fy- mice. These values were significantly smaller than in untreated slices of knockout mice (P=0.01), and there was also a tendency for wild-type animals to show a reduction in STP after application of AP5 (P=0.05).

Next, we used two different approaches to investigate the role of voltage-gated Ca^{2+} channels in LTP at direct perforant path projections to the CA3 field. We studied influences of an agonist and an antagonist of L-type voltage dependent Ca^{2+} channels in L1fy+ and L1fy- mice.

Application of 10 μM nifedipine (the L-type voltage dependent Ca^{2+} channel antagonist) 15 min before and during delivering 2 trains of HFS caused a significant decrease in the level of LTP in both wild-type and knockout mice. No statistically significant difference between genotypes was observed in the presence of nifedipine. LTP was 115.9±3.4% in L1fy- animals and 109.7±2.8% in L1fy+ (Figure 21B). Comparison of the levels of LTP between untreated and nifedipine applied slices revealed that, nifedipine caused statistically significant reduction of the LTP level in case of wild-type animals, while the knockout slices were not much affected. STP in L1fy- slices treated with nifedipine was 207.6±11.39% and in L1fy+ case it was 172.6±11.7%. This apparent difference was not statistically significant (P=0.058) and also no significant difference was observed between treated and untreated slices of both genotypes.

Application of 15 μM BAY K 8644 (agonist of L-type voltage dependent Ca^{2+} channels) for 15 min to disinhibited slices, in contrast to nifedipine, caused an increase in the level of LTP in both genotypes after delivering of two trains of HFS. No statistically significant difference was seen between genotypes any more. STP was 183.24±8.95% in L1fy- and 171.94±3.66% in L1fy+ mice. LTP in L1fy- was 129.01±8.55% and in L1fy+ it reached 130.32±6.67% (Figure 21C). Treatment of slices by BAY K 8644 did not cause any statistically significant changes in

terms of short- or long-term potentiation for wild-type animals, but resulted in statistically significant increase of LTP and decrease of STP levels in L1fy+ mice ($P<0.05$) compared to untreated slices.

Thus, our results show that both NMDA and L-type voltage-dependent Ca^{2+} channels are implicated in long-term potentiation at direct perforant path synapses in the CA3 field. Since antagonist and agonist of L-type voltage-dependent Ca^{2+} channels abolished the difference in LTP between L1 conditional knockout and wild-type animals, these channels are good candidates to be responsible for impairment of LTP in L1fy+ mice.

1.5.2. Influence of L1 on L-VDCC currents

Based on the fact, that the L-VDCC antagonist nifedipine and agonist BAY K 8644 abolished difference between levels of LTP in slices from L1fy+ and L1fy- mice, we speculated that deficiency in L1 molecule could alter activity of L-VDCCs. A direct way to check influence of cell adhesion molecule L1 on above mentioned channels was to record L-VDCC currents in transfected CHO cells, which had been grown on poly-L-lysine plus L1 coated coverslips, and compare these with currents from cells grown on poly-L-lysine alone.

Application of voltage step protocol to both experimental groups of cells elicited similar peak and steady state currents (Figure 22 B, C). Maximal amplitude of peak currents was 0.94±0.21 nA for cells grown on L1 coated coverslips and 0.72±0.11 nA for control ones. The similar situation was observed for steady state currents, where maximal amplitude was 0.59±0.13 nA and 0.47±0.07 nA for L1 coated and control coverslips, respectively. No difference has been observed in term of peak and steady state current density, i.e. a ratio between currents and cell capacitance, as well (Figure 22 D, E). Maximal peak current density was 47.5±7.6 pA/pF and 65.8±15.2 pA/pF for control and L1 coated coverslips respectively and maximal steady state current density was 28.84±4.3 pA/pF for control cells and 40.9±9.1 pA/pF for L1 coated ones. Thus, our experiments showed that there was no difference between cells grown with or without L1 molecule in all measured parameters of L-VDCC currents.

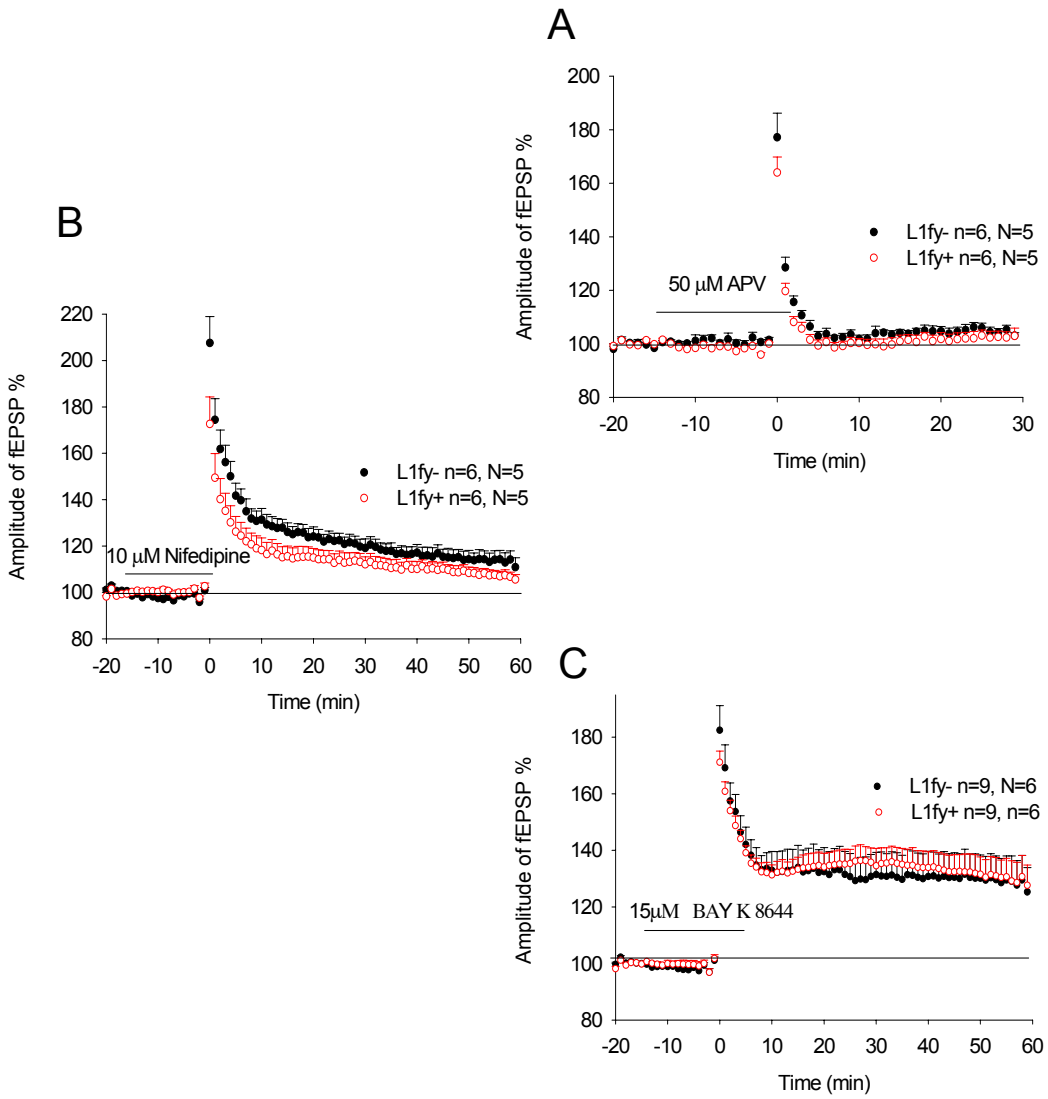

Figure 21. Short- and long-term potentiation induced by 2 trains of HFS delivered to the direct perforant path projections in the CA3 field, in presence of A) antagonist of NMDA receptors, APV; B) antagonist of voltage-dependent Ca^{2+} channels, nifedipine and C) agonist of voltage-dependent Ca^{2+} channels BAY-K 8644. N represents the number of tested mice, n is the number of tested slices.

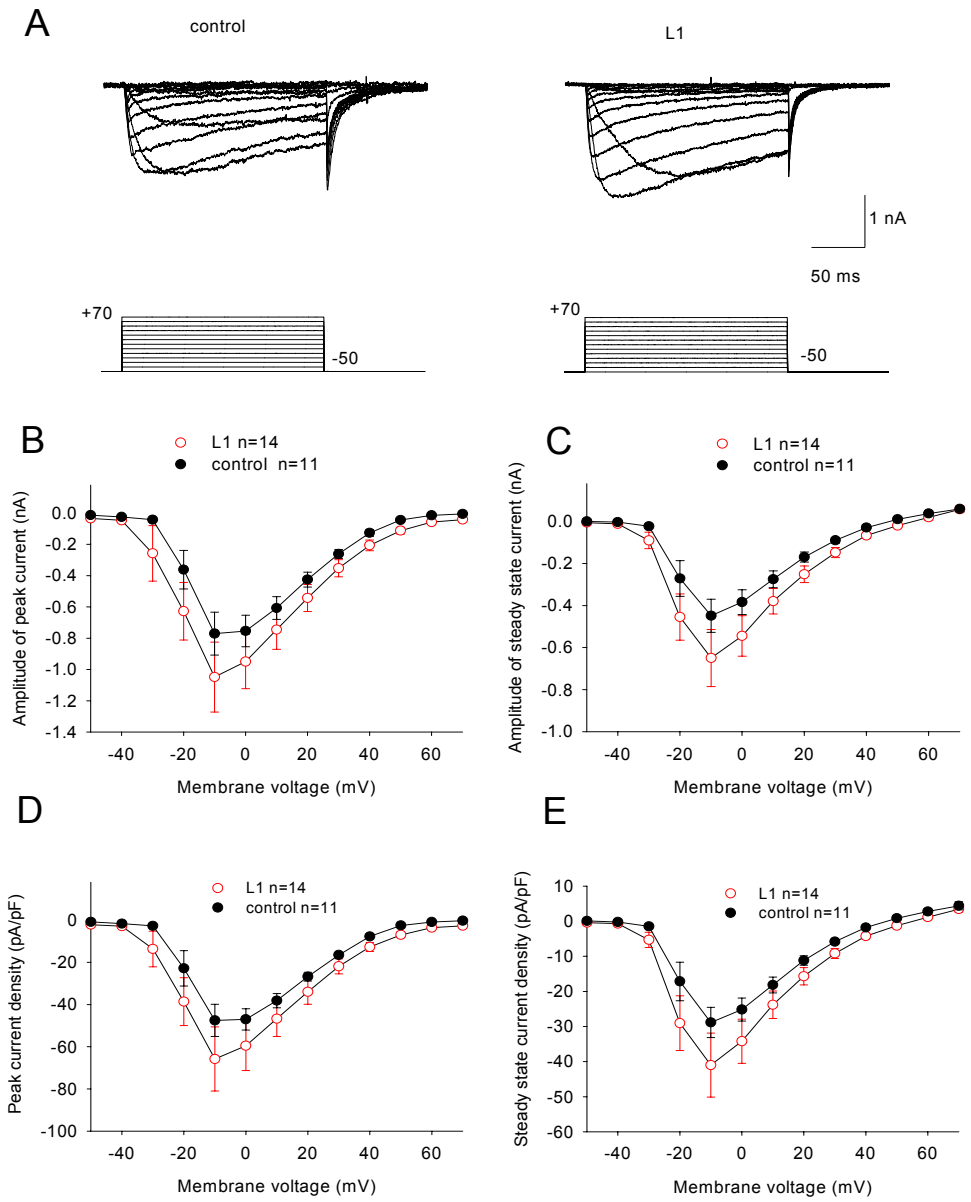

Figure 22. Influence of L1 on L-VDCC currents. A) representative recordings from cells grown on control (left panel) and L1 coated (right panel) coverslips. I-V activation curve for peak (B) and steady state (C) currents and their densities, (D) and (E) respectively. n is number of recorded cells.

1.6. Summary for 3 month-old L1 conditional knockout mice

All data collected from 3 month-old L1 conditional knockout mice and corresponding wild-types are summarized in a table, which shows basal synaptic transmission, paired-pulse facilitation, short- and long-term potentiation in all studied synapses in knockout mice.

Parameter	LPP-DG	MPP-DG	MF-CA3	A/C-CA3	PP-CA1	PP-CA3
Basal Synaptic Transmission	=	=	=	=	=	=
Paired-Pulse Facilitation	=	=	=	=	=	=
Post-Tetanic or Short-term Potentiation	↑	=	=	=	=	=
Long-Term Potentiation	=	=	=	=	↓	↓
Frequency Facilitation			=			

LPP, lateral perforant path; MPP, medial perforant path; MF, mossy fibers; A/C, associational/commissural projections; PP, direct perforant path projections; DG, dentate gyrus; CA1 and CA3, subfields of the hippocampus. =, there is no statistically significant difference between knockout and wild type mice; ↓ , parameter is less in knockouts than in wild type mice; ↑ , parameter is increased in knockouts.

1.7. Cholinergic modulation of excitatory transmission in the CA3 area of the hippocampus in L1fy- and L1fy+ mice

The hippocampal formation receives different inputs from various brain regions (Johnston and Amaral, 2004). Among them are cholinergic projections which are considered to be important modulators of hippocampal functions. Cholinergic fibers that innervate hippocampus mainly arrive through the fornix/fimbria and originate in the medial septal niclei and the vertical limb of the nucleus of the diagonal band of Broca (Gray and McNaughton, 1983).

Muscarinic and nicotinic receptors are found on both principal cells and interneurons in the CA3 region (Levey et al., 1995, Mcquiston and Madison 1999). It has been shown that muscarine strongly blocks associational/commissural-CA3 responses, but has almost no effect on mossy fiber-CA3 synapses (Vogt and Regehr, 2001).

Our aim was to investigate influence of muscarine on the fEPSP and HFS induced long-term potentiation of associational/commissural and perforant path projections to the CA3 neurons in L1 conditional knockouts and corresponding wild-types. For this purpose we first washed 1 μM muscarine during 15 minutes in slices prepared from L1fy- mice and then investigated HFS induced LTP under muscarine treatment. As Figure 23A shows 1 μM muscarine reduced fEPSPs up to 45.03±4.1% of the baseline and similar level of decrease (40.5±6.9%), was observed in slices where HFS was delivered for LTP induction. Tetanic activation of A/C fibers after muscarine treatment caused increase of responses up to 103.1±4.7%. To find out whether this increase of fEPSPs after HFS was due to the tetanic stimulation or due to the washing out of compound we compared LTP recordings with normal wash in and wash out paradigms. Figure 23A shows that, without delivering of HFS, wash out of muscarine caused increase of responses up to 91.08±5.7% of the baseline. Difference between results obtained after tetanic stimulation and normal wash out did not reach statistical significance with P=0.15.

We also checked effect of muscarine on the perforant path projections to the CA3 pyramidal neurons. As Figure 23B shows 1 μM muscarine caused reduction of responses up to 59.3±6.1% of the baseline in slices were no tetanic stimulation was delivered and 67.5±7.1%, were LTP was induced by HFS. Reduction of fEPSPs in both cases was statistically significantly different from that observed for A/C fibers. Tetanic stimulation of perforant path fibers in muscarine treated wild-type slices induced increase of fEPSPs up to 90.2±3.8%, and simple wash out of muscarine without HFS changed responses up to 78.4±9.1% of the baseline. This difference did not reach statistical significance.

The same group of experiments were performed for L1fy+ mice and similarly to wild-types, we investigated effects of muscarine on field potentials induced by the activation of either associational/commissural or perforant pathway, and also HFS evoked LTP.

For A/C pathway, washing in of 1 μM muscarine caused reduction of responses to 52.2±2.9% of the baseline and in slices were HFS was delivered for LTP induction, decrease of fEPSPs by muscarine was 47.7±5.6% (Figure 23C). After washing out, responses tended to increase and in slices which did not undergo LTP this increase was up to 86.4±5.5%, and in slices, where HFS was delivered it was 94.5±6.8% of the baseline. The difference did not reach statistical significance. Application of 1 μM muscarine had reducing effect on perforant path evoked fEPSPs too and this decrease reached 75.2±7.1% of the baseline in slices where no HFS was delivered and 62.9±6.6% in slices which later underwent LTP. Washing out of muscarine brought about increase of responses and at the end of recordings amplitude was 75.6±3.04% of the baseline in slices were no long-term potentiation was induced and 86.6±4.5% in slices which were tetanically stimulated by HFS. The difference did not reach statistical significance (P=0.1; Figure 23D).

Since the increase of fEPSPs after tetanic stimulation is not statistically significantly different from results obtained after simple washing out of the compound, we can conclude that HFS fails to induce LTP in muscarine treated slices for both, wild-type and knockout animals.

To compare effects of muscarine in two different genotypes we plotted together results received from activation of either associational/commissural or perforant path projections in L1fy- and L1fy+ mice. Figure 24 shows that there was no statistically significant difference between genotypes either in terms of block of responses due to the muscarine application or in terms of HFS induced LTP at both, associational/commissural (A) and perforant path projections (B).

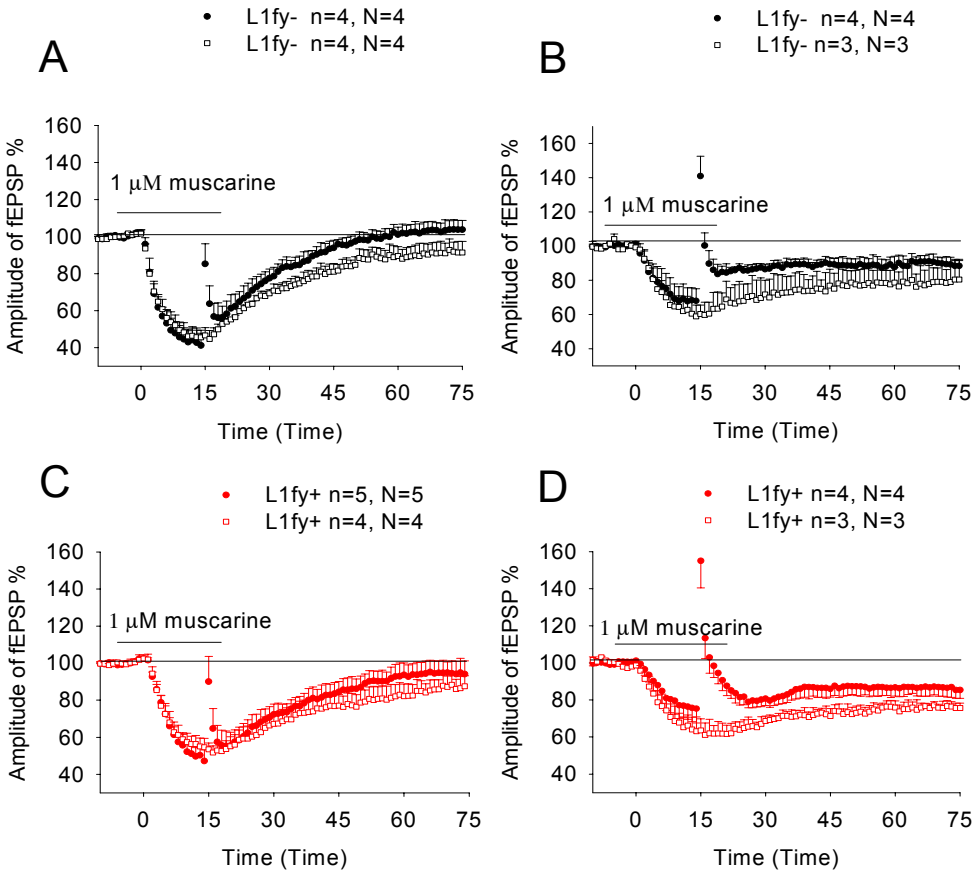

Figure 23. Effects of muscarine on associational/commissural (A) and (C) and perforant path (B) and (D) evoked potentials in the CA3 field. Filled circles show recordings in slices with HFS and open squares - with no tetanic activation. N represents the number of mice, n is the number of slices.

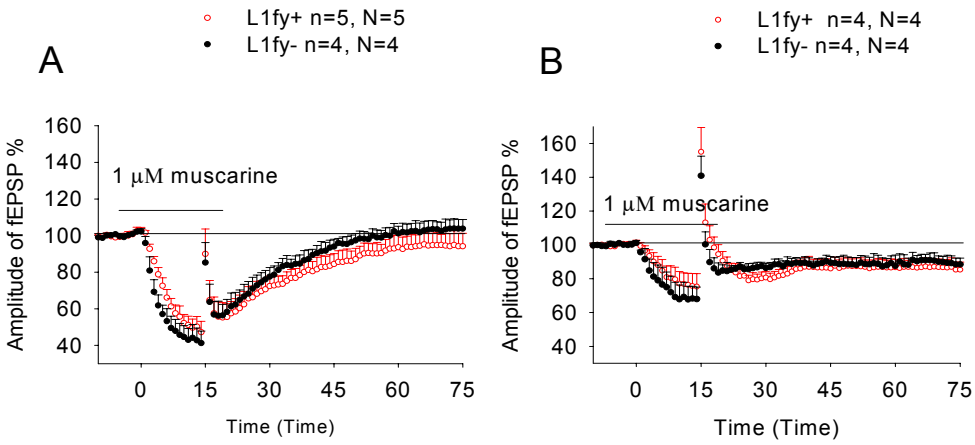

Figure 24. Effects of muscarine on the HFS evoked LTP of the associational/commissural (A) and perforant path (B) projections to the CA3 field. N represents the number of mice, n is the number of slices.

2. Characteristics of interaction between direct perforant path and associational-commissural projections to the CA3 pyramidal neurons

CA3 pyramidal neurons are extremely interesting in terms of their diverse excitatory inputs. They receive three different projections from different sources, 1. direct perforant path fibers from layer II of the entorhinal cortex; 2. mossy fibers from dentate granule cells and 3. associational/commissural projections from other ipsi- or contralateral CA3 pyramidal cells.

Due to this feature CA3 neurons are the best targets, within the hippocampus, for studying interactions between different excitatory pathways. Our investigation was focused on the associational/commissural and direct perforant path projections.

To study this phenomenon we used single and co-stimulation of above mentioned pathways and recorded fEPSPs from both, direct perforant path synapses onto the distal part and associational/commissural synapses onto the middle area of the CA3 apical dendrites.

2.1. Effects of co-stimulation of direct perforant path and associational-commissural projections on the perforant path synapses onto CA3 pyramidal neurons

Since direct perforant path projections are located in stratum lacunosum-moleculare of the CA3 field, our recording electrode was placed in this area and at the beginning of experiments we stimulated only perforant path fibers to elicit fEPSPs of these synapses. After responses were found, we applied additional simultaneous stimulation of the associational/commisural projections and compared elicited fEPSPs with the original, single stimulation evoked responses.

Figure 25A shows that co-stimulation of direct perforant path and associational/commissural fibers evoked statistically significantly smaller fEPSPs than the single stimulation of perforant path projections. For comparison, the amplitude of fEPSPs induced by single stimulation was taken as 100% and as one can see on the Figure 25A simultaneous stimulation of the associational/commisural and direct perforant pathways induced responses which were 81.9± 3.2% of original fEPSPs, $P<0.01$.

We also checked whether inhibitory interneurons, which are abundant in the CA3 field, played any role in the decrease of responses at direct perforant path synapses onto the CA3 pyramidal cells. For this purpose we applied 100 μM picrotoxin to the bath solution during 10 minutes and then observed fEPSPs upon single stimulation and co-stimulation of two pathways.

As shown on Figure 25B, disinhibition of slices caused at least partial recovery of responses after co-stimulation of direct perforant path and associational/commissural projections,

which were 91.6±4.0 % of original fEPSPs (P=0.06). This is underestimation of responses since co-stimulation elicited firing of neurons and these population spikes may lead to a bias of amplitude measurements. Thus, our results indicate that, the reduction of fEPSPs after simultaneous stimulation of these two pathways could be due to the feed forward inhibition.

2.2. Effects of co-stimulation of associational/commissural and direct perforant path projections on the associational/commissural synapses onto CA3 pyramidal neurons

In contrast to direct perforant path projections, associational/commissural synapses onto the CA3 neurons are located in stratum radiatum of the CA3 field. Therefore, in the next set of experiments the recording electrode was placed in the stratum radiatum. To induce responses at these synapses, we first stimulated Schaffer collaterals and evoked associational/commissural responses in the CA3 area (see Materials and Methods) and then additionally applied simultaneous stimulation of the perforant path projections.

Figure 26A shows that co-stimulation of direct perforant path and Schaffer collateral fibers induced similar fEPSPs to that one which was recorded after single activation of associational/commissural projections. For comparison, the amplitude of fEPSPs induced by single stimulation was taken as 100% and as one can see on the Figure 26A co-stimulation elicited responses that were 100.5± 1.7 % of original fEPSPs.

As in the case of direct perforant path synapses, here we also studied modulation of fEPSPs after co-stimulation of two pathways. As shown on Figure 26B, disinhibition of slices by 100 μM picrotoxin did not cause any significant changes of results and simultaneous stimulation of associational/commissural and direct perforant path projections did not bring about strong decrease of responses. Similarly to previous cases, the amplitude of fEPSPs evoked by single stimulation was taken as 100% and, co-activation elicited responses that were 95.7±4.6% of original fEPSP.

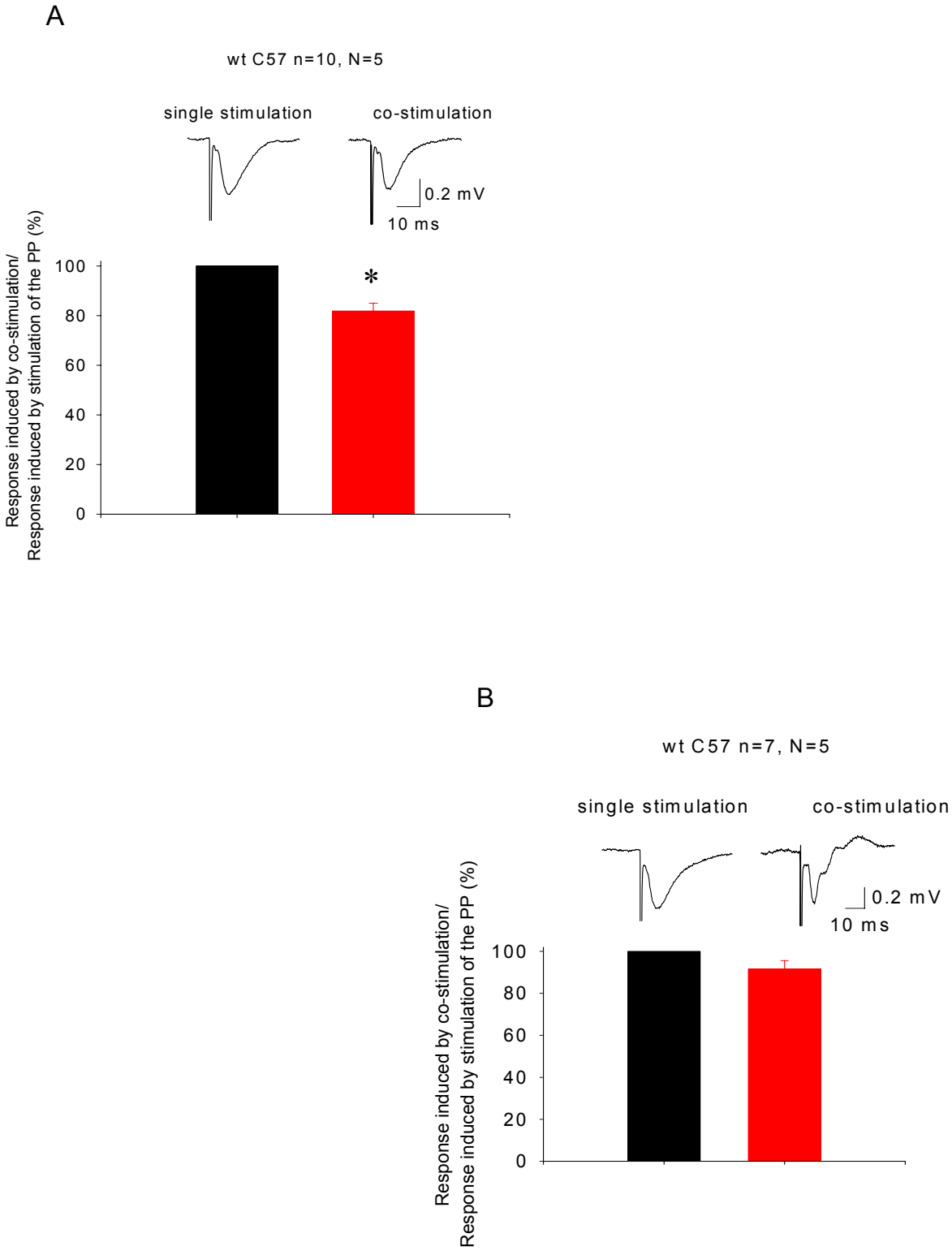

Figure 25. Effects of co-stimulation of direct perforant path and associational/commissural projections on perforant path synapses to the CA3 pyramidal neurons without (A) and with (B) Picrotoxin. Red column represents results received after co-stimulation and black column – after single stimulation (was set to 100%) of perforant path fibers. Upper panels show fEPSPs. N represents the number of tested mice, n is the number of tested slices.

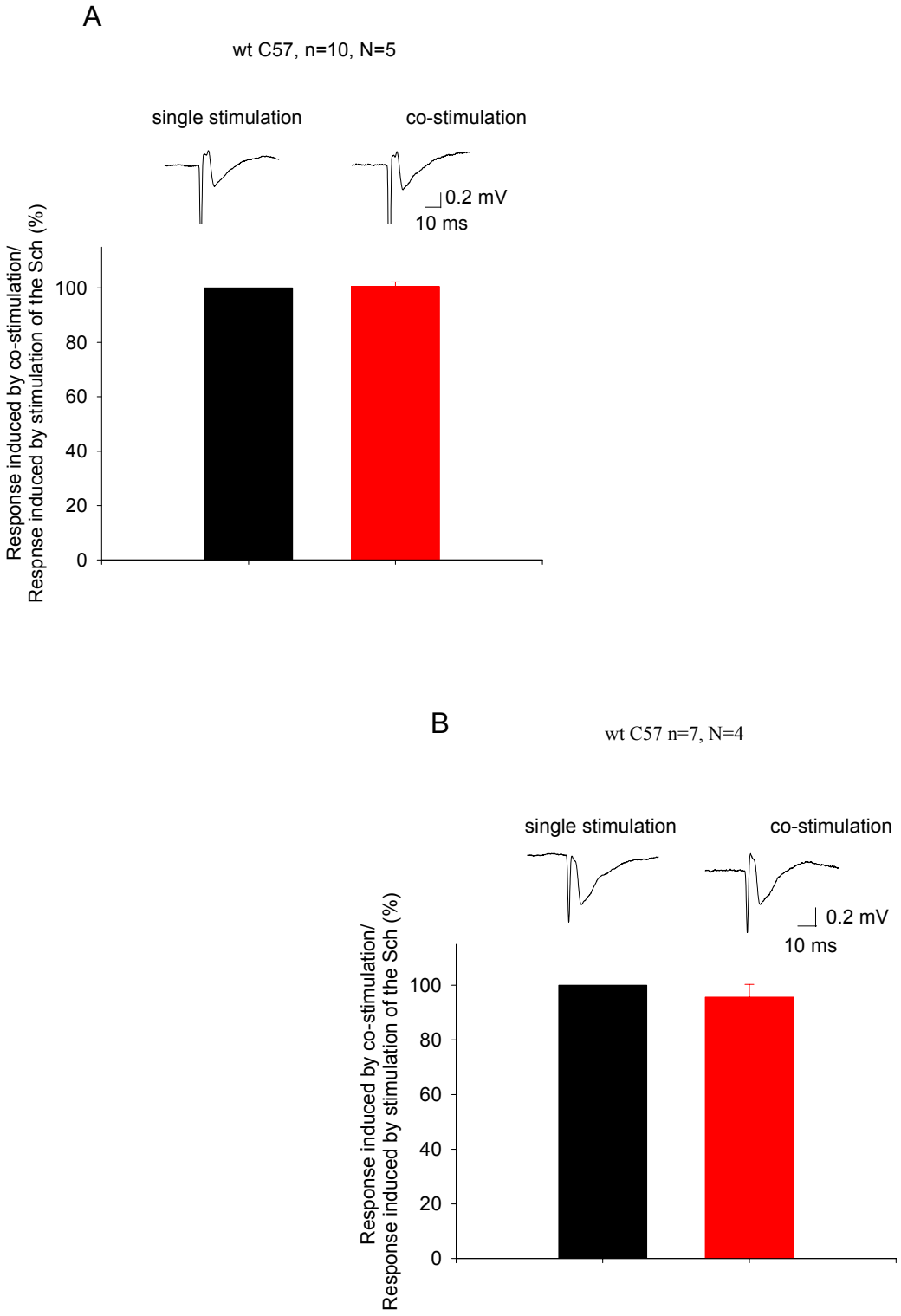

Figure 26. Effects of co-stimulation of associational/commissural and direct perforant path projections on associational/commissural synapses to the CA3 pyramidal neurons without (A) and with (B) picrotoxin. Red and black columns represent results received after co-stimulation and single stimulation, respectively. Upper panels show fEPSPs. N represents the number of tested mice, n is the number of tested slices

3. Analysis of CHL1 constitutive knockout mice and corresponding wild- types

Like in the L1 conditional knockout mice, we investigated synaptic transmission and plasticity in all major excitatory pathways in 3 month-old CHL1 constitutive knockouts and corresponding wild-types.

The first step again was to analyze synaptic transmission and plasticity in perforant path projections to the dentate gyrus, which include lateral and medial perforant path fibers.

3.1. Analysis of lateral perforant path projections to the dentate gyrus

Placing the stimulating and recording electrodes in the outer part of the molecular layer in the dentate gyrus allowed us to find lateral perforant path responses, which facilitated with 50 ms interstimulus interval paired-pulse stimulation. Facilitation of responses under such conditions was 118.6±2.9% for CHL1+/+ and 120.4±2.8% for CHL1-/- mice. After finding proper responses we checked the relationship between the amplitude of fEPSPs versus intensity of stimulation. As shown on Figure 27A, there was no statistically significant difference in terms of maximal amplitude of responses between two genotypes. Analysis showed that maximal amplitude of fEPSPs in wild-type animals (CHL1+/+) was 1.11±0.06 mV and in knockouts (CHL1-/-) it was 1.19±0.09 mV. Intensity of stimulation required for the induction of these responses in CHL1+/+ was 96.2±5.6 μA and in CHL1-/- it was 75.7±5.7 μA. ANOVA analysis revealed that there was a statistically significant difference in terms of intensity of stimulation between two genotypes, also t-test showed that all points except the first one were different between genotypes.

Long-term potentiation was induced by 5 trains of high frequency stimulation delivered to disinhibited slices. Figure 27B shows that there was no difference in terms of short- and long-term potentiation between two genotypes. Level of STP was 132.1±8.3 % in CHL1+/+ mice and 131.3±4.5 % in CHL1-/- ones. The level of LTP was 122.0±2.8 % in CHL1+/+ mice and 119.9±3.3 % in CHL-/- animals.

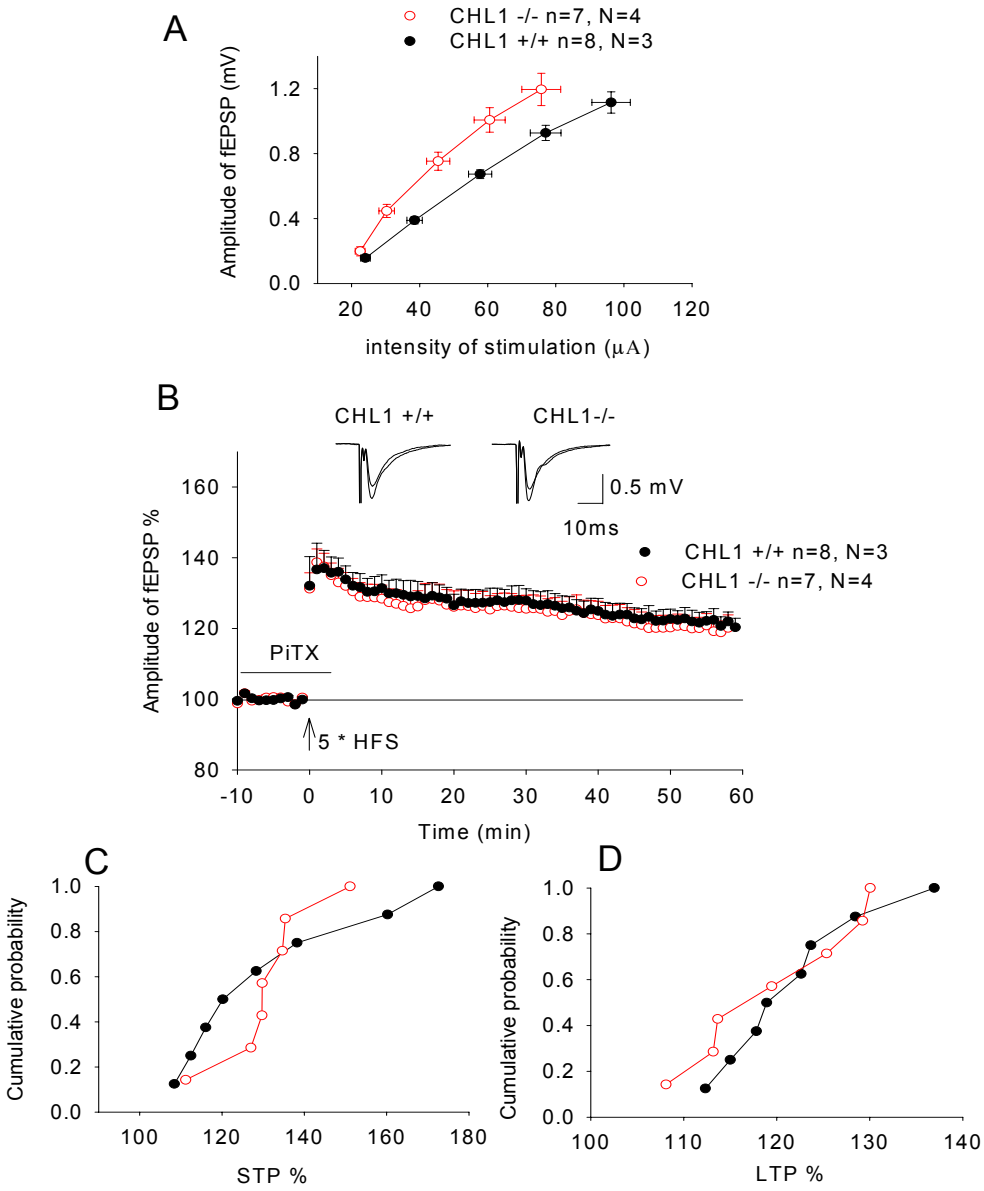

Figure 27. A) Input-output curves for amplitudes of fEPSPs evoked by stimulation of lateral perforant path projections to the dentate gyrus at different stimulation strengths. B) Short- and long-term potentiation induced by 5 trains of HFS. Upper panel shows fEPSPs recorded before and 50-60 min after HFS for both genotypes. C-D) Cumulative plots representing levels of short-term potentiation (STP) measured 1 min after HFS (C) and long-term potentiation (LTP) measured 50-60 min after HFS (D). Each symbol represents a single experiment. Cumulative probability at any given value x is the probability to observe potentiation less or equal to x. N represents the number of tested mice, n is the number of tested slices.

3.2. Analysis of medial perforant path projections to the dentate gyrus

For induction and registration of medial perforant path responses in the dentate gyrus we placed stimulating and recording electrodes in the inner part of the molecular layer. After finding responses which exhibited paired-pulse depression with 50 ms interstimulus intervals we assessed amplitudes of fEPSPs versus intensity of stimulation. PPD was 81.2±0.8% in wild-type animals and 80.2±1.4% in CHL1 -/- mice. Figure 28A shows that maximal amplitude of fEPSPs was 1.71±0.2 mV in CHL1+/+ mice and 2.02±0.1 mV in CHL1-/-. The intensity of stimulation required to elicit these responses in CHL1+/+ animals was 73.12±5.6 μA and in CHL1-/- mice it was 55.62±2.4 μA. This difference is statistically significant ($P<0.05$).

Figure 28B shows that 5 trains of HFS delivered with 100% of stimulation intensity caused similar STP and LTP in disinhibited slices of two compared genotypes. Level of STP in CHL1+/+ mice was 141.2±11.7 % and in CHL1-/- mice it was 144.0±4.6%. The level of LTP in CHL1+/+ mice was 147.3±11.5 % and in CHL1-/- mice it was 138.1±7.2%.

3.3. Analysis of mossy fiber projections to the CA3 field

Mossy fibers transmit signals from the dentate gyrus to the CA3 field. Analysis of physiological characteristics of mossy fiber projections to the CA3 field in CHL1 constitutive knockouts and corresponding wild-type mice revealed that there was no difference between genotypes in terms of frequency dependent facilitation and block of responses by DCG IV (Figure 29A and B).

Two trains of HFS delivered to slices which were pre-treated by 50 μM APV (to block NMDA receptors), induced similar PTP and LTP in slices from both genotypes. PTP in CHL1 +/+ was 1050.9±150.6 % and in CHL1 -/- mice it was 883.3±61.4 %. ($P=0.3$). The level of LTP in CHL1 +/+ mice was 168.7±38.1% and in CHL1-/- animals it was 166.9±4.6 % (Figure 29C).

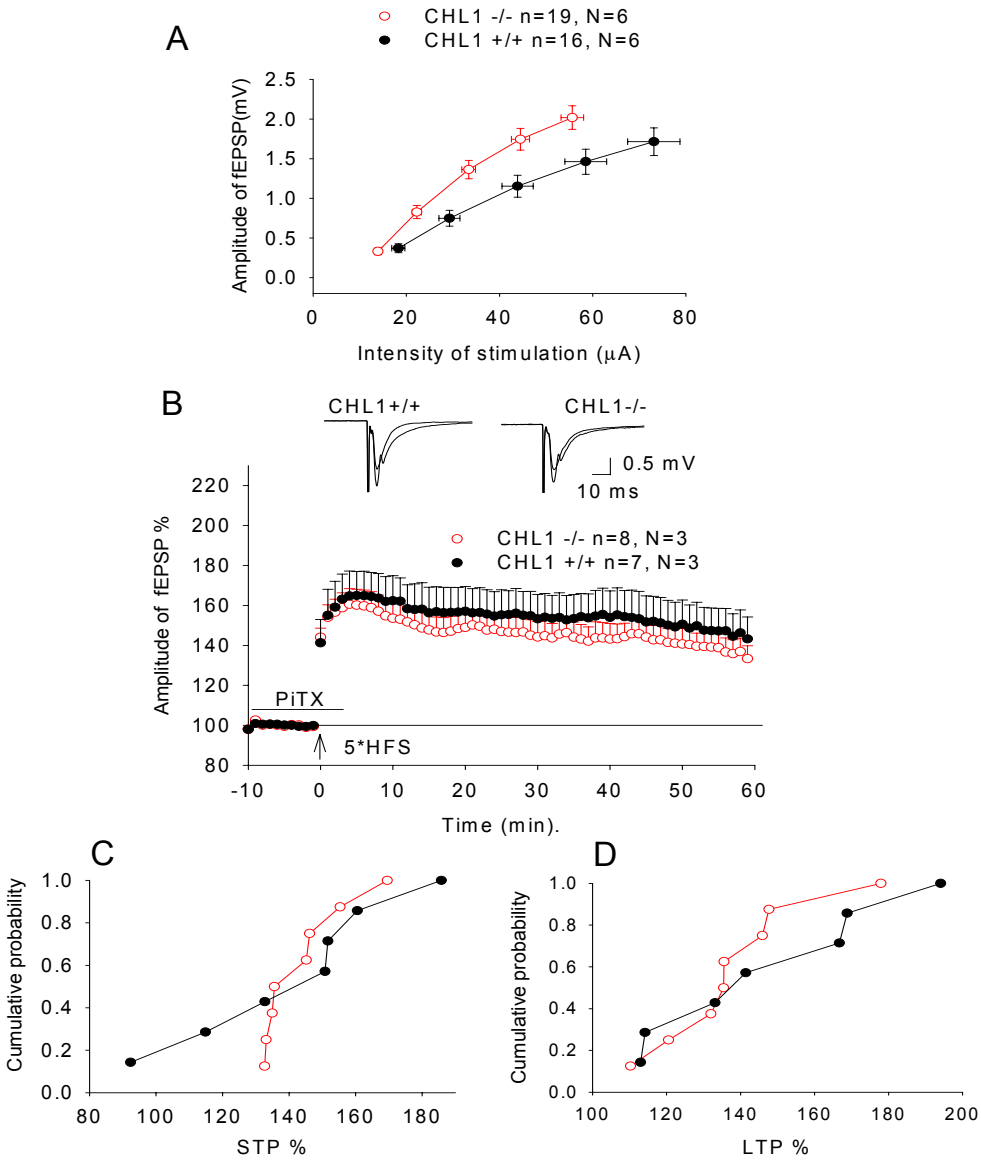

Figure 28. A) Input-output curves for amplitudes of fEPSPs evoked by stimulation of medial perforant path projections to the dentate gyrus at different stimulation strengths. B) Short- and long-term potentiation induced by 5 trains of HFS. Upper panel shows fEPSPs recorded before and 50-60 min after HFS for both genotypes. C-D) Cumulative plots representing levels of short-term potentiation (STP) measured 1 min after HFS (C) and long-term potentiation (LTP) measured 50-60 min after HFS (D). Each symbol represents a single experiment. Cumulative probability at any given value x is the probability to observe potentiation less or equal to x. N represents the number of tested mice, n is the number of tested slices.

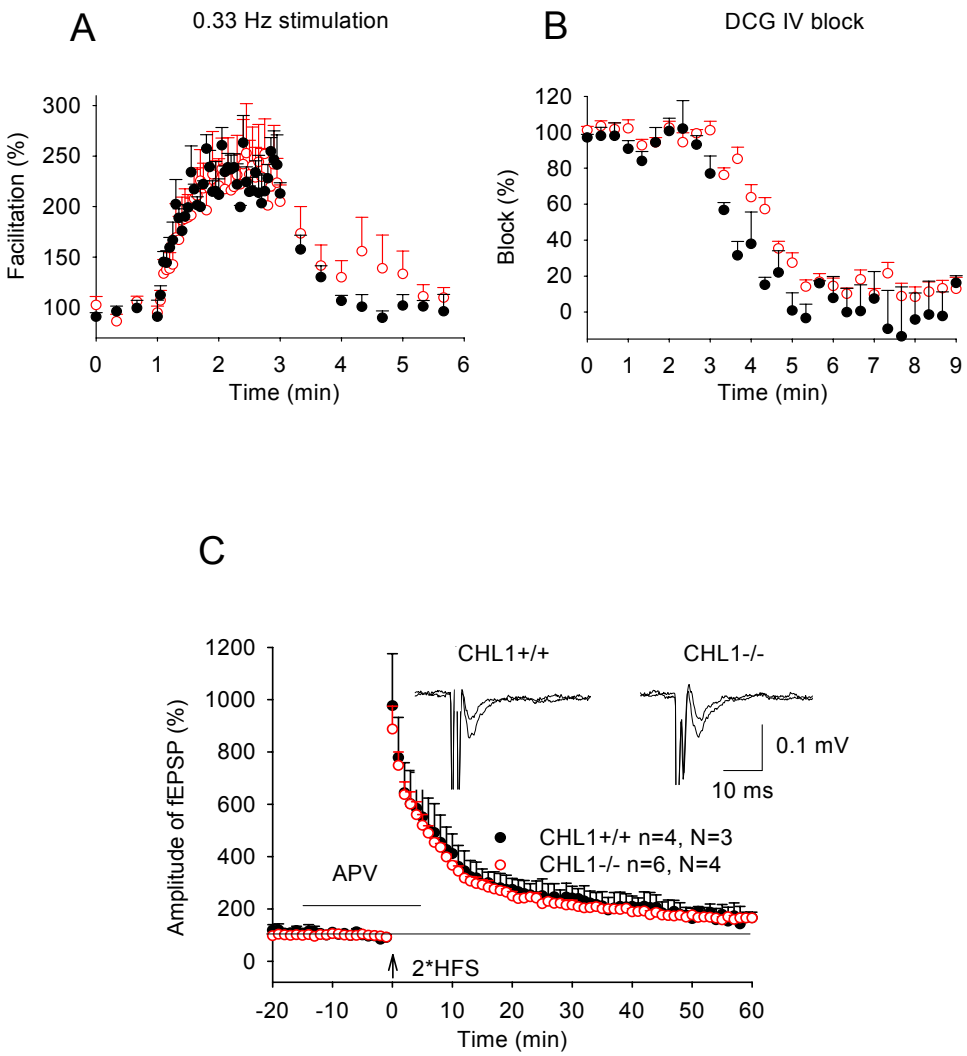

Figure 29. A) Frequency-dependent facilitation of mossy fiber responses with 0.33 Hz stimulation. B) Block of responses with group II mGluR agonist DCG IV. C) Post-tetanic and long-term potentiation induced by 2 trains of HFS in the presence of NMDA receptor antagonist APV. Upper panel shows fEPSPs recorded before and 50-60 min after HFS for both genotypes. N represents number of tested mice, n is number of tested slices.

3.4. Analysis of associational/commissural projections to the CA3 field

Like in other cases, first step of this set of experiments was to study the relationship between the amplitude of fEPSPs and intensity of stimulation. As shown on Figure 30A, no difference between genotypes was observed in terms of maximal amplitude of responses or intensity of stimulation. The maximal amplitude of fEPSPs was 432.6±42.6 μV in CHL1 +/+ mice and 406.7±30.2 μV in CHL1 -/- mice. The maximal responses were elicited with intensity of stimulation 192.4±4.07 μA in CHL1 +/+ and 193.3±4.8 μA in CHL1-/- mice. None of statistical tests showed any differences between two genotypes.

Paired-pulse facilitation evaluation with ANOVA analysis showed that there was no difference between CHL1+/+ and CHL1-/- mice with 10, 20, 50, 100 and 200 ms interstimulus interval paired stimulations (Figure 30B).

LTP was induced by two trains of HFS and no statistically significant differences were revealed either in STP or in LTP. The level of STP in CHL1+/+ mice was 173.7±6.9 % and in CHL1-/- mice it was 177.5±7.5 %. The level of LTP in CHL1+/+ animals was 130.5±3.6 % and in CHL1-/- mice it was 123.5±3.4 % (P=0.17; Figure 30C).

3.5. Analysis of Schaffer collateral/commissural projections to the CA1 field

Information from CA3 to the CA1 field is transmitted via Schaffer collaterals to the ipsilateral hippocampus and via commissural projections to the contralateral one. To record CA3-CA1 responses we placed stimulating and recording electrodes in the stratum radiatum of the CA1 field.

Similar to other pathways, at the beginning of recordings we assessed a relationship between the amplitude of responses and intensity of stimulation. As shown on Figure 31A, there was no difference in terms of maximal amplitude between genotypes. Evaluations revealed that CHL1+/+ mice had 1.34±0.12 mV of maximal fEPSPs and CHL1-/- had 1.37±0.07 mV. Maximal responses were elicited with intensity of stimulation which was 64.3±4.8 μA for CHL1+/+ mice and 76.2±4.2 μA for CHL1-/- mice (P=0.08). ANOVA and t-test showed deference neither in terms of amplitude, nor in terms of stimulation intensity.

Analysis of paired-pulse facilitation with 10, 20, 50, 100 and 200 ms interstimulus intervals with ANOVA test showed that there was no statistically significant difference between two genotypes (Figure 31B).

Two trains of high frequency stimulation induced short- and long-term potentiation, which did not show any difference between CHL1+/+ and CHL1-/- mice. STP in CHL1+/+ was

178.5±5.0 % and in CHL1-/- it was 181.8±10.0 %. The levels of LTP were 115.6±3.6 % and 112.3±2.4 % in CHL1 +/+ and CHL1 -/- mice, respectively (Figure 31C). The profile and level of long-term potentiation was similar to that in wild-type mice, as shown by Evers and colleagues (Evers et al., 2002).

3.6. Analysis of direct perforant path projections to the CA1 field

CA1 pyramidal neurons receive information on the one hand from the CA3 field via Shaffer collateral/commissural projections and on the other hand from the entorhinal cortex via direct perforant path projections. These fibers originate from layer III of the entorhinal cortex and make synapses onto the distal parts of apical dendrites.

Our investigation revealed that there was no statistically significant difference in maximal amplitude of the fEPSPs between two genotypes (Figure 32A). Maximal amplitudes of responses were 0.94±0.09 mV and 0.87±0.07 mV in CHL1+/+ and CHL1-/- mice, respectively. The intensity of stimulation required to elicit these fEPSPs in case of CHL1+/+ mice was 150.0±15.3 μA and 187.5±15.8 μA for CHL1-/- mice. ANOVA did not reveal statistical significant difference between stimulus-response curves ($P>0.1$).

Paired-pulse facilitation with 10, 20, 50, 100 and 200 ms interstimulus intervals did not show any abnormalities in CHL1 -/- mice (Figure 32B).

Long-term potentiation was induced by 2 trains of HFS delivered with 100% of stimulation intensity to disinhibited slices. STP was 186.2±4.5 % in CHL1+/+ mice and 189.6±4.1 % in CHL1-/- animals. The level of LTP in CHL1+/+ mice was 111.7±3.3 % and in CHL1-/- it was 110.9±3.1 %. Thus, no statistically significant difference was observed for STP and LTP between two compared genotypes (Figure 32C).

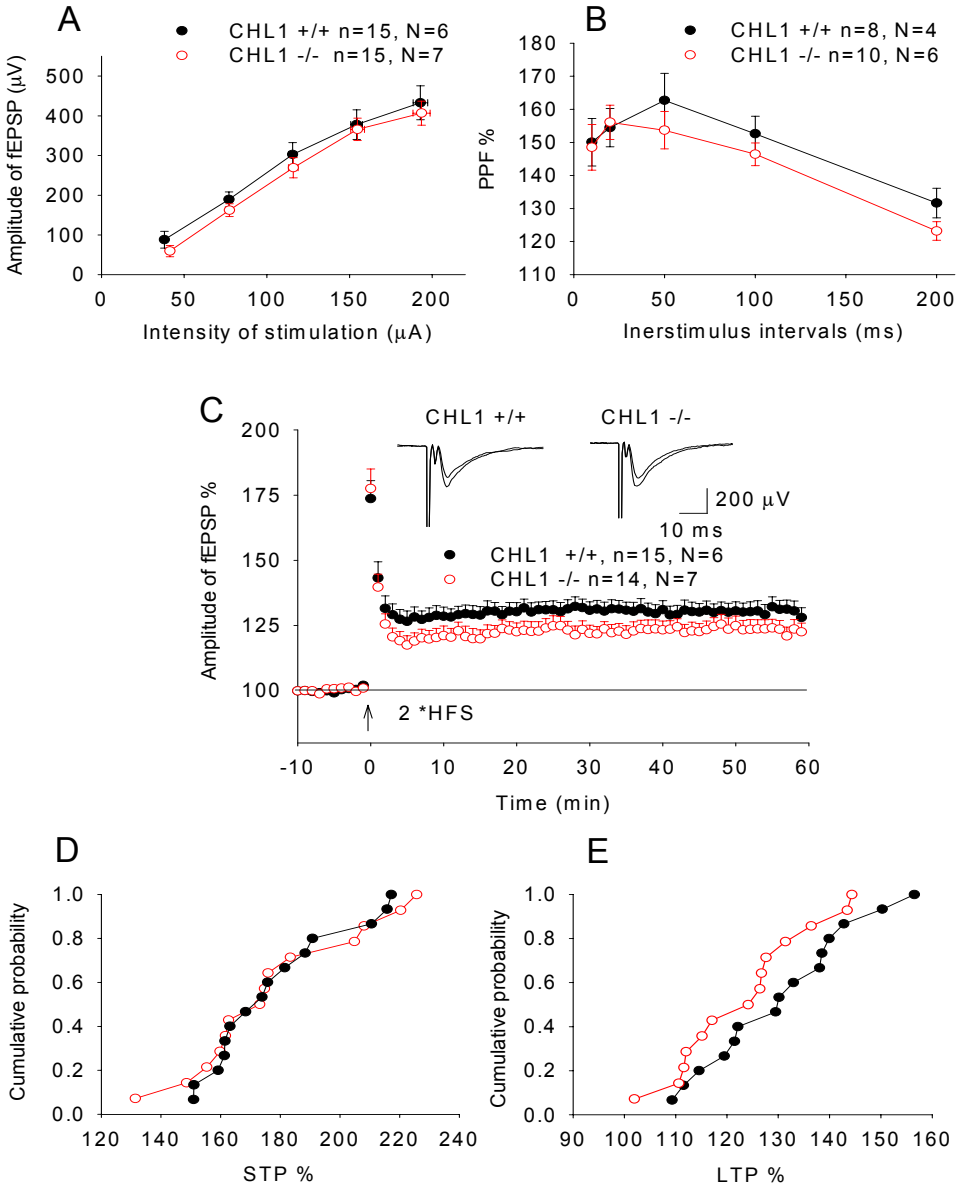

Figure 30. A) Input-output curves for amplitudes of fEPSPs evoked by stimulation of associational/commissural projections to the CA3 field at different stimulation strengths. B) Paired-pulse facilitation with 10, 20, 50, 100 and 200 ms interstimulus intervals. C) Short- and long-term potentiation induced by 2 trains of HFS. Upper panel shows fEPSPs recorded before and 50-60 min after HFS for both genotypes. D-E) Cumulative plots representing levels of short-term potentiation (PTP) measured 1 min after HFS (D) and long-term potentiation (LTP) measured 50-60 min after HFS (E). Each symbol represents a single experiment. Cumulative probability at any given value x is the probability to observe potentiation less or equal to x. N represents the number of tested mice, n is the number of tested slices.

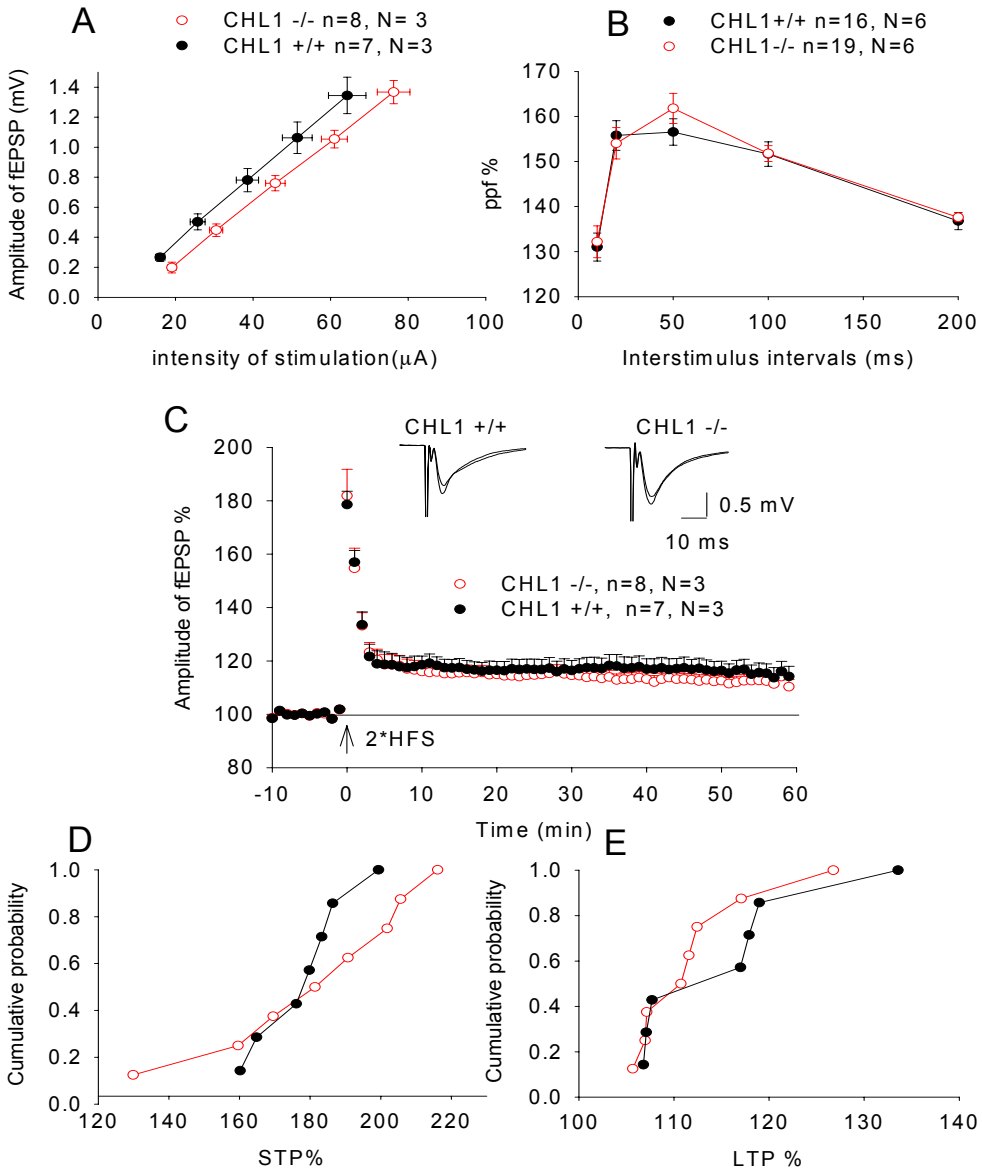

Figure 31. A) Input-output curves for amplitudes of fEPSPs evoked by stimulation of CA3 axons in the CA1 field at different stimulation strengths. B) Paired-pulse facilitation with 10, 20, 50, 100 and 200 ms interstimulus intervals. C) Short- and long-term potentiation induced by 2 trains of HFS. Upper panel shows fEPSPs recorded before and 50-60 min after HFS for both genotypes. D-E) Cumulative plots representing levels of STP measured 1 min after HFS (D) and LTP measured 50-60 min after HFS (E). Each symbol represents a single experiment. Cumulative probability at any given value x is the probability to observe potentiation less or equal to x. N represents the number of tested mice, n is the number of tested slices.

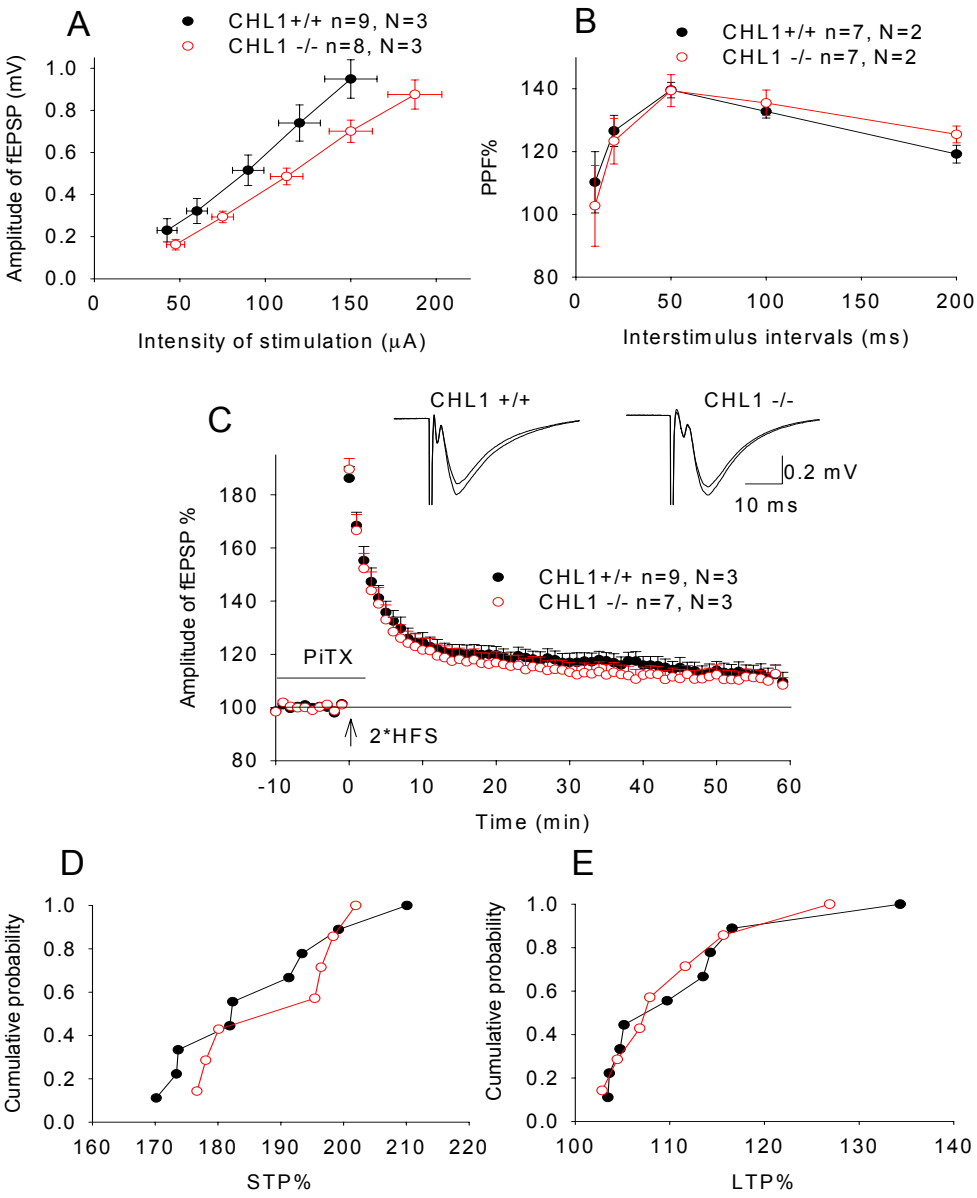

Figure 32. A) Input-output curves for amplitudes of fEPSPs evoked by stimulation of direct perforant path projections to the CA1 field at different stimulation strengths. B) Paired-pulse facilitation with 10, 20, 50, 100 and 200 ms interstimulus intervals. C) Short- and long-term potentiation induced by 2 trains of HFS. Upper panels show fEPSPs recorded before and 50-60 min after HFS for both genotypes. D-E) Cumulative plots representing levels of STP measured 1 min after HFS (D) and LTP measured 50-60 min after HFS (E). Each symbol represents a single experiment. Cumulative probability at any given value x is the probability to observe potentiation less or equal to x. N represents the number of tested mice, n is the number of tested slices.

3.7. Analysis of direct perforant path projections to the CA3 field

Neurons in the layer II of the entorhinal cortex send perforant path fibers to the dentate gyrus, and also provide a direct input to the CA3 field that is responsible for monosynaptic activation of CA3 pyramidal cells.

Analysis of direct perforant path projections to the CA3 field showed that there was no statistically significant difference in the maximal amplitude of responses between CHL1 constitutive knockouts and corresponding wild-types. Figure 33A shows that in CHL1+/+ the maximal amplitude of fEPSP was 0.75±0.05 mV and in CHL1-/- it was 0.71±0.03 mV. For induction of these responses we used maximal intensity of stimulation which in case of CHL1+/+ was 150.0±7.4 μA and for CHL1-/- mice was 158.4±11.3 μA. ANOVA did not show statistically significant difference in terms of intensity of stimulation and amplitude of responses.

No difference was also observed for paired-pulse facilitation with 10, 20, 50, 100 and 200 ms interstimulus intervals (Figure 33B).

Two trains of HFS delivered with 100% of stimulation intensity to disinhibited slices evoked STP which was 193.1±5.2 % in CHL1+/+ mice and 183.5±7.5 % in CHL1-/- ones. The level of LTP was 114.2±2.5 % in CHL1+/+ and 112.8±3.1 % in CHL1-/- animals (Figure 33C).

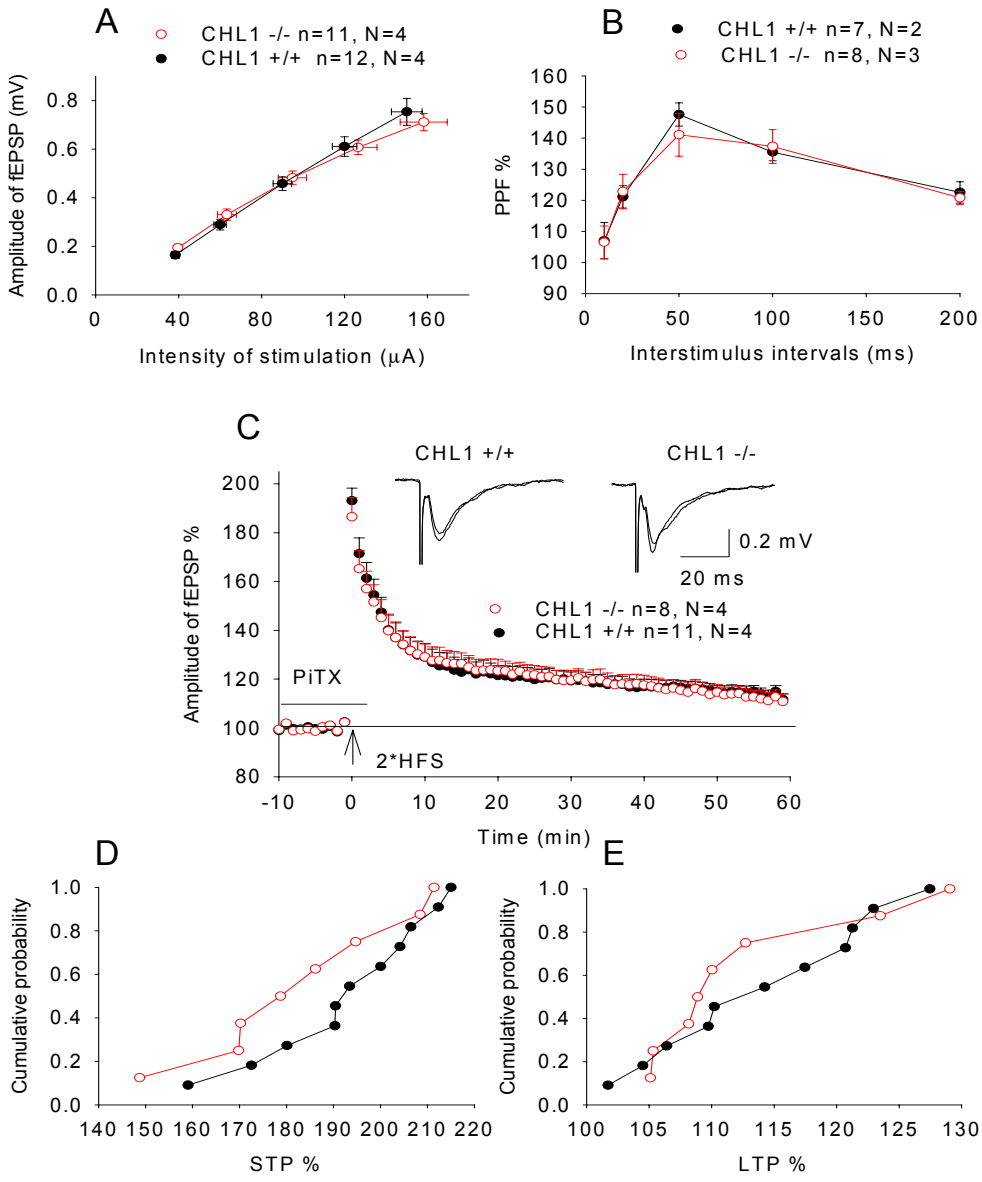

Figure 33. A) Input-output curves for amplitudes of fEPSPs evoked by stimulation of direct perforant path projections to the CA3 field at different stimulation strengths. B) Paired-pulse facilitation with 10, 20, 50, 100 and 200 ms interstimulus intervals. C) Short- and long-term potentiation induced by 2 trains of HFS. Upper panel shows fEPSPs recorded before and 50-60 min after HFS for both genotypes. D-E) Cumulative plots representing levels of short-term potentiation (STP) measured 1 min after HFS (D) and long-term potentiation (LTP) measured 50-60 min after HFS (E). Each symbol represents a single experiment. Cumulative probability at any given value x is the probability to observe potentiation less or equal to x. N represents the number of tested mice, n – the number of tested slices.

3.8. Summary for 3 month-old CHL1 constitutive knockout mice

To summarize data received from 3 month-old CHL1 constitutive knockout mice and corresponding wild-types, I would like to introduce the summary table, which shows basal synaptic transmission, paired-pulse facilitation; short- and long-term potentiation in knockout mice.

Parameter	LPP-DG	MPP-DG	MF-CA3	A/C-CA3	S/C-CA1	PP-CA1	PP-CA3
Basal Synaptic Transmission	↑	↑	=	=	=	=	=
Paired-Pulse Facilitation (PPF)	=	=	=	=	=	=	=
Post-Tetanic or Short-term Potentiation (PTP or STP)	=	=	=	=	=	=	=
Long-Term Potentiation (LTP)	=	=	=	=	=	=	=
Frequency Facilitation			=				

LPP, lateral perforant path; MPP, medial perforant path; MF, mossy fibers; A/C, associational/commissural projections; S/C, Schaffer collateral/commissural projections; PP, direct perforant path projections; DG, dentate gyrus; CA1 and CA3, subfields of the hippocampus. =, parameter is equal in knockout and wild type animals; ↓ , parameter is less in knockouts than in wild type mice; ↑ , parameter is increased in knockouts.

3.9. Analysis of Schaffer collateral/commissural projections to the CA1 field in 1 month-old animals

After 3 month-old CHL1 constitutive knockout animals did not show any serious abnormalities in all main excitatory hippocampal pathways, we decided to check whether there were some alterations in mice of other ages.

Since the Schaffer collateral projections to the CA1 field are considered to be very vulnerable, we decided to focus our attention on this pathway.

As Figure 34A shows, there was no statistically significant change in terms of maximal amplitude of responses and intensity of stimulation in CHL1 constitutive knockout animals at one month of age. Analysis revealed that maximal amplitude of fEPSPs in CHL1+/+ mice was 1.30±0.06 mV and in CHL1-/- it was 1.13±0.06 mV. The maximal stimulation intensity required for the induction of these responses in CHL1+/+ was 118.0±7.6 μA and in CHL1-/- – 120.0±14.3 μA.

Paired-path facilitation with 10, 20, 50, 100 and 200 ms interstimulus intervals did not show any abnormalities in 1 month-old CHL1 constitutive knockout mice (Figure 34B).

For induction of long-term potentiation, we used 5 trains of TBS which evoked statistically significantly stronger short- and long-term potentiation in wild-types, than in knockout mice (Figure 34C). Level of STP in CHL1+/+ was 183.34±8.46% and in CHL1-/- it was 143.54±4.24%, $P<0.01$. The level of LTP in CHL1+/+ was 148.41±4.51% and in CHL1-/- it was 123.69±3.11%, $P<0.01$.

Possible mechanisms underling impairment of LTP at Schaffer collateral/commissural-CA1 synapses in 1 month-old CHL1-/- mice

Since there was a strong reduction in both STP and LTP in CHL1-/- mice, we decided to verify whether this phenotype is due to enhanced inhibitory transmission in the CA1 field, which may impair induction of LTP at Schaffer collateral/commissural projections to the CA1 field. For this purpose we recorded long-term potentiation in above mentioned projections in the presence of 100 μM picrotoxin.

Figure 35A shows that in disinhibited slices 5xTBS induced similar short- and long-term potentiation. Level of STP in CHL1+/+ mice was 178.69±12.34% and in CHL1-/- it was 203.39±16.79%. The level of LTP in CHL1+/+ was 161.88±11.45% and in CHL1-/- – 152.41±12.49%.

Based on these results we presume that impairment of LTP could be due to the increased GABAergic inhibitory activity in CHL1 constitutive knockout mice.

3.10. Analysis of Schaffer collateral/commissural projections to the CA1 field in 2 month-old animals

Next we investigated 2 month-old animals using TBS protocol. As it is shown in Figure 36A no statistically significant change was observed in terms of basal synaptic activity at Schaffer collateral/commissural synapses in the CA1 field, as we descriebed above for the series of experiments using HFS. Maximal amplitude of responses in CHL1+/+ was 1.06±0.06 mV and in CHL1-/- – 0.93±0.04 mV. Maximal intensity of stimulation which induced these fEPSPs in CHL1+/+ was 73.0±7.60 μA and in CHL1-/- it was 76.36±3.63 μA.

Analysis of paired-pulse facilitation with ANOVA test showed that there was no statistically significant difference between genotypes for all tested interstimulus intervals (Figure 36B).

Five trains of TBS induced similar short- and long-term potentiation in both genotypes. Figure 36C shows that in CHL1+/+ STP was 155.47±7.87% and in CHL1-/- – 170.27±8.48% and the level of LTP in CHL1+/+ was 129.19±4.48% and in CHL1-/- it was 131.80±2.94%.

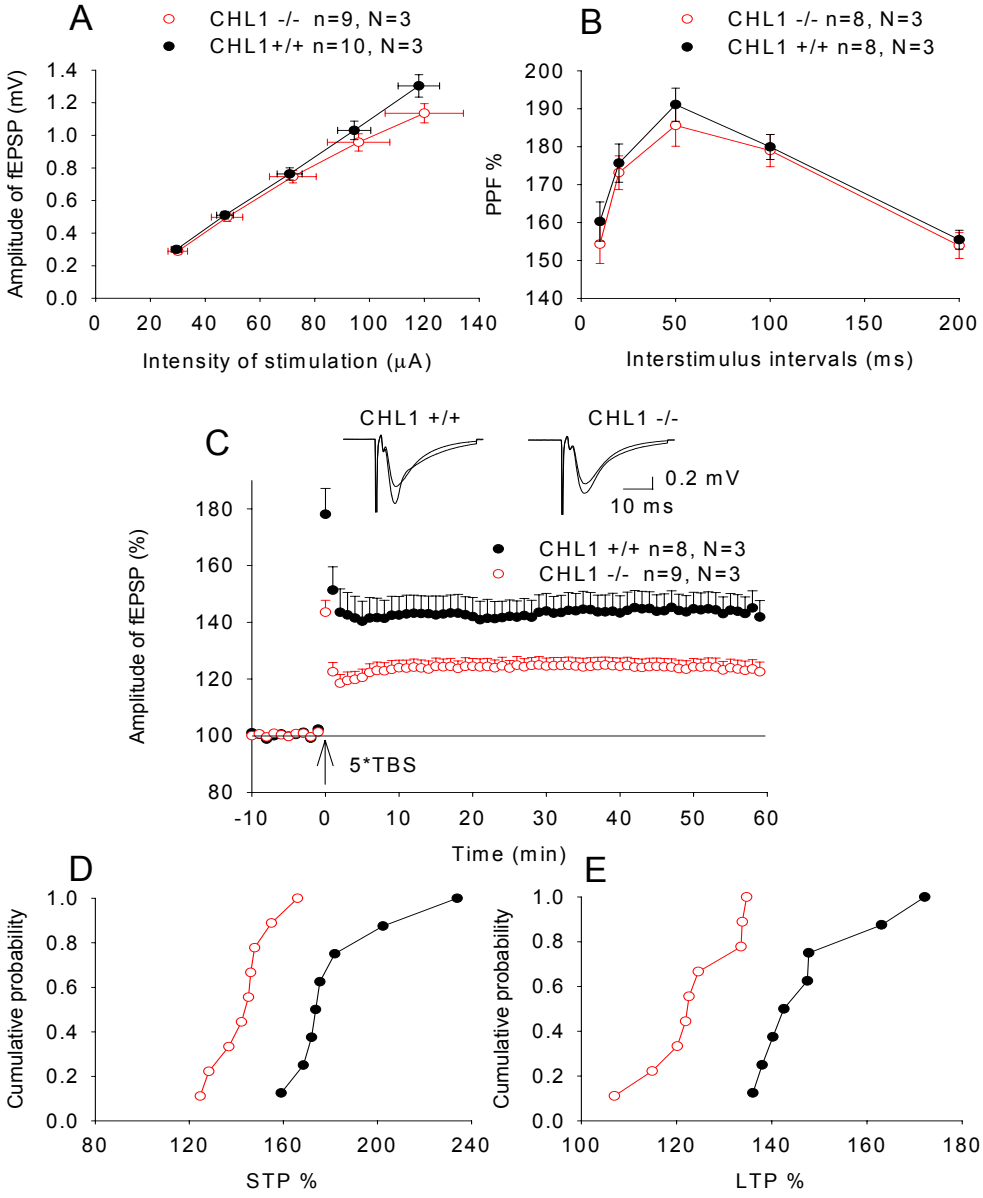

Figure 34. A) Input-output curves for amplitudes of fEPSPs evoked by stimulation of Schaffer collateral/commissural projections to the CA1 field at different stimulation strengths. B) Paired-pulse facilitation with 10, 20, 50, 100 and 200 ms interstimulus intervals. C) Short and long-term potentiation induced by 5 trains of TBS. Upper panel shows fEPSPs recorded before and 50-60 min after TBS for both genotypes. D-E) Cumulative plots representing levels of short-term potentiation (STP) measured 1 min after TBS (D) and long-term potentiation (LTP) measured 50-60 min after TBS (E). Each symbol represents a single experiment. Cumulative probability at any given value x is the probability to observe potentiation less or equal to x. N represents the number of tested mice, n – the number of tested slices.

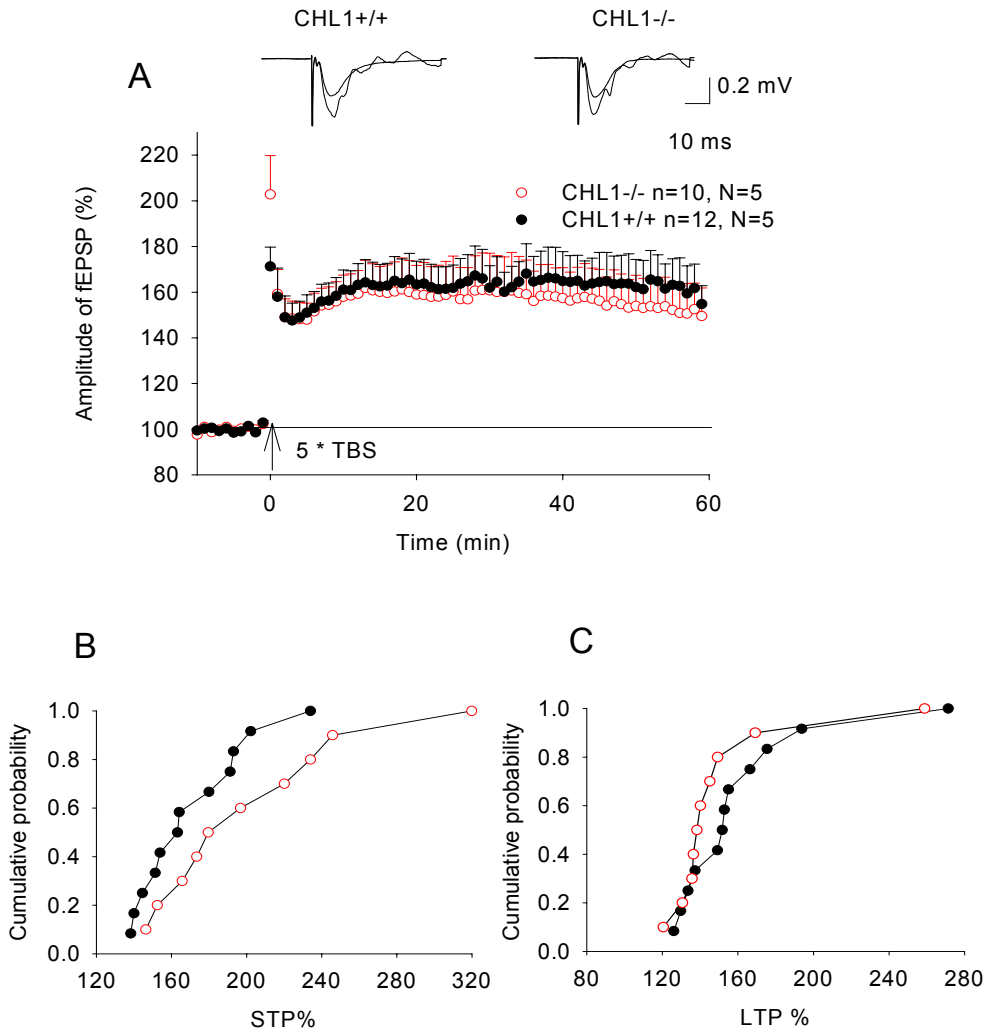

Figure 35. A) Short- and long-term potentiation induced by 5 trains of TBS applied to Schaffer collateral/commissural projections to the CA1 field. Upper panel shows fEPSPs recorded before and 50-60 min after TBS for both genotypes. B-C) Cumulative plots representing levels of short-term potentiation (STP) measured 1 min after TBS (B) and long-term potentiation (LTP) measured 50-60 min after TBS (C). Each symbol represents a single experiment. Cumulative probability at any given value x is the probability to observe potentiation less or equal to x. N represents the number of tested mice, n – the number of tested slices.

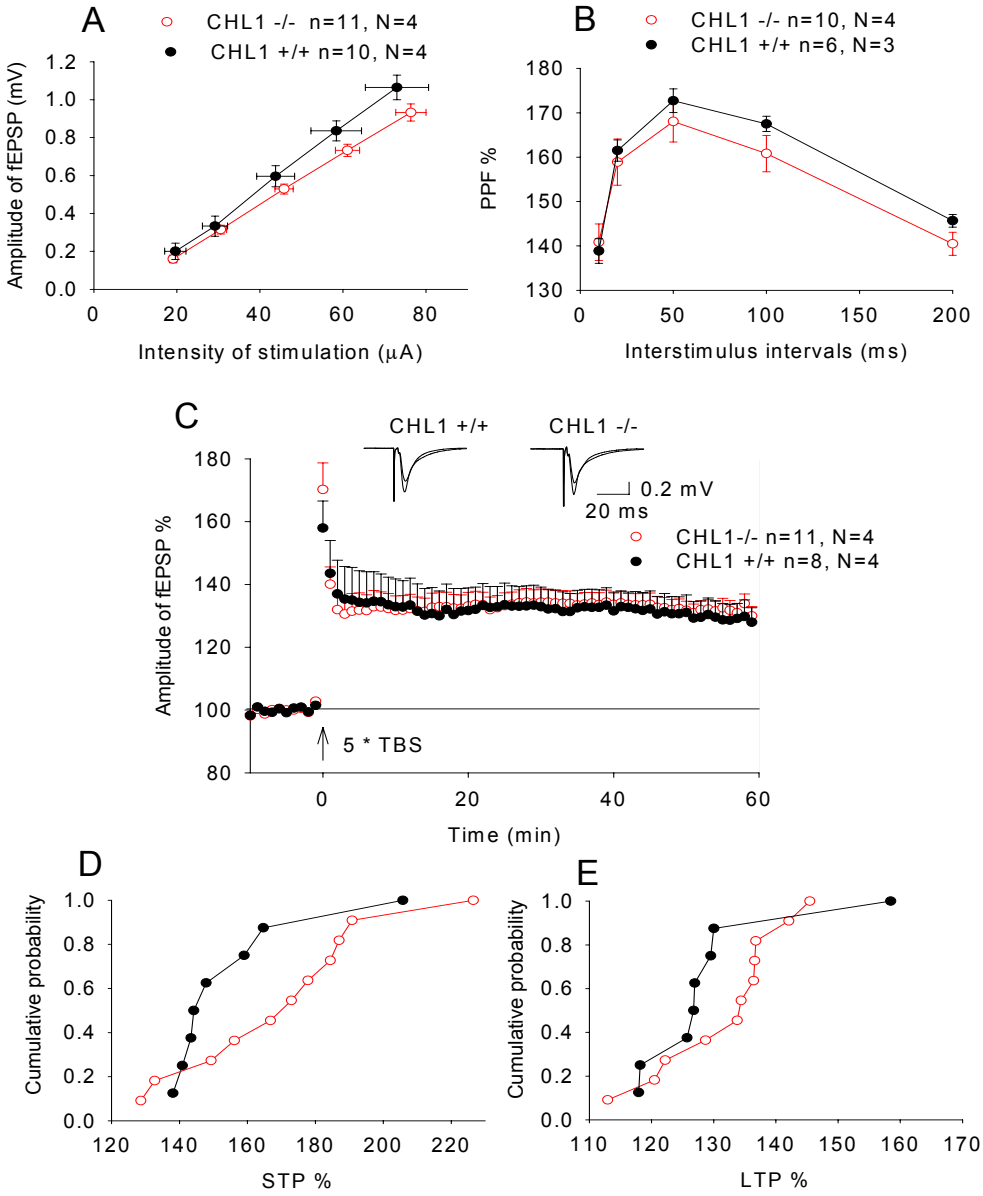

Figure 36. A) Input-output curves for amplitudes of fEPSPs evoked by stimulation of Schaffer collateral/commissural projections to the CA1 field at different stimulation strengths. B) Paired-pulse facilitation with 10, 20, 50, 100 and 200 ms interstimulus intervals. C) Short- and long-term potentiation induced by 5 trains of TBS. Upper panel shows fEPSPs recorded before and 50-60 min after TBS for both genotypes. D-E) Cumulative plots representing levels of short-term potentiation (STP) measured 1 min after TBS (D) and long-term potentiation (LTP) measured 50-60 min after TBS (E). Each symbol represents a single experiment. Cumulative probability at any given value x is the probability to observe potentiation less or equal to x. N represents the number of tested mice, n – the number of tested slices.

3.11. Analysis of Schaffer collateral/commissural projections to the CA1 field in 9 month-old animals

The last age group we studied was 9 month-old mice. Figure 37A shows that there was a tendency of decreased basal synaptic activity in CHL1 constitutive knockouts, but it did not reach statistical significance. Maximal amplitude of fEPSP in CHL1+/+ mice was 0.83±0.06 mV and in CHL1-/- – 0.77±0.05 mV. The maximal intensity of stimulation necessary for induction of these responses in CHL1+/+ was 73.75±3.96 μA and in CHL1 -/- it was 68.58±6.43 μA. ANOVA analysis did not show any statistically significant differences between two genotypes, and comparison with two month-old animals revealed that responses were smaller in aged mice than in younger ones and the difference was statistically significant with $P<0.05$.

No difference between genotypes was found in paired-pulse facilitation with 10, 20, 50, 100 and 200 ms interstimulus intervals (Figure 37B).

Five trains of TBS induced much higher levels of STP and LTP in wild-types, than in knockout mice ($P<0.05$). STP in CHL1+/+ was 168.21±7.40% and it did not show statistically significant difference from two months old animals, and the level of STP in CHL1-/- was 148.4±4.5%. Long-term potentiation in CHL1+/+ was 127.4±3.0%, and similarly to STP did not differ from two month-old wild-type animals. The level of LTP in CHL1-/- was however statistically significantly smaller than in wild-type mice (114.4±2.3%, $P<0.01$) (Figure 37C).

Our results suggest that the developmental state of the animal is important for the expression of abnormalities induced by CHL1 deficiency.

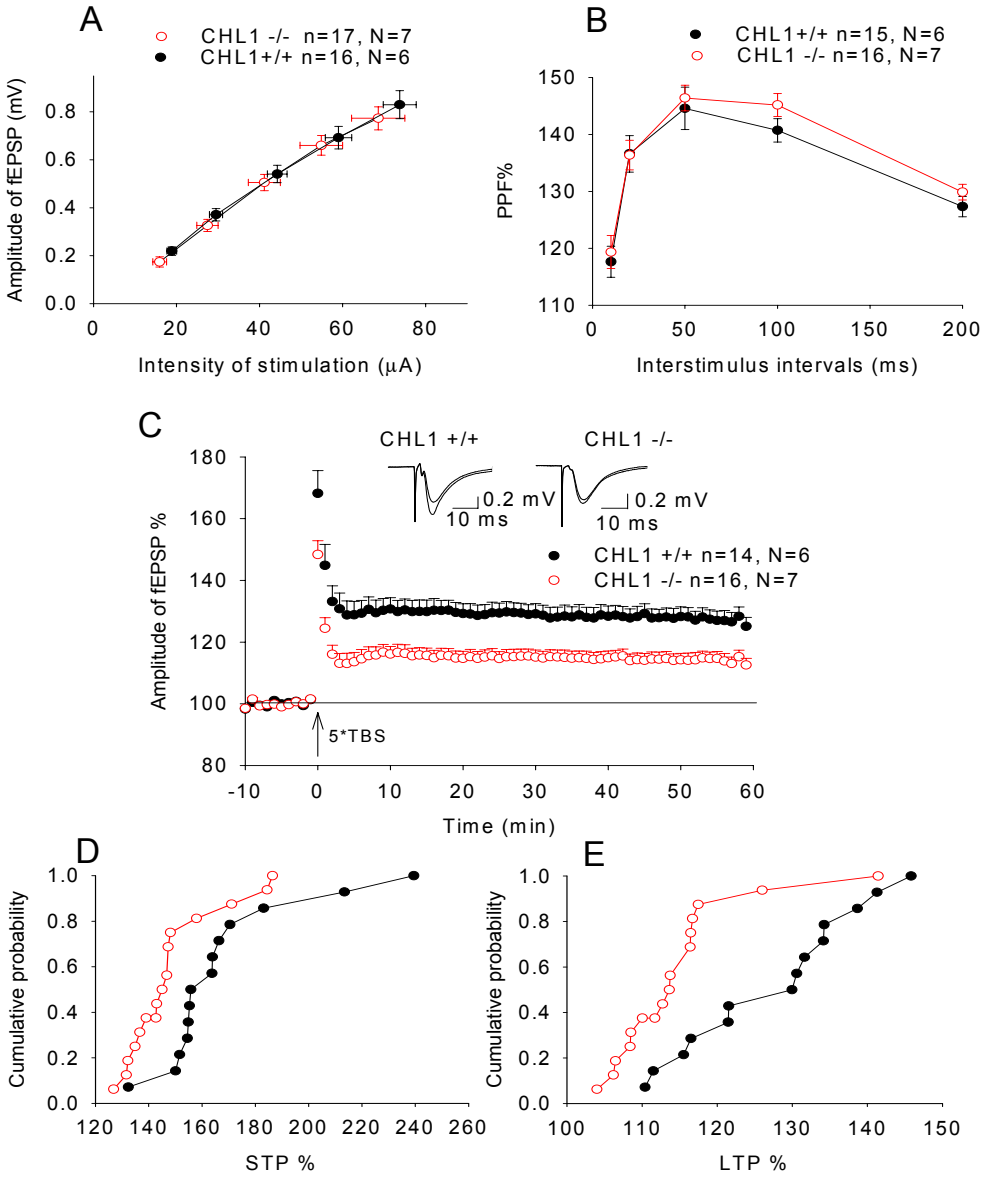

Figure 37. A) Input-output curves for amplitudes of fEPSPs evoked by stimulation of Schaffer collateral/commissural projections to the CA1 field at different stimulation strengths. B) Paired-pulse facilitation with 10, 20, 50, 100 and 200 ms interstimulus intervals. C) Short- and long-term potentiation induced by 5 trains of TBS. Upper panel shows fEPSPs recorded before and 50-60 min after TBS for both genotypes. D-E) Cumulative plots representing levels of short-term potentiation (STP) measured 1 min after TBS (D) and long-term potentiation (LTP) measured 50-60 min after TBS (E). Each symbol represents a single experiment. Cumulative probability at any given value x is the probability to observe potentiation less or equal to x. N represents the number of tested mice, n – the number of tested slices.

VIII. Discussion

Since neural cell adhesion molecules are not only implicated in cell interaction during nervous system development, but also have been recognized as important mediators of synaptic plasticity, we have been interested in analysis of different forms of plasticity in mice lacking one of two members of the immunoglobulin superfamily of cell adhesion molecules, L1 or CHL1.

Synaptic plasticity has been described in different parts of the brain, among them is the hippocampus, which is one of the most intensively studied areas in the central nervous system. Most of *in vitro* electrophysiological studies in the hippocampal formation have been done on Schaffer collateral/commissural projections to the CA1 field, because it is easy to find responses at these synapses and induce different forms of synaptic plasticity, including long-term potentiation. However, it is well known, that the hippocampal formation is a complex system and its complexity is related to multiple projections, which have different origin and targets. Therefore our investigation involved different excitatory synapses within the hippocampal formation, where we compared main physiological characteristics such as basal synaptic transmission, paired-pulse facilitation short- and long-term potentiation in L1 conditional, CHL1 constitutive knockouts and their corresponding wild-type mice.

In our study we used L1 conditional knockout mice that have been generated to dissociate the functional roles of L1 in the adult brain from developmental abnormalities. Previous investigations, dedicated to these knockouts, revealed that they showed different phenotype from that observed in L1 constitutive knockout mice. Namely, in contrast to constitutive ones these mutants did not show the overt morphological and behavioural abnormalities, but they had increased basal excitatory synaptic transmission in CA1 region of the hippocampus and decreased anxiety in the open field and elevated plus-maze. At the same time they shared some features with constitutive knockouts and among these features were altered place learning in the water maze and normal short- and long-term potentiation in the CA1 region (Bliss et al., 2000;Law et al., 2003). Thus, abnormalities in synaptic plasticity underlying impaired place learning in L1 mutants are most likely to be outside of CA3-CA1 synapses. Our main findings indicate that the conditional ablation of L1 molecule induces specific impairment of long-term potentiation in perforant path projections to pyramidal cells.

CHL1 shares the basic structural plan of L1 family members and it is a relatively newly identified member expressed in subpopulations of developing neurons in the central and peripheral nervous systems. CHL1 expression persists at low levels in the mature brain in areas of high plasticity (Hillenbrand et al., 1999; Liu et al., 2000). The structural resemblance and the differences between CHL1 and the other members of the L1 family of CAMs suggest that this

molecule might have both similar and distinct functions. Our results show that the deficiency in CHL1 molecule does not cause any severe electrophysiological abnormalities in young adult CHL1 constitutive knockout mice, except for elevated levels of basal synaptic transmission in the dentate gyrus. However, it leads to impairment of synaptic plasticity in juvenile and aged mice.

1. Deficiency in L1 induces synapse specific impairments in adult mouse hippocampus

Analysis of several excitatory pathways in the hippocampal formation of adult L1 conditional knockout mice revealed that ablation of L1 during the development affects long-term potentiation only at certain synapses, while others stay intact.

As mentioned above, the previous study of Schaffer collateral/commissural projections to the CA1 field showed that there was no difference between adult L1 conditional knockouts and corresponding wild-types in terms of short- and long-term potentiation, but basal synaptic activity was significantly elevated in knockout animals (Law et al., 2003). The normal relationship between stimulation strength and amplitude of presynaptic fiber volley in L1 conditional knockout mice suggested that L1 deficiency led to an increased postsynaptic response generated by a single axon rather than to modifications in the threshold of excitability of Schaffer collaterals. Additional analysis of polyspiking activity indicated that activity-dependent disinhibition and excitability of CA1 pyramidal cells were also normal in *L1fy*+ mice (Law et al., 2003).

Our present experiments revealed that, similarly to Schaffer collateral/commissural projections to the CA1 field, no difference was observed in terms of long-term potentiation at medial and lateral perforant path projections to the dentate gyrus, and mossy fiber and associational/commissural projections to the CA3 field. In contrast to Schaffer collateral/commissural pathway, no elevation was detected in basal synaptic activity. Above described data indicate that, upon deficiency in L1 molecule signal transfer from the entorhinal cortex to the hippocampus along the trisynaptic pathway is without any gross abnormalities in young adult conditional knockout mice.

Transmission of signals via dentate gyrus is not the only way that information reaches the hippocampus, an additional possibility is by direct perforant path projections, which originate from superficial layers of the entrohinal cortex and bring information to the CA3 and CA1 fields. In spite of a fact that both perforant path fibers come from the entorhinal cortex they do not have the same origin. Fibers projecting to the CA3 field come from layer II of the entorhinal cortex,

and fibers projecting to the CA1 field arise from layer III (Johnston and Amaral, 2004). Our study highlights that, although the short-term potentiation is unaltered at direct perforant path projections, the long-term potentiation is impaired in L1 conditional knockout mice. The striking fact is that both synapses are located in the stratum lacunosum-moleculare of the CA1 and CA3 fields, which includes distal parts of the pyramidal apical dendrites. This fact could be of special interest since the staining of adult rat hippocampus with L1 antibodies revealed that there is relatively high expression of L1 in the stratum lacunosum-moleculare and mossy fiber bundles (Schuster et al., 2001; Law et al., 2003). Thus, combined data suggest that synaptic plasticity in direct perforant path projections to the CA1 and CA3 fields may be important for normal place learning, which is altered in L1 conditional knockout mice (Law et al., 2003).

1.1. Deficit in voltage-dependent Ca^{2+} channels underlies impairment in LTP at the direct perforant path projections to the CA3 field in L1 conditional knockout mice

After discovering the impairment of LTP at the direct perforant path projections to the CA1 and CA3 fields, we performed pharmacological analysis to dissect which receptors or channels could underlie this abnormality. Since long-term potentiation is considered to be related to the elevation of intracellular Ca^{2+} concentration (see the review of the literature), the most interesting candidates were NMDA receptors and voltage-dependent Ca^{2+} channels (VDCCs).

The role of NMDA receptors was assessed by using of APV (the antagonist of the NMDA receptor). Our investigation showed that a blockade of the NMDA receptors resulted in a decrease in the level of short-term potentiation and a block of LTP. This result is in accordance with published data in rats (McMahon and Barrionuevo, 2002), and demonstrates that NMDA receptors are absolutely crucial for induction of LTP at above-mentioned synapses in both L1 deficient and wild-type mice.

Voltage-dependent Ca^{2+} channels provide another major route of Ca^{2+} entry in neurons and play a crucial role in many forms of synaptic plasticity, since they couple membrane depolarization to Ca^{2+}-dependent signal transduction. Electrophysiological investigation of these channels in L1 conditional knockout mice was of particular interest since several studies have demonstrated modulation of VDCCs by cell adhesion molecules. For instance, it has been found that the infusion of the soluble juxtamembrane domain of N-cadherin into chick ciliary neurons caused a substantial decrease in the amplitude of the high-threshold voltage-activated calcium current and this effect was reversed by inhibition of RhoA or its downstream effector, Rho-associated kinase (Piccoli et al., 2004). Studies dedicated to the influence of integrins on VDCCs uncovered that alphavbeta3 and alpha5 beta1 integrins differentially linked through intracellular

signaling pathways to the L-type Ca^{2+} channel and thereby altered control of Ca^{2+} influx in vascular smooth muscle. Antibodies against alphavbeta3 had inhibitory effect and insoluble antabodies against alpha5 beta1 - enhancing effect on VDCC currents (Wu et al., 1998). Alpha5beta1 integrin appears to regulate the function of the L-type calcium channel via a tyrosine phosphorylation cascade involving Src and various focal adhesion proteins (Wu et al., 2001). L1 and its binding partner NCAM are also known to influence voltage-dependent Ca^{2+} channels in cell lines or developing neurons. Addition of L1 and NCAM antibodies, and the purified molecules themselves, elicited cell type-specific responses that could be modulated by the substrate on which the cells were maintained. Depending on the cell type, cells responded to the addition of the purified molecules, by a rise in intracellular Ca^{2+} levels, which could be either dependent or independent of the opening of VDCCs. In neurons, extracellular homophilic binding or binding of antibodies led to an increase of L- and N-type Ca^{2+} currents via second messenger pathway involving a pertussis-toxin sensitive trimeric G-protein (Bohlen Und et al., 1992).

Our experiments in adult hippocampal neurons showed that pharmacological manipulations with L-type VDCCs using the antagonist nifedipine and agonist BAY K 8644 abolished observed difference in LTP at direct perforant path synapses to the CA3 field between L1fy- and L1fy+ mice. Application of nifedipine caused statistically significant decrease of LTP level in wild-type animals, while knockouts were not much affected. This is very similar to the outcome of a previous study on mice deficient in extracellular matrix glycoprotein tenascin-C (Evers et al., 2002), in which nifedipine reduced LTP in CA3-CA1 synapses in wild-type but not tenascin-C deficient mice. Application of BAY K 8644 had an opposite, increasing, effect on long-term potentiation in L1 deficient mice, while it had no effect in wild-types. Since both treatments abolished the statistically significant difference between genotypes, it is plausible to conclude that the observed difference could be due to the impaired action of voltage-dependent Ca^{2+} channels in L1 conditional knockout mice.

1.1.1. Influence of L1 on L-VDCC currents

Since pharmacological manipulations with L-type VDCCs eliminated difference in long-term potentiation observed at direct perforant path synapses to the CA3 field, next logical step was to check the influence of L1 molecule on Ca^{2+} currents. Also previous studies have revealed that there is a connection between L1, Ca^{2+} channels, intracellular Ca^{2+} concentration and downstream cascades. Investigations related to the influence of cell adhesion molecules on the second messenger system demonstrated that application of polyclonal anti L1 and NCAM antibodies to the rat PC12 pheochromocytoma cell line induced an increase in intracellular Ca^{2+}

concentration. Since blockers of voltage-dependent Ca^{2+} channels (verapamil and diltiazem) had a suppressing effect on this increase, these data suggest that L-type VDCCs were at least partially responsible for elevations of intracellular Ca^{2+} level (Schuch et al., 1989).

It has also been demonstrated that L1 as well as several other cell adhesion molecules such as NCAM and N-cadherin (Povlsen et al., 2003) promote neurite outgrowth by activating a second messenger pathway that involves influx of Ca^{2+} via VDCCs into neurons as a consequence of activation of an FGF (fibroblast growth factor) receptor and production of arachidonic acid. The CaM kinase activity is specifically required downstream of calcium influx in the cell adhesion molecule and FGF signaling pathway leading to axonal growth (Williams et al., 1995).

Our experiments, in which we investigated Ca^{2+} currents in L-type VDCC-transfected CHO cells, no difference between cells grown on control or L1 coated substrates in terms of amplitude and density of peak and steady-state Ca^{2+} currents was found. This indicates that there was no direct *trans* action of L1 molecule on L-type VDCCs composed of Cav1.2 channel subunit α_1 and two subunits β_1b and $\alpha_2\delta_1$. However, it should be taken into consideration that there are several different combinations of α and auxiliary subunits resulting in different functional L-type voltage-dependent Ca^{2+} channel and only one of these combinations was investigated in the present study. Thus, we can not exclude that L1 directly interacts with other subtype of L-type VDCCs. Another possibility is that L1 may interact with channels in a *cis* configuration, although it is unlikely in view of preferential presynaptic expression of L1 and postsynaptic localization of L-type VDCCs involved in induction of LTP. Other scenarios may involve interactions between L1 and other molecules that modulate L-type VDCCs, for instance, interactions between L1 and FGF receptors (Povlsen et al., 2003), or between L1 and integrins (Felding-Habermann et al., 1997;Montgomery et al., 1996). Since L1 affects diverse second messenger systems, such as MAP kinase and inositol phosphates (Bohlen et al., 1992; Schuch et al., 1989), it is also plausible to assume that L1 may affect expression of these channels.

1.2. Modulating effect of the cholinergic system on excitatory synapses of the CA3 field in L1fy- and L1fy+ animals

The cholinergic system is involved in higher brain functions, including attention, learning and memory (Blokland, 1995). It has been shown that pharmacological manipulations of cholinergic system had modulating effect on neocortical LTP. The cholinergic agonist facilitated long-term potentiation induction and the antagonist blocked it in a component-specific modulatory manner (Boyd et al., 2000). It has also been shown that physiologically released acetylcholine enhances synaptic plasticity in the CA1 field of the hippocampus through the

postsynaptic M_1 subtype of muscarinic receptor activation (Shinoe et al., 2005). Acetylcholine may act not only on muscarinic, but also on nicotinic receptors. Experiments have shown that nicotine facilitates the induction of long-term potentiation in the hippocampal CA1 region. Mechanisms underlying this effect could be that nicotine has desensitizing effect on alpha7 nicotinic acetylcholine receptors, which are present on feedforward interneurons. Activation of these receptors by acetylcholine prevents LTP induction by inhibiting pyramidal cells. Nicotine reduces this inhibitory influence and hence causes facilitation of LTP (Yamazaki et al., 2005).

Muscarinic cholinergic agonists are also shown to affect synaptic plasticity in the CA3 region of the hippocampal slice. Long-term potentiation of the mossy fiber-CA3 synapse was blocked by muscarine. Low concentrations of muscarine (1 μM) had a little effect on low-frequency synaptic stimulation but significantly reduced the magnitude and probability of LTP induction (Williams and Johnston, 1988). It has also been shown that application of muscarinic acetylcholine receptor agonists to hippocampal slices produces network oscillations (Fisahn et al., 2002). Intracortical application of cholinergic antagonists showed that the enhancement of gamma oscillations and response synchronization is mediated by acetylcholine and muscarinic receptors (Rodriguez et al., 2004). Cholinergic projections have selective blocking effect on different excitatory synapses of the CA3 field (Vogt and Regeher, 2001).

Our study showed that activation of cholinergic system by its agonist muscarine, caused a reduction of field EPSPs not only at associational/commissural – CA3 synapses, but also at direct perforant path synapses to the same field. As expected from previous studies (Hasselmo and Schnell, 1994), the effect of muscarine was stronger at intrinsic, i.e. associative, than at extrinsic, i.e. formed by cortical axons, projections. This might be important for suppressing intrinsic activity of the CA3 neurons and increase an impact of sensory information coming from the entorhinal cortex. Muscarinic treatment of slices strongly decreased the level of long-term potentiation in both projections, which most likely is a secondary effect to the reduction of fEPSPs, since such reduction leads to low levels of depolarization during theta-burst stimulation.

Comparison of cholinergic modulation of associational/commissural and perforant path projections to the CA3 field in L1fy- and L1fy+ mice revealed that there was no genotype-specific difference either in terms of the level of block of responses by muscarine and the level of potentiation induced by high-frequency stimulation at both types of synapses.

2. Co-activation of the associational/commissural and perforant path projections has inhibitory effect on the perforant path – CA3 synapses

Investigation of synaptic transmission and plasticity at a specific excitatory connection is of a great importance and interest to understand mechanisms of signal processing at this synapse.

However, in the brain, different types of synapses do not work separately from each other. Therefore it is very interesting to investigate characteristics of functional interactions between different projections.

For this purpose we focused our attention on the CA3 field of the hippocampus which is abundant in various fibers differing in their origin and projections. We investigated characteristics of communication between the associational/commissural and perforant path synapses in the CA3 field and found out that indeed, there is an interaction between these projections and associational/commissural fibers have suppressing effect on the perforant path – CA3 synapses. Interestingly this inhibitory effect is abolished by picrotoxin ($GABA_A$ receptor antagonist), which indicates that the effect of associational/commissural fibers on perforant path-CA3 synapses could be mediated by feed forward inhibition.

In contrast to inhibitory influence of associational/commissural pathway on direct perforant path synapses in the CA3 field, perforant path fibers have no effect on the associational – CA3 synapses. Our findings might mean that, reverbaration of the signal within the CA3 field along the associational/commissural fibers decreases the input of new sensory information from the entorhinal cortex.

3. Deficiency in CHL1 does not induce any gross physiological abnormalities in adult mouse hippocampus

Like for L1 conditional knockout mice, in adult CHL1 constitutive ones all available excitatory hippocampal pathways have been checked and revealed that deficiency in CHL1 molecule did not cause any gross electrophysiological abnormalities in all investigated projections. However, the intensity of stimulation used to elicit maximal fEPSPs in medial and lateral perforant path projections was significantly smaller in CHL1 deficient than wild-type animals, although there were no alterations in terms of amplitudes of responses, short- or long-term potentiation. Based on the fact that prespike-presynaptic fiber volley was similar for both genotypes in medial and lateral perforant path fibers, one can assume that in CHL1 deficient mice excitability of fibers was higher than in corresponding wild-types.

There are several studies showing that altered basal synaptic activity in the dentate gyrus could be related to different behavioural paradigms. For example, various degrees of periodic novel environment exposure for 19 days in freely moving rats led to increased fEPSPs in the dentate gyrus of the hippocampus, but only when animals were kept in nominally low-stress housing conditions. However, enriched environment exposure did not change the level of long-term potentiation induced by a moderately strong high-frequency tetanus (Irvine et al., 2006). Since the main behavioural alteration shown by CHL1 knockout mice is a delayed reactivity to

respond and possibly detect environmental stimuli, one can think that these mice are impaired in extracting relevant information from the environment (Morellini; Kähler and Schachner, unpublished data). In this context, it is noteworthy that the dentate gyrus is the primary input of information coming from the entorhinal cortex and acts as an interface between the hippocampus and the rest of the cortical mantle. In light of enhanced basal excitatory synaptic transmission in the dentate gyrus of CHL1 deficient mice it is tempting to speculate that this abnormality could lead to a lower signal-to-noise ratio (i.e. ratio between activity elicited by an environmental stimulus and baseline activity) in CHL1 knockout mice, explaining why they have some deficits in detecting and processing the relevant information among the diverse environmental stimuli to which they are exposed. Altered basal synaptic activity in the dentate gyrus is also of a great interest in light of altered exploratory behavior observed in CHL1 knockout mice (Montag-Sallaz et al., 2002), since learning through exploration was demonstrated to increase synaptic field potentials in the dentate gyrus and was accompanied by formation of new synapses (Andersen et al., 1996).

Morphological data show that in CHL1 constitutive knockouts the mossy fiber projections are misguided (Montag-Sallaz et al., 2002; Demyanenko et al., 2004). Since it has been shown that in NCAM knockout mice abnormal lamination of mossy fibers corresponds to abolished LTP (Cramer et al., 1998) one could expect to find abnormal electrophysiological properties of mossy fiber synapses in CHL1 knockouts too, but our study showed that despite altered morphology, electrophysiologically these synapses were normal and neither frequency-dependent facilitation, nor short- and long-term potentiation were different between knockout and wild-type mice. Thus, our study provides an example showing a lack of one-to-one relationships between morphological and electrophysiological abnormalities in mossy fiber synapses.

Further analyses of basal synaptic transmission, paired-pulse facilitation and high frequency-induced short- and long-term potentiation at associational/commissural – CA3, Schaffer collateral/commissural – CA1, direct perforant path – CA3 and – CA1 synapses demonstrated that absence of CHL1 molecule did not cause any alterations in young adult mice. This perfectly corresponds to behavioral observations, according to which CHL1 deficient mice exhibit normal cognitive function in the step-through passive avoidance and spontaneous alternation tests (Morellini, Kähler and Schachner, unpublished data).

3.1. Different influences of CHL1 on Schaffer collateral/commissural - CA1 synapses in various age groups

Changes that take place in the nervous system during individual development are always of a great importance. Morphological analysis of CHL1 knockout mice revealed an age-dependent changes in different morphological characteristics (Thilo, Irintchev and Schachner, unpublished data). Evaluation of gross-anatomical parameters demonstrated various alterations of brain wet weight in different age groups of CHL1 knockout mice. Brain mass of the CHL1-/- was smaller at 1 month of age (-6%), similar at 2 months and 8% -10% larger at 6 and 12 months. Similar age-related differences were observed for the brain volume. Accordingly, specific weight (unit mass per unit volume) was similar in CHL1-/- and CHL1+/+ littermates. Investigation of numerical density (i.e., number per unit volume) of all cells, in the motor cortex revealed that while no difference between 2-month-old CHL1+/+ and CHL1-/- animals was found, the total cell density in the cortex of 6- and 12-month-old mutant mice was significantly lower compared to the age-matched control animals. The density of microglial cells in the hippocampus also showed age-dependent alterations. At 1 and 2 months of age it was abnormally high in knockout mice, but no abnormalities were detected in 6 and 12 months old animals. Number of PV^+ interneurons, was also varying during development. In 3 week-old mice, the number of PV^+ interneurons was 94% higher in CHL1 deficient mice than in wild-types (Nikonenko et al., 2006). At 2 months of age no difference between knockouts and controls was observed, while at 6 and 12 months they declined to about 80% of the values estimated for control mice. All above described data indicate that CHL1 deficiency caused age-dependent alterations, which stimulated us to investigate electrophysiological characteristics in different age groups.

Our investigation revealed that in young mice deficiency in CHL1 molecule was crucial for theta-burst induced short- and long-term potentiation while basal synaptic transmission and paired-pulse facilitations were not altered. We focused our attention on inhibitory transmission, based on morphological and electrophysiological data, according to which in young CHL1 constitutive knockout mice the length and linear density of active zones in symmetric synapses on CA1 pyramidal cell bodies, and number of perisomatic puncta containing inhibitory axonal markers were increased. Density and total number of parvalbumin-positive interneurons was very high and perisomatic inhibitory currents were also increased (Nikonenko et al., 2006). Therefore, it could be expected that an increased inhibitory synaptic input to pyramidal cells would have profound effects on hippocampal functions. To verify our hypotheses we investigated effects of disinhibition of slices on short- and long-term potentiation at Schaffer collateral/commissural – CA1 synapses. We found out that the blocker of $GABA_A$ transmission

picrotoxin abolished differences between genotypes and thus provided evidence that impairment of short- and long-term potentiation in young animals was mainly due to the increased inhibition.

Since number of parvalbumin-positive interneurons was normal in 2 month-old CHL1 knockout mice (Thilo, Irintchev and Schachner, unpublished data), it was interesting to explore characteristics of short- and long-term potentiation in this age group and check whether normal inhibition corresponded to unchanged STP and LTP or not. Experiments showed that theta-burst stimulation induced similar levels of potentiation in both CHL1+/+ and CHL1 -/- mice and since two different protocols of tetanic stimulation (TBS and HFS) did not reveal abnormalities in adult CHL1 constitutive knockouts, we concluded that impairment of LTP observed for juvenile mice was age- rather than protocol-dependent.

The last investigated age group was 9 month-old and here we also detected impaired STP and LTP, which were not accompanied by altered basal synaptic transmission or paired-pulse facilitation. The impairment of long-term potentiation at this age could be somehow related to the high degree of degeneration of the cells that has been detected in aged CHL1 knockout animals.

Thus, our study suggests that systematic analysis of major excitatory synapses in the hippocampal formation is beneficial to understand 1) how synaptic transmission and plasticity are regulated by cell adhesion molecules and 2) how synaptic transmission and plasticity at different types of synapses may be related to different aspects of animal behavior.

IX. Reference List

Amann,J., Kidd,V.J., and Lahti,J.M. (1997). Characterization of putative human homologues of the yeast chromosome transmission fidelity gene, CHL1. J.Biol.Chem. *272*, 3823-3832.

Andersen,P. and Bliss,T., and Skrede, K. (1971). Lamellar organization of hippocampal axcitatory pathways. Exp.Brain Res *13*, 222-238.

Andersen,P., Moser,E., Moser,M.B., and Trommald,M. (1996). Cellular correlates to spatial learning in the rat hippocampus. J.Physiol Paris *90*, 349.

Angeloni,D., Lindor,N.M., Pack,S., Latif,F., Wei,M.H., and Lerman,M.I. (1999a). CALL gene is haploinsufficient in a 3p- syndrome patient. Am.J.Med.Genet. *86*, 482-485.

Angeloni,D., Wei,M.H., and Lerman,M.I. (1999b). Two single nucleotide polymorphisms (SNPs) in the CALL gene for association studies with IQ. Psychiatr.Genet. *9*, 165-167.

Aniksztejn,L. and Ben Ari,Y. (1991). Novel form of long-term potentiation produced by a K+ channel blocker in the hippocampus. Nature *349*, 67-69.

Appel,F., Holm,J., Conscience,J.F., and Schachner,M. (1993). Several extracellular domains of the neural cell adhesion molecule L1 are involved in neurite outgrowth and cell body adhesion. J.Neurosci. *13*, 4764-4775.

Applegate,M.D., Kerr,D.S., and Landfield,P.W. (1987). Redistribution of synaptic vesicles during long-term potentiation in the hippocampus. Brain Res. *401*, 401-406.

Asou,H., Miura,M., Kobayashi,M., and Uyemura,K. (1992). The cell adhesion molecule L1 has a specific role in neural cell migration. Neuroreport *3*, 481-484.

Barnes,C.A. (1979). Memory deficits associated with senescence: a neurophysiological and behavioral study in the rat. J.Comp Physiol Psychol. *93*, 74-104.

Barnes,C.A. and McNaughton,B.L. (1985). An age comparison of the rates of acquisition and forgetting of spatial information in relation to long-term enhancement of hippocampal synapses. Behav.Neurosci. *99*, 1040-1048.

Bartsch,U., Kirchhoff,F., and Schachner,M. (1989). Immunohistological localization of the adhesion molecules L1, N-CAM, and MAG in the developing and adult optic nerve of mice. J.Comp Neurol. *284*, 451-462.

Baudry,M., Arst,D., Oliver,M., and Lynch,G. (1981). Development of glutamate binding sites and their regulation by calcium in rat hippocampus. Brain Res. *227*, 37-48.

Bear,M.F. (1996). A synaptic basis for memory storage in the cerebral cortex. Proc.Natl.Acad.Sci.U.S.A *93*, 13453-13459.

Becker,C.G., Lieberoth,B.C., Morellini,F., Feldner,J., Becker,T., and Schachner,M. (2004). L1.1 is involved in spinal cord regeneration in adult zebrafish. J.Neurosci. *24*, 7837-7842.

REFERENCE LIST

Bennett,V. and Chen,L. (2001). Ankyrins and cellular targeting of diverse membrane proteins to physiological sites. Curr.Opin.Cell Biol. *13*, 61-67.

Benson,D.L., Schnapp,L.M., Shapiro,L., and Huntley,G.W. (2000). Making memories stick: cell-adhesion molecules in synaptic plasticity. Trends Cell Biol. *10*, 473-482.

Berzhanskaya,J., Urban,N.N., and Barrionuevo,G. (1998). Electrophysiological and pharmacological characterization of the direct perforant path input to hippocampal area CA3. J.Neurophysiol. *79*, 2111-2118.

Bianchine JW,L.R., Jr. (1974). The MASA syndrome: a new heritable mental retardation syndrome. Clin Genet *5*, 298-306.

Bickers D,A.R. (1949). Hereditary stenosis of the aqueduct of Sylvius as a cause of congenital hydrocephalus. Brain *72:* 246-262.

Bliss,T., Errington,M., Fransen,E., Godfraind,J.M., Kauer,J.A., Kooy,R.F., Maness,P.F., and Furley,A.J. (2000). Long-term potentiation in mice lacking the neural cell adhesion molecule L1. Curr.Biol. *10*, 1607-1610.

Blokland,A. (1995). Acetylcholine: a neurotransmitter for learning and memory? Brain Res.Brain Res.Rev. *21*, 285-300.

Bohlen Und,H.F., Taylor,J., and Schachner,M. (1992). Cell Type-specific Effects of the Neural Adhesion Molecules L1 and N-CAM on Diverse Second Messenger Systems. Eur.J.Neurosci. *4*, 896-909.

Bortolotto,Z.A., Bashir,Z.I., Davies,C.H., and Collingridge,G.L. (1994). A molecular switch activated by metabotropic glutamate receptors regulates induction of long-term potentiation. Nature *368*, 740-743.

Bortolotto,Z.A. and Collingridge,G.L. (1993). Characterisation of LTP induced by the activation of glutamate metabotropic receptors in area CA1 of the hippocampus. Neuropharmacology *32*, 1-9.

Bortolotto,Z.A. and Collingridge,G.L. (1998). Involvement of calcium/calmodulin-dependent protein kinases in the setting of a molecular switch involved in hippocampal LTP. Neuropharmacology *37*, 535-544.

Boyd,T.E., Trepel,C., and Racine,R.J. (2000). Cholinergic modulation of neocortical long-term potentiation in the awake, freely moving rat. Brain Res. *881*, 28-36.

Breindl,A., Derrick,B.E., Rodriguez,S.B., and Martinez,J.L., Jr. (1994). Opioid receptor-dependent long-term potentiation at the lateral perforant path-CA3 synapse in rat hippocampus. Brain Res.Bull. *33*, 17-24.

Bronzino,J.D., Abu-Hasaballah,K., Austin-LaFrance,R.J., and Morgane,P.J. (1994). Maturation of long-term potentiation in the hippocampal dentate gyrus of the freely moving rat. Hippocampus *4*, 439-446.

Brummendorf,T., Hubert,M., Treubert,U., Leuschner,R., Tarnok,A., and Rathjen,F.G. (1993). The axonal recognition molecule F11 is a multifunctional protein: specific domains mediate interactions with Ng-CAM and restrictin. Neuron *10*, 711-727.

REFERENCE LIST

Brummendorf,T. and Rathjen,F.G. (1995). Cell adhesion molecules 1: immunoglobulin superfamily. Protein Profile. *2*, 963-1108.

Buchs,P.A. and Muller,D. (1996). Induction of long-term potentiation is associated with major ultrastructural changes of activated synapses. Proc.Natl.Acad.Sci.U.S.A *93*, 8040-8045.

Buhusi,M., Midkiff,B.R., Gates,A.M., Richter,M., Schachner,M., and Maness,P.F. (2003). Close homolog of L1 is an enhancer of integrin-mediated cell migration. J.Biol.Chem. *278*, 25024-25031.

Burden-Gulley,S.M., Payne,H.R., and Lemmon,V. (1995). Growth cones are actively influenced by substrate-bound adhesion molecules. J.Neurosci. *15*, 4370-4381.

Burwell,R.D. (2000). The parahippocampal region: corticocortical connectivity. Ann.N.Y.Acad.Sci. *911*, 25-42.

Casey,M., Maguire,C., Kelly,A., Gooney,M.A., and Lynch,M.A. (2002). Analysis of the presynaptic signaling mechanisms underlying the inhibition of LTP in rat dentate gyrus by the tyrosine kinase inhibitor, genistein. Hippocampus *12*, 377-385.

Carter,A.G. and Sabatini,B.L. (2004). State-dependent calcium signaling in dendritic spines of striatal medium spiny neurons. Neuron *44*, 483-493.

Castellani,V., Chedotal,A., Schachner,M., Faivre-Sarrailh,C., and Rougon,G. (2000). Analysis of the L1-deficient mouse phenotype reveals cross-talk between Sema3A and L1 signaling pathways in axonal guidance. Neuron *27*, 237-249.

Castillo,P.E., Weisskopf,M.G., and Nicoll,R.A. (1994). The role of Ca2+ channels in hippocampal mossy fiber synaptic transmission and long-term potentiation. Neuron *12*, 261-269.

Chaisuksunt,V., Campbell,G., Zhang,Y., Schachner,M., Lieberman,A.R., and Anderson,P.N. (2000a). The cell recognition molecule CHL1 is strongly upregulated by injured and regenerating thalamic neurons. J.Comp Neurol. *425*, 382-392.

Chaisuksunt,V., Zhang,Y., Anderson,P.N., Campbell,G., Vaudano,E., Schachner,M., and Lieberman,A.R. (2000b). Axonal regeneration from CNS neurons in the cerebellum and brainstem of adult rats: correlation with the patterns of expression and distribution of messenger RNAs for L1, CHL1, c-jun and growth-associated protein-43. Neuroscience *100*, 87-108.

Chang,S., Rathjen,F.G., and Raper,J.A. (1987). Extension of neurites on axons is impaired by antibodies against specific neural cell surface glycoproteins. J.Cell Biol. *104*, 355-362.

Chapman,C.A., Perez,Y., and Lacaille,J.C. (1998). Effects of GABA(A) inhibition on the expression of long-term potentiation in CA1 pyramidal cells are dependent on tetanization parameters. Hippocampus *8*, 289-298.

Chapman,V.M., Keitz,B.T., Stephenson,D.A., Mullins,L.J., Moos,M., and Schachner,M. (1990). Linkage of a gene for neural cell adhesion molecule, L1 (CamL1) to the Rsvp region of the mouse X chromosome. Genomics *8*, 113-118.

REFERENCE LIST

Chen,Q.Y., Chen,Q., Feng,G.Y., Lindpaintner,K., Chen,Y., Sun,X., Chen,Z., Gao,Z., Tang,J., and He,L. (2005). Case-control association study of the close homologue of L1 (CHL1) gene and schizophrenia in the Chinese population. Schizophr.Res. *73*, 269-274.

Chen,S., Mantei,N., Dong,L., and Schachner,M. (1999). Prevention of neuronal cell death by neural adhesion molecules L1 and CHL1. J.Neurobiol. *38*, 428-439.

Chicurel,M.E. and Harris,K.M. (1992). Three-dimensional analysis of the structure and composition of CA3 branched dendritic spines and their synaptic relationships with mossy fiber boutons in the rat hippocampus. J.Comp Neurol. *325*, 169-182.

Chinestra,P., Aniksztejn,L., Diabira,D., and Ben Ari,Y. (1993). (RS)-alpha-methyl-4-carboxyphenylglycine neither prevents induction of LTP nor antagonizes metabotropic glutamate receptors in CA1 hippocampal neurons. J.Neurophysiol. *70*, 2684-2689.

Claiborne,B.J., Amaral,D.G., and Cowan,W.M. (1986). A light and electron microscopic analysis of the mossy fibers of the rat dentate gyrus. J.Comp Neurol. *246*, 435-458.

Cohen,N.R., Taylor,J.S., Scott,L.B., Guillery,R.W., Soriano,P., and Furley,A.J. (1998). Errors in corticospinal axon guidance in mice lacking the neural cell adhesion molecule L1. Curr.Biol. *8*, 26-33.

Colbert,C.M. and Levy,W.B. (1993). Long-term potentiation of perforant path synapses in hippocampal CA1 in vitro. Brain Res. *606*, 87-91.

Collingridge,G.L., Kehl,S.J., and McLennan,H. (1983). Excitatory amino acids in synaptic transmission in the Schaffer collateral-commissural pathway of the rat hippocampus. J.Physiol *334*, 33-46.

Conte,R.A., Pitter,J.H., and Verma,R.S. (1995). Molecular characterization of trisomic segment 3p24.1-->3pter: a case with review of the literature. Clin.Genet. *48*, 49-53.

Corsellis,J.A. and Bruton,C.J. (1983). Neuropathology of status epilepticus in humans. Adv.Neurol. *34*, 129-139.

Cremer,H., Chazal,G., Carleton,A., Goridis,C., Vincent,J.D., and Lledo,P.M. (1998). Long-term but not short-term plasticity at mossy fiber synapses is impaired in neural cell adhesion molecule-deficient mice. Proc.Natl.Acad.Sci.U.S.A *95*, 13242-13247.

Cunningham,B.A. (1995). Cell adhesion molecules as morphoregulators. Curr.Opin.Cell Biol. *7*, 628-633.

Dahme,M., Bartsch,U., Martini,R., Anliker,B., Schachner,M., and Mantei,N. (1997). Disruption of the mouse L1 gene leads to malformations of the nervous system. Nat.Genet. *17*, 346-349.

Davis,J.Q. and Bennett,V. (1993). Ankyrin-binding activity of nervous system cell adhesion molecules expressed in adult brain. J.Cell Sci.Suppl *17*, 109-117.

Davis,J.Q. and Bennett,V. (1994). Ankyrin binding activity shared by the neurofascin/L1/NrCAM family of nervous system cell adhesion molecules. J.Biol.Chem. *269*, 27163-27166.

DeBernardo,A.P. and Chang,S. (1996). Heterophilic interactions of DM-GRASP: GRASP-NgCAM interactions involved in neurite extension. J.Cell Biol. *133*, 657-667.

Debiec,H., Christensen,E.I., and Ronco,P.M. (1998). The cell adhesion molecule L1 is developmentally regulated in the renal epithelium and is involved in kidney branching morphogenesis. J.Cell Biol. *143*, 2067-2079.

Demyanenko,G.P., Schachner,M., Anton,E., Schmid,R., Feng,G., Sanes,J., and Maness,P.F. (2004). Close homolog of L1 modulates area-specific neuronal positioning and dendrite orientation in the cerebral cortex. Neuron *44*, 423-437.

Derrick,B.E. and Martinez,J.L., Jr. (1994). Frequency-dependent associative long-term potentiation at the hippocampal mossy fiber-CA3 synapse. Proc.Natl.Acad.Sci.U.S.A *91*, 10290-10294.

Desmond,N.L. and Levy,W.B. (1988). Synaptic interface surface area increases with long-term potentiation in the hippocampal dentate gyrus. Brain Res. *453*, 308-314.

Diamond,D.M., Dunwiddie,T.V., and Rose,G.M. (1988). Characteristics of hippocampal primed burst potentiation in vitro and in the awake rat. J.Neurosci. *8*, 4079-4088.

Dityatev,A., Dityateva,G., and Schachner,M. (2000). Synaptic strength as a function of post- versus presynaptic expression of the neural cell adhesion molecule NCAM. Neuron *26*, 207-217.

Djabali,M., Mattei,M.G., Nguyen,C., Roux,D., Demengeot,J., Denizot,F., Moos,M., Schachner,M., Goridis,C., and Jordan,B.R. (1990). The gene encoding L1, a neural adhesion molecule of the immunoglobulin family, is located on the X chromosome in mouse and man. Genomics *7*, 587-593.

Do,V.H., Martinez,C.O., Martinez,J.L., Jr., and Derrick,B.E. (2002). Long-term potentiation in direct perforant path projections to the hippocampal CA3 region in vivo. J.Neurophysiol. *87*, 669-678.

Doller,H.J. and Weight,F.F. (1982). Perforant pathway activation of hippocampal CA1 stratum pyramidale neurons: electrophysiological evidence for a direct pathway. Brain Res. *237*, 1-13.

Drumheller,T., McGillivray,B.C., Behrner,D., MacLeod,P., McFadden,D.E., Roberson,J., Venditti,C., Chorney,K., Chorney,M., and Smith,D.I. (1996). Precise localisation of 3p25 breakpoints in four patients with the 3p-syndrome. J.Med.Genet. *33*, 842-847.

Durand,G.M., Kovalchuk,Y., and Konnerth,A. (1996). Long-term potentiation and functional synapse induction in developing hippocampus. Nature *381*, 71-75.

Eckhardt,M., Bukalo,O., Chazal,G., Wang,L., Goridis,C., Schachner,M., Gerardy-Schahn,R., Cremer,H., and Dityatev,A. (2000). Mice deficient in the polysialyltransferase ST8SiaIV/PST-1 allow discrimination of the roles of neural cell adhesion molecule protein and polysialic acid in neural development and synaptic plasticity. J.Neurosci. *20*, 5234-5244.

Empson,R.M. and Heinemann,U. (1995). Perforant path connections to area CA1 are predominantly inhibitory in the rat hippocampal-entorhinal cortex combined slice preparation. Hippocampus *5*, 104-107.

Errington,M.L., Lynch,M.A., and Bliss,T.V. (1987). Long-term potentiation in the dentate gyrus: induction and increased glutamate release are blocked by D(-)aminophosphonovalerate. Neuroscience *20*, 279-284.

Evers,M.R., Salmen,B., Bukalo,O., Rollenhagen,A., Bosl,M.R., Morellini,F., Bartsch,U., Dityatev,A., and Schachner,M. (2002). Impairment of L-type Ca2+ channel-dependent forms of hippocampal synaptic plasticity in mice deficient in the extracellular matrix glycoprotein tenascin-C. J.Neurosci. *22*, 7177-7194.

Faissner,A., Kruse,J., Nieke,J., and Schachner,M. (1984). Expression of neural cell adhesion molecule L1 during development, in neurological mutants and in the peripheral nervous system. Brain Res. *317*, 69-82.

Fannon,A.M. and Colman,D.R. (1996). A model for central synaptic junctional complex formation based on the differential adhesive specificities of the cadherins. Neuron *17*, 423-434.

Felding-Habermann,B., Silletti,S., Mei,F., Siu,C.H., Yip,P.M., Brooks,P.C., Cheresh,D.A., O'Toole,T.E., Ginsberg,M.H., and Montgomery,A.M. (1997). A single immunoglobulin-like domain of the human neural cell adhesion molecule L1 supports adhesion by multiple vascular and platelet integrins. J Cell Biol. *139*, 1567-1581.

Feldman,D.E., Nicoll,R.A., and Malenka,R.C. (1999). Synaptic plasticity at thalamocortical synapses in developing rat somatosensory cortex: LTP, LTD, and silent synapses. J.Neurobiol. *41*, 92-101.

Fifkova,E. and Van Harreveld,A. (1977). Long-lasting morphological changes in dendritic spines of dentate granular cells following stimulation of the entorhinal area. J.Neurocytol. *6*, 211-230.

Fink,C.C. and Meyer,T. (2002). Molecular mechanisms of CaMKII activation in neuronal plasticity. Curr.Opin.Neurobiol. *12*, 293-299.

Fisahn,A., Yamada,M., Duttaroy,A., Gan,J.W., Deng,C.X., McBain,C.J., and Wess,J. (2002). Muscarinic induction of hippocampal gamma oscillations requires coupling of the M1 receptor to two mixed cation currents. Neuron *33*, 615-624.

Fischer,G., Kunemund,V., and Schachner,M. (1986). Neurite outgrowth patterns in cerebellar microexplant cultures are affected by antibodies to the cell surface glycoprotein L1. J.Neurosci. *6*, 605-612.

Fransen,E., Lemmon,V., Van Camp,G., Vits,L., Coucke,P., and Willems,P.J. (1995). CRASH syndrome: clinical spectrum of corpus callosum hypoplasia, retardation, adducted thumbs, spastic paraparesis and hydrocephalus due to mutations in one single gene, L1. Eur.J.Hum.Genet *3*, 273-284.

Fransen,E., Schrander-Stumpel,C., Vits,L., Coucke,P., Van Camp,G., and Willems,P.J. (1994). X-linked hydrocephalus and MASA syndrome present in one family are due to a single missense mutation in exon 28 of the L1CAM gene. Hum.Mol.Genet *3*, 2255-2256.

Freund,T.F. and Buzsaki,G. (1996). Interneurons of the hippocampus. Hippocampus *6*, 347-470.

Frints,S.G., Marynen,P., Hartmann,D., Fryns,J.P., Steyaert,J., Schachner,M., Rolf,B., Craessaerts,K., Snellinx,A., Hollanders,K., D'Hooge,R., De Deyn,P.P., and Froyen,G. (2003). CALL interrupted in a patient with non-specific mental retardation: gene dosage-

dependent alteration of murine brain development and behavior. Hum.Mol.Genet. *12*, 1463-1474.

Fukunaga,K., Muller,D., and Miyamoto,E. (1996). CaM kinase II in long-term potentiation. Neurochem.Int. *28*, 343-358.

Gaarskjaer,F.B. (1986). The organization and development of the hippocampal mossy fiber system. Brain Res. *396*, 335-357.

Gashler,A. and Sukhatme,V.P. (1995). Early growth response protein 1 (Egr-1): prototype of a zinc-finger family of transcription factors. Prog.Nucleic Acid Res.Mol.Biol. *50*, 191-224.

Geinisman,Y., deToledo-Morrell,L., and Morrell,F. (1991). Induction of long-term potentiation is associated with an increase in the number of axospinous synapses with segmented postsynaptic densities. Brain Res. *566*, 77-88.

Geinisman,Y., deToledo-Morrell,L., and Morrell,F. (1994). Comparison of structural synaptic modifications induced by long-term potentiation in the hippocampal dentate gyrus of young adult and aged rats. Ann.N.Y.Acad.Sci. *747*, 452-466.

Geinisman,Y., Toledo-Morrell,L., and Morrell,F. (1986). Aged rats need a preserved complement of perforated axospinous synapses per hippocampal neuron to maintain good spatial memory. Brain Res. *398*, 266-275.

Geinisman,Y., Toledo-Morrell,L., Morrell,F., Heller,R.E., Rossi,M., and Parshall,R.F. (1993). Structural synaptic correlate of long-term potentiation: formation of axospinous synapses with multiple, completely partitioned transmission zones. Hippocampus *3*, 435-445.

Gereau,R.W. and Conn,P.J. (1994). Presynaptic enhancement of excitatory synaptic transmission by beta-adrenergic receptor activation. J.Neurophysiol. *72*, 1438-1442.

Gerring,S.L., Spencer,F., and Hieter,P. (1990). The CHL 1 (CTF 1) gene product of Saccharomyces cerevisiae is important for chromosome transmission and normal cell cycle progression in G2/M. EMBO J. *9*, 4347-4358.

Goldspink,D.F. (1988). Protein turnover and growth of the rat brain from the foetus to old age. J.Neurochem. *50*, 1364-1368.

Gooney,M. and Lynch,M.A. (2001). Long-term potentiation in the dentate gyrus of the rat hippocampus is accompanied by brain-derived neurotrophic factor-induced activation of TrkB. J.Neurochem. *77*, 1198-1207.

Gooney,M., Shaw,K., Kelly,A., O'Mara,S.M., and Lynch,M.A. (2002). Long-term potentiation and spatial learning are associated with increased phosphorylation of TrkB and extracellular signal-regulated kinase (ERK) in the dentate gyrus: evidence for a role for brain-derived neurotrophic factor. Behav.Neurosci. *116*, 455-463.

Gordon-Weeks,P.R. and Fischer,I. (2000). MAP1B expression and microtubule stability in growing and regenerating axons. Microsc.Res.Tech. *48*, 63-74.

Gray,J.A. and McNaughton,N. (1983). Comparison between the behavioural effects of septal and hippocampal lesions: a review. Neurosci.Biobehav.Rev. *7*, 119-188.

Green,J.D. (1964). The Hippocampus. Physiol Rev. *44*, 561-608.

Greenstein,Y.J., Pavlides,C., and Winson,J. (1988). Long-term potentiation in the dentate gyrus is preferentially induced at theta rhythm periodicity. Brain Res. *438*, 331-334.

Grover,L.M. and Teyler,T.J. (1990). Two components of long-term potentiation induced by different patterns of afferent activation. Nature *347*, 477-479.

Grumet,M., Friedlander,D.R., and Edelman,G.M. (1993). Evidence for the binding of Ng-CAM to laminin. Cell Adhes.Commun. *1*, 177-190.

Gutwein,P., Oleszewski,M., Mechtersheimer,S., Agmon-Levin,N., Krauss,K., and Altevogt,P. (2000). Role of Src kinases in the ADAM-mediated release of L1 adhesion molecule from human tumor cells. J Biol.Chem. *275*, 15490-15497.

Hamill,O.P., Marty,A., Neher,E., Sakmann,B., and Sigworth,F.J. (1981). Improved patch-clamp techniques for high-resolution current recording from cells and cell-free membrane patches. Pflugers Arch. *391*, 85-100.

Hankin,M.H. and Lagenaur,C.F. (1994). Cell adhesion molecules in the early developing mouse retina: retinal neurons show preferential outgrowth in vitro on L1 but not N-CAM. J.Neurobiol. *25*, 472-487.

Hanse,E. and Gustafsson,B. (1992). Postsynaptic, but not presynaptic, activity controls the early time course of long-term potentiation in the dentate gyrus. J.Neurosci. *12*, 3226-3240.

Harris,E.W. and Cotman,C.W. (1986). Long-term potentiation of guinea pig mossy fiber responses is not blocked by N-methyl D-aspartate antagonists. Neurosci.Lett. *70*, 132-137.

Hasselmo,M.E. and Schnell,E. (1994). Laminar selectivity of the cholinergic suppression of synaptic transmission in rat hippocampal region CA1: computational modeling and brain slice physiology. J.Neurosci. *14*, 3898-3914.

Henze,D.A., Urban,N.N., and Barrionuevo,G. (2000). The multifarious hippocampal mossy fiber pathway: a review. Neuroscience *98*, 407-427.

Higgins,J.J., Rosen,D.R., Loveless,J.M., Clyman,J.C., and Grau,M.J. (2000). A gene for nonsyndromic mental retardation maps to chromosome 3p25-pter. Neurology *55*, 335-340.

Hillenbrand,R., Molthagen,M., Montag,D., and Schachner,M. (1999). The close homologue of the neural adhesion molecule L1 (CHL1): patterns of expression and promotion of neurite outgrowth by heterophilic interactions. Eur.J.Neurosci. *11*, 813-826.

Hirota,Y. and Lahti,J.M. (2000). Characterization of the enzymatic activity of hChlR1, a novel human DNA helicase. Nucleic Acids Res. *28*, 917-924.

Holm,J., Appel,F., and Schachner,M. (1995). Several extracellular domains of the neural cell adhesion molecule L1 are involved in homophilic interactions. J.Neurosci. Res. *42*, 9-20.

Holm, J., Hillenbrand,R., Steuber,V., Bartsch,U., Moos,M., Lubbert,H., Montag,D., and Schachner,M. (1996). Structural features of a close homologue of L1 (CHL1) in the mouse: a new member of the L1 family of neural recognition molecules. Eur.J.Neurosci. *8*, 1613-1629.

Hortsch M (1996). The L1 family of neural cell adhesion molecules: old proteins performing new tricks. Neuron *17:* 587-593.

Hortsch, M. (2000). Structural and functional evolution of the L1 family: are four adhesion molecules better than one? Mol.Cell Neurosci. *15*, 1-10.

Huang,Y.Y. and Malenka,R.C. (1993). Examination of TEA-induced synaptic enhancement in area CA1 of the hippocampus: the role of voltage-dependent Ca2+ channels in the induction of LTP. J.Neurosci. *13*, 568-576.

Ignelzi,MA.Jr., Miller,DR., Soriano,P., Maness,PF. (1994). Impaired neurite outgrowth of src-minus cerebellar neurons on the cell adhesion molecule L1. Neuron *12:* 873-884.

Irintchev,A., Koch,M., Needham,L.K., Maness,P., and Schachner,M. (2004). Impairment of sensorimotor gating in mice deficient in the cell adhesion molecule L1 or its close homologue, CHL1. Brain Res. *1029*, 131-134.

Irvine,G.I., Logan,B., Eckert,M., and Abraham,W.C. (2006). Enriched environment exposure regulates excitability, synaptic transmission, and LTP in the dentate gyrus of freely moving rats. Hippocampus *16*, 149-160.

Isaac,J.T., Crair,M.C., Nicoll,R.A., and Malenka,R.C. (1997). Silent synapses during development of thalamocortical inputs. Neuron *18*, 269-280.

Isaac,J.T., Nicoll,R.A., and Malenka,R.C. (1995). Evidence for silent synapses: implications for the expression of LTP. Neuron *15*, 427-434.

Ito,I., Futai,K., Katagiri,H., Watanabe,M., Sakimura,K., Mishina,M., and Sugiyama,H. (1997). Synapse-selective impairment of NMDA receptor functions in mice lacking NMDA receptor epsilon 1 or epsilon 2 subunit. J.Physiol *500 (Pt 2)*, 401-408.

Itoh,K., Sakurai,Y., Asou,H., and Umeda,M. (2000). Differential expression of alternatively spliced neural cell adhesion molecule L1 isoforms during oligodendrocyte maturation. J.Neurosci.Res. *60*, 579-586.

Itoh,K., Shimono,K., and Lemmon,V. (2005). Dephosphorylation and internalization of cell adhesion molecule L1 induced by theta burst stimulation in rat hippocampus. Mol.Cell Neurosci. *29*, 245-249.

Jaffe,D. and Johnston,D. (1990). Induction of long-term potentiation at hippocampal mossy-fiber synapses follows a Hebbian rule. J.Neurophysiol. *64*, 948-960.

Jia,Z., Agopyan,N., Miu,P., Xiong,Z., Henderson,J., Gerlai,R., Taverna,F.A., Velumian,A., MacDonald,J., Carlen,P., Abramow-Newerly,W., and Roder,J. (1996). Enhanced LTP in mice deficient in the AMPA receptor GluR2. Neuron *17*, 945-956.

Jia,Z., Lu,Y., Henderson,J., Taverna,F., Romano,C., Abramow-Newerly,W., Wojtowicz,J.M., and Roder,J. (1998). Selective abolition of the NMDA component of long-term potentiation in mice lacking mGluR5. Learn.Mem. *5*, 331-343.

Johnston D and Amaral D.G (2004). hippocampus. In The synaptic organization of the brain, Shepherd G.M, ed. OXFORD, UNIVERSITY PRESS), pp. 455-494.

Jones,S.W. (2003). Calcium channels: unanswered questions. J.Bioenerg.Biomembr. *35*, 461-475.

Jouet,M., Rosenthal,A., Armstrong,G., MacFarlane,J., Stevenson,R., Paterson,J., Metzenberg,A., Ionasescu,V., Temple,K., and Kenwrick,S. (1994). X-linked spastic paraplegia (SPG1), MASA syndrome and X-linked hydrocephalus result from mutations in the L1 gene. Nat.Genet *7*, 402-407.

Kadmon,G., Bohlen,H., Horstkorte,R., Eckert,M., Altevogt,P., Schachner,M. (1995). Evidence for cis interaction and cooperative signalling by the heat- stable antigen nectadrin (murine CD24) and the cell adhesion molecule L1 in neurons. Eur J Neurosci *7:* 993-1004.

Kadmon,G. and Altevogt,P. (1997). The cell adhesion molecule L1: species- and cell-type-dependent multiple binding mechanisms. Differentiation *61*, 143-150.

Kallunki,P., Edelman,G.M., and Jones,F.S. (1997). Tissue-specific expression of the L1 cell adhesion molecule is modulated by the neural restrictive silencer element. J.Cell Biol. *138*, 1343-1354.

Kalus,I., Bormann,U., Mzoughi,M., Schachner,M. and Kleene,R. (2006). Proteolytic cleavage of the neural cell adhesion molecule NCAM by ADAM17/TACE is involved in neurite outgrowth. in press.

Kamiguchi,H. and Lemmon,V. (2000). Recycling of the cell adhesion molecule L1 in axonal growth cones. J.Neurosci. *20*, 3676-3686.

Kamiguchi,H., Long,K.E., Pendergast,M., Schaefer,A.W., Rapoport,I., Kirchhausen,T., and Lemmon,V. (1998). The neural cell adhesion molecule L1 interacts with the AP-2 adaptor and is endocytosed via the clathrin-mediated pathway. J.Neurosci. *18*, 5311-5321.

Kamiguchi,H. and Yoshihara,F. (2001). The role of endocytic l1 trafficking in polarized adhesion and migration of nerve growth cones. J.Neurosci. *21*, 9194-9203.

Kaplan,P. (1983). X linked recessive inheritance of agenesis of the corpus callosum. J.Med.Genet *20*, 122-124.

Kater,S.B. and Rehder,V. (1995). The sensory-motor role of growth cone filopodia. Curr.Opin.Neurobiol. *5*, 68-74.

Katsuki,H., Kaneko,S., Tajima,A., and Satoh,M. (1991). Separate mechanisms of long-term potentiation in two input systems to CA3 pyramidal neurons of rat hippocampal slices as revealed by the whole-cell patch-clamp technique. Neurosci.Res. *12*, 393-402.

Kauer,J.A., Malenka,R.C., and Nicoll,R.A. (1988). NMDA application potentiates synaptic transmission in the hippocampus. Nature *334*, 250-252.

Kelly,A. and Lynch,M.A. (2000). Long-term potentiation in dentate gyrus of the rat is inhibited by the phosphoinositide 3-kinase inhibitor, wortmannin. Neuropharmacology *39*, 643-651.

Kelly,A., Maguire,C., and Lynch,M.A. (2000a). Deficits in nerve growth factor release and tyrosine receptor kinase phosphorylation are associated with age-related impairment in long-term potentiation in the dentate gyrus. Neuroscience *95*, 359-365.

Kelly,A., Mullany,P.M., and Lynch,M.A. (2000b). Protein synthesis in entorhinal cortex and long-term potentiation in dentate gyrus. Hippocampus *10*, 431-437.

Kenwrick,S., Ionasescu,V., Ionasescu,G., Searby,C., King,A., Dubowitz,M., and Davies,K.E. (1986). Linkage studies of X-linked recessive spastic paraplegia using DNA probes. Hum.Genet *73*, 264-266.

Kenwrick,S., Watkins,A., and De Angelis,E. (2000). Neural cell recognition molecule L1: relating biological complexity to human disease mutations. Hum.Mol.Genet. *9*, 879-886.

Kiyama,Y., Manabe,T., Sakimura,K., Kawakami,F., Mori,H., and Mishina,M. (1998). Increased thresholds for long-term potentiation and contextual learning in mice lacking the NMDA-type glutamate receptor epsilon1 subunit. J.Neurosci. *18*, 6704-6712.

Kobayashi,K., Manabe,T., and Takahashi,T. (1996). Presynaptic long-term depression at the hippocampal mossy fiber-CA3 synapse. Science *273*, 648-650.

Kobayashi,K. and Poo,M.M. (2004). Spike train timing-dependent associative modification of hippocampal CA3 recurrent synapses by mossy fibers. Neuron *41*, 445-454.

Kohl,A., Giese,K.P., Mohajeri,M.H., Montag,D., Moos,M., and Schachner,M. (1992). Analysis of promoter activity and 5' genomic structure of the neural cell adhesion molecule L1. J.Neurosci.Res. *32*, 167-177.

Kowitz,A., Kadmon,G., Eckert,M., Schirrmacher,V., Schachner,M., and Altevogt,P. (1992). Expression and function of the neural cell adhesion molecule L1 in mouse leukocytes. Eur.J.Immunol. *22*, 1199-1205.

Kuhn,T.B., Stoeckli,E.T., Condrau,M.A., Rathjen,F.G., and Sonderegger,P. (1991). Neurite outgrowth on immobilized axonin-1 is mediated by a heterophilic interaction with L1(G4). J.Cell Biol. *115*, 1113-1126.

Kujat,R., Miragall,F., Krause,D., Dermietzel,R., and Wrobel,K.H. (1995). Immunolocalization of the neural cell adhesion molecule L1 in non-proliferating epithelial cells of the male urogenital tract. Histochem.Cell Biol. *103*, 311-321.

Kunz,S., Ziegler,U., Kunz,B., and Sonderegger,P. (1996). Intracellular signaling is changed after clustering of the neural cell adhesion molecules axonin-1 and NgCAM during neurite fasciculation. J.Cell Biol. *135*, 253-267.

Kutsuwada,T., Sakimura,K., Manabe,T., Takayama,C., Katakura,N., Kushiya,E., Natsume,R., Watanabe,M., Inoue,Y., Yagi,T., Aizawa,S., Arakawa,M., Takahashi,T., Nakamura,Y., Mori,H., and Mishina,M. (1996). Impairment of suckling response, trigeminal neuronal pattern formation, and hippocampal LTD in NMDA receptor epsilon 2 subunit mutant mice. Neuron *16*, 333-344.

Lagenaur,C. and Lemmon,V. (1987). An L1-like molecule, the 8D9 antigen, is a potent substrate for neurite extension. Proc.Natl.Acad.Sci.U.S.A *84*, 7753-7757.

Landfield,P.W., McGaugh,J.L., and Lynch,G. (1978a). Impaired synaptic potentiation processes in the hippocampus of aged, memory-deficient rats. Brain Res. *150*, 85-101.

Landfield,P.W., Waymire,J.C., and Lynch,G. (1978b). Hippocampal aging and adrenocorticoids: quantitative correlations. Science *202*, 1098-1102.

Langdon,R.B., Johnson,J.W., and Barrionuevo,G. (1995). Posttetanic potentiation and presynaptically induced long-term potentiation at the mossy fiber synapse in rat hippocampus. J.Neurobiol. *26*, 370-385.

Law,J.W., Lee,A.Y., Sun,M., Nikonenko,A.G., Chung,S.K., Dityatev,A., Schachner,M., and Morellini,F. (2003). Decreased anxiety, altered place learning, and increased CA1 basal excitatory synaptic transmission in mice with conditional ablation of the neural cell adhesion molecule L1. J.Neurosci. *23*, 10419-10432.

Lee,A., Westenbroek,R.E., Haeseleer,F., Palczewski,K., Scheuer,T., and Catterall,W.A. (2002). Differential modulation of Ca(v)2.1 channels by calmodulin and Ca2+-binding protein 1. Nat.Neurosci. *5*, 210-217.

Lemmon,V., Farr,K.L., and Lagenaur,C. (1989). L1-mediated axon outgrowth occurs via a homophilic binding mechanism. Neuron *2*, 1597-1603.

Letourneau,P.C. and Shattuck,T.A. (1989). Distribution and possible interactions of actin-associated proteins and cell adhesion molecules of nerve growth cones. Development *105*, 505-519.

Levey,A.I., Edmunds,S.M., Koliatsos,V., Wiley,R.G., and Heilman,C.J. (1995). Expression of m1-m4 muscarinic acetylcholine receptor proteins in rat hippocampus and regulation by cholinergic innervation. J.Neurosci. *15*, 4077-4092.

Li,Y., Erzurumlu,R.S., Chen,C., Jhaveri,S., and Tonegawa,S. (1994). Whisker-related neuronal patterns fail to develop in the trigeminal brainstem nuclei of NMDAR1 knockout mice. Cell *76*, 427-437.

Liao,D., Hessler,N.A., and Malinow,R. (1995). Activation of postsynaptically silent synapses during pairing-induced LTP in CA1 region of hippocampal slice. Nature *375*, 400-404.

Liao,D., Zhang,X., O'Brien,R., Ehlers,M.D., and Huganir,R.L. (1999). Regulation of morphological postsynaptic silent synapses in developing hippocampal neurons. Nat.Neurosci. *2*, 37-43.

Lindner,J., Rathjen,F.G., and Schachner,M. (1983). L1 mono- and polyclonal antibodies modify cell migration in early postnatal mouse cerebellum. Nature *305*, 427-430.

Liu,Q., Dwyer,N.D., and O'Leary,D.D. (2000). Differential expression of COUP-TFI, CHL1, and two novel genes in developing neocortex identified by differential display PCR. J.Neurosci. *20*, 7682-7690.

Lom,B., Hopker,V., McFarlane,S., Bixby,J.L., and Holt,C.E. (1998). Fibroblast growth factor receptor signaling in Xenopus retinal axon extension. J.Neurobiol. *37*, 633-641.

Lorente de No (1934). Studies on the structure of the cerebral cortex II. Comunication of the study of the ammonic system. J.Psychol.Neurol. *46*, 113-177.

Lu,Y.M., Jia,Z., Janus,C., Henderson,J.T., Gerlai,R., Wojtowicz,J.M., and Roder,J.C. (1997). Mice lacking metabotropic glutamate receptor 5 show impaired learning and reduced CA1 long-term potentiation (LTP) but normal CA3 LTP. J.Neurosci. *17*, 5196-5205.

Luscher,C. and Frerking,M. (2001). Restless AMPA receptors: implications for synaptic transmission and plasticity. Trends Neurosci. *24*, 665-670.

Luthi,A., Mohajeri,H., Schachner,M., and Laurent,J.P. (1996). Reduction of hippocampal long-term potentiation in transgenic mice ectopically expressing the neural cell adhesion molecule L1 in astrocytes. J.Neurosci.Res. *46*, 1-6.

Luthi,A., Laurent,J.P., Figurov,A., Muller,D., and Schachner,M. (1994). Hippocampal long-term potentiation and neural cell adhesion molecules L1 and NCAM. Nature *372*, 777-779.

Lynch,M.A. (2004). Long-term potentiation and memory. Physiol Rev. *84*, 87-136.

Lynch,M.A. and Voss,K.L. (1994). Membrane arachidonic acid concentration correlates with age and induction of long-term potentiation in the dentate gyrus in the rat. Eur.J.Neurosci. *6*, 1008-1014.

Lynch,M.A., Voss,K.L., Rodriguez,J., and Bliss,T.V. (1994). Increase in synaptic vesicle proteins accompanies long-term potentiation in the dentate gyrus. Neuroscience *60*, 1-5.

Malenka,R.C., Kauer,J.A., Perkel,D.J., Mauk,M.D., Kelly,P.T., Nicoll,R.A., and Waxham,M.N. (1989). An essential role for postsynaptic calmodulin and protein kinase activity in long-term potentiation. Nature *340*, 554-557.

Malhotra,J.D., Tsiotra,P., Karagogeos,D., and Hortsch,M. (1998). Cis-activation of L1-mediated ankyrin recruitment by TAG-1 homophilic cell adhesion. J.Biol.Chem. *273*, 33354-33359.

Malinow,R. and Malenka,R.C. (2002). AMPA receptor trafficking and synaptic plasticity. Annu.Rev.Neurosci. *25*, 103-126.

Malinow,R., Schulman,H., and Tsien,R.W. (1989). Inhibition of postsynaptic PKC or CaMKII blocks induction but not expression of LTP. Science *245*, 862-866.

Manahan-Vaughan,D. (1997). Group 1 and 2 metabotropic glutamate receptors play differential roles in hippocampal long-term depression and long-term potentiation in freely moving rats. J.Neurosci. *17*, 3303-3311.

Martina,M., Royer,S., and Pare,D. (2001). Propagation of neocortical inputs in the perirhinal cortex. J.Neurosci. *21*, 2878-2888.

Martinez,C.O., Do,V.H., Martinez,J.L., Jr., and Derrick,B.E. (2002). Associative long-term potentiation (LTP) among extrinsic afferents of the hippocampal CA3 region in vivo. Brain Res. *940*, 86-94.

Martini,R. and Schachner,M. (1986). Immunoelectron microscopic localization of neural cell adhesion molecules (L1, N-CAM, and MAG) and their shared carbohydrate epitope and myelin basic protein in developing sciatic nerve. J.Cell Biol. *103*, 2439-2448.

McGahon,B., Clements,M.P., and Lynch,M.A. (1997). The ability of aged rats to sustain long-term potentiation is restored when the age-related decrease in membrane arachidonic acid concentration is reversed. Neuroscience *81*, 9-16.

McGahon,B. and Lynch,M.A. (1998). Analysis of the interaction between arachidonic acid and metabotropic glutamate receptor activation reveals that phospholipase C acts as a coincidence detector in the expression of long-term potentiation in the rat dentate gyrus. Hippocampus *8*, 48-56.

McGahon,B., Maguire,C., Kelly,A., and Lynch,M.A. (1999a). Activation of p42 mitogen-activated protein kinase by arachidonic acid and trans-1-amino-cyclopentyl-1,3-dicarboxylate impacts on long-term potentiation in the dentate gyrus in the rat: analysis of age-related changes. Neuroscience *90*, 1167-1175.

McGahon,B.M., Martin,D.S., Horrobin,D.F., and Lynch,M.A. (1999b). Age-related changes in LTP and antioxidant defenses are reversed by an alpha-lipoic acid-enriched diet. Neurobiol.Aging *20*, 655-664.

McGahon,B.M., Martin,D.S., Horrobin,D.F., and Lynch,M.A. (1999c). Age-related changes in synaptic function: analysis of the effect of dietary supplementation with omega-3 fatty acids. Neuroscience *94*, 305-314.

McGahon,B.M., Murray,C.A., Horrobin,D.F., and Lynch (1999d). Age-related changes in oxidative mechanisms and LTP are reversed by dietary manipulation. Neurobiol.Aging *20*, 643-653.

McGuinness,N., Anwyl,R., and Rowan,M. (1991). Trans-ACPD enhances long-term potentiation in the hippocampus. Eur.J.Pharmacol. *197*, 231-232.

McLay,R.N., Freeman,S.M., Harlan,R.E., Kastin,A.J., and Zadina,J.E. (1999). Tests used to assess the cognitive abilities of aged rats: their relation to each other and to hippocampal morphology and neurotrophin expression. Gerontology *45*, 143-155.

McMahon,D.B. and Barrionuevo,G. (2002). Short- and long-term plasticity of the perforant path synapse in hippocampal area CA3. J.Neurophysiol. *88*, 528-533.

McNaughton,B.L. (1980). Evidence for two physiologically distinct perforant pathways to the fascia dentata. Brain Res. *199*, 1-19.

McQuiston,A.R. and Madison,D.V. (1999). Muscarinic receptor activity has multiple effects on the resting membrane potentials of CA1 hippocampal interneurons. J.Neurosci. *19*, 5693-5702.

Meberg,P.J., Valcourt,E.G., and Routtenberg,A. (1995). Protein F1/GAP-43 and PKC gene expression patterns in hippocampus are altered 1-2 h after LTP. Brain Res.Mol.Brain Res. *34*, 343-346.

Mechtersheimer,S., Gutwein,P., Agmon-Levin,N., Stoeck,A., Oleszewski,M., Riedle,S., Postina,R., Fahrenholz,F., Fogel,M., Lemmon,V., and Altevogt,P. (2001). Ectodomain shedding of L1 adhesion molecule promotes cell migration by autocrine binding to integrins. J Cell Biol. *155*, 661-673.

Meiri,K.F., Saffell,J.L., Walsh,F.S., and Doherty,P. (1998). Neurite outgrowth stimulated by neural cell adhesion molecules requires growth-associated protein-43 (GAP-43) function and is associated with GAP-43 phosphorylation in growth cones. J.Neurosci. *18*, 10429-10437.

Meshul,C.K. and Hopkins,W.F. (1990). Presynaptic ultrastructural correlates of long-term potentiation in the CA1 subfield of the hippocampus. Brain Res. *514*, 310-319.

Milev,P., Friedlander,D.R., Sakurai,T., Karthikeyan,L., Flad,M., Margolis,R.K., Grumet,M., and Margolis,R.U. (1994). Interactions of the chondroitin sulfate proteoglycan phosphacan, the extracellular domain of a receptor-type protein tyrosine phosphatase, with neurons, glia, and neural cell adhesion molecules. J Cell Biol. *127*, 1703-1715.

Miura,M., Asou,H., Kobayashi,M., and Uyemura,K. (1992). Functional expression of a full-length cDNA coding for rat neural cell adhesion molecule L1 mediates homophilic intercellular adhesion and migration of cerebellar neurons. J.Biol.Chem. *267*, 10752-10758.

Montag-Sallaz,M., Schachner,M., and Montag,D. (2002). Misguided axonal projections, neural cell adhesion molecule 180 mRNA upregulation, and altered behavior in mice deficient for the close homolog of L1. Mol.Cell Biol. *22*, 7967-7981.

Montgomery,A.M., Becker,J.C., Siu,C.H., Lemmon,V.P., Cheresh,D.A., Pancook,J.D., Zhao,X., and Reisfeld,R.A. (1996). Human neural cell adhesion molecule L1 and rat homologue NILE are ligands for integrin alpha v beta 3. J Cell Biol. *132*, 475-485.

Moody,T.D., Thomas,M.J., Makhinson,M., and O'Dell,T.J. (1998). 5-Hz stimulation of CA3 pyramidal cell axons induces a beta-adrenergic modulated potentiation at synapses on CA1, but not CA3, pyramidal cells. Brain Res. *794*, 75-79.

Moos,M., Tacke,R., Scherer,H., Teplow,D., Fruh,K., and Schachner,M. (1988). Neural adhesion molecule L1 as a member of the immunoglobulin superfamily with binding domains similar to fibronectin. Nature *334*, 701-703.

Morales,M. and Goda,Y. (1999). Nomadic AMPA receptors and LTP. Neuron *23*, 431-434.

Morris,R.G. (1999). D.O. Hebb: The Organization of Behavior, Wiley: New York; 1949. Brain Res.Bull. *50*, 437.

Moya,G.E., Michaelis,R.C., Holloway,L.W., and Sanchez,J.M. (2002). Prenatal diagnosis of L1 cell adhesion molecule mutations. Capabilities and limitations. Fetal Diagn.Ther. *17*, 115-119.

Mullany,P. and Lynch,M.A. (1997). Changes in protein synthesis and synthesis of the synaptic vesicle protein, synaptophysin, in entorhinal cortex following induction of long-term potentiation in dentate gyrus: an age-related study in the rat. Neuropharmacology *36*, 973-980.

Mullany,P.M. and Lynch,M.A. (1998). Evidence for a role for synaptophysin in expression of long-term potentiation in rat dentate gyrus. Neuroreport *9*, 2489-2494.

Muller,D., Wang,C., Skibo,G., Toni,N., Cremer,H., Calaora,V., Rougon,G., and Kiss,J.Z. (1996). PSA-NCAM is required for activity-induced synaptic plasticity. Neuron *17*, 413-422.

Muller,W. and Connor,J.A. (1991). Dendritic spines as individual neuronal compartments for synaptic Ca2+ responses. Nature *354*, 73-76.

Murase,S. and Schuman,E.M. (1999). The role of cell adhesion molecules in synaptic plasticity and memory. Curr.Opin.Cell Biol. *11*, 549-553.

Murray,C.A. and Lynch,M.A. (1998a). Dietary supplementation with vitamin E reverses the age-related deficit in long term potentiation in dentate gyrus. J.Biol.Chem. *273*, 12161-12168.

Murray,C.A. and Lynch,M.A. (1998b). Evidence that increased hippocampal expression of the cytokine interleukin-1 beta is a common trigger for age- and stress-induced impairments in long-term potentiation. J.Neurosci. *18*, 2974-2981.

Nadel,L. and Moscovitch,M. (1997). Memory consolidation, retrograde amnesia and the hippocampal complex. Curr.Opin.Neurobiol. *7*, 217-227.

Nadel,L., Samsonovich,A., Ryan,L., and Moscovitch,M. (2000). Multiple trace theory of human memory: computational, neuroimaging, and neuropsychological results. Hippocampus *10*, 352-368.

Nakazawa,K., Quirk,M.C., Chitwood,R.A., Watanabe,M., Yeckel,M.F., Sun,L.D., Kato,A., Carr,C.A., Johnston,D., Wilson,M.A., and Tonegawa,S. (2002). Requirement for hippocampal CA3 NMDA receptors in associative memory recall. Science *297*, 211-218.

Nayak,A., Zastrow,D.J., Lickteig,R., Zahniser,N.R., and Browning,M.D. (1998). Maintenance of late-phase LTP is accompanied by PKA-dependent increase in AMPA receptor synthesis. Nature *394*, 680-683.

Nayak,A.S., Moore,C.I., and Browning,M.D. (1996). Ca2+/calmodulin-dependent protein kinase II phosphorylation of the presynaptic protein synapsin I is persistently increased during long-term potentiation. Proc.Natl.Acad.Sci.U.S.A *93*, 15451-15456.

Nayeem,N., Silletti,S., Yang,X., Lemmon,V.P., Reisfeld,R.A., Stallcup,W.B., and Montgomery,A.M. (1999). A potential role for the plasmin(ogen) system in the posttranslational cleavage of the neural cell adhesion molecule L1. J Cell Sci. *112 (Pt 24)*, 4739-4749.

Nicoll,R.A. and Malenka,R.C. (1995). Contrasting properties of two forms of long-term potentiation in the hippocampus. Nature *377*, 115-118.

Nikonenko,A.G., Sun,M., Lepsveridze,E., Apostolova,I., Petrova,I., Irintchev,A., Dityatev, A., and Schachner,M. (2006). Enhanced perisomatic inhibition and impaired long-term potentiation in the CA1 region of juvenile CHL1-deficient mice. European Journal of Neurosci. *23*, 1839-1852.

Nishimune,H., Bernreuther,C., Carroll,P., Chen,S., Schachner,M., and Henderson,C.E. (2005). Neural adhesion molecules L1 and CHL1 are survival factors for motoneurons. J.Neurosci.Res. *80*, 593-599.

Nolte,C., Moos,M., and Schachner,M. (1999). Immunolocalization of the neural cell adhesion molecule L1 in epithelia of rodents. Cell Tissue Res. *298*, 261-273.

O'Connor,J.J., Rowan,M.J., and Anwyl,R. (1995). Tetanically induced LTP involves a similar increase in the AMPA and NMDA receptor components of the excitatory postsynaptic current: investigations of the involvement of mGlu receptors. J.Neurosci. *15*, 2013-2020.

O'Mara,S.M., Commins,S., and Anderson,M. (2000). Synaptic plasticity in the hippocampal area CA1-subiculum projection: implications for theories of memory. Hippocampus *10*, 447-456.

Ouyang,Y., Rosenstein,A., Kreiman,G., Schuman,E.M., and Kennedy,M.B. (1999). Tetanic stimulation leads to increased accumulation of Ca(2+)/calmodulin-dependent protein kinase II via dendritic protein synthesis in hippocampal neurons. J.Neurosci. *19*, 7823-7833.

Payne,H.R., Burden,S.M., and Lemmon,V. (1992). Modulation of growth cone morphology by substrate-bound adhesion molecules. Cell Motil.Cytoskeleton *21*, 65-73.

Perrin,F.E., Rathjen,F.G., and Stoeckli,E.T. (2001). Distinct subpopulations of sensory afferents require F11 or axonin-1 for growth to their target layers within the spinal cord of the chick. Neuron *30*, 707-723.

Persohn,E. and Schachner,M. (1990). Immunohistological localization of the neural adhesion molecules L1 and N-CAM in the developing hippocampus of the mouse. J.Neurocytol. *19*, 807-819.

Piccoli,G., Rutishauser,U., and Bruses,J.L. (2004). N-cadherin juxtamembrane domain modulates voltage-gated Ca2+ current via RhoA GTPase and Rho-associated kinase. J.Neurosci. *24*, 10918-10923.

Povlsen,G.K., Ditlevsen,D.K., Berezin,V., and Bock,E. (2003). Intracellular signaling by the neural cell adhesion molecule. Neurochem.Res. *28*, 127-141.

Pozzo-Miller,L.D., Gottschalk,W., Zhang,L., McDermott,K., Du,J., Gopalakrishnan,R., Oho,C., Sheng,Z.H., and Lu,B. (1999). Impairments in high-frequency transmission, synaptic vesicle docking, and synaptic protein distribution in the hippocampus of BDNF knockout mice. J.Neurosci. *19*, 4972-4983.

Pratte,M., Rougon,G., Schachner,M., and Jamon,M. (2003). Mice deficient for the close homologue of the neural adhesion cell L1 (CHL1) display alterations in emotional reactivity and motor coordination. Behav.Brain Res. *147*, 31-39.

Quinlan,E.M., Olstein,D.H., and Bear,M.F. (1999). Bidirectional, experience-dependent regulation of N-methyl-D-aspartate receptor subunit composition in the rat visual cortex during postnatal development. Proc.Natl.Acad.Sci.U.S.A *96*, 12876-12880.

Ramakers,G.M., Pasinelli,P., Hens,J.J., Gispen,W.H., and De Graan,P.N. (1997). Protein kinase C in synaptic plasticity: changes in the in situ phosphorylation state of identified pre- and postsynaptic substrates. Prog.Neuropsychopharmacol.Biol.Psychiatry *21*, 455-486.

Rathjen,F.G. and Schachner,M. (1984). Immunocytological and biochemical characterization of a new neuronal cell surface component (L1 antigen) which is involved in cell adhesion. EMBO J. *3*, 1-10.

Rauch,U., Gao,P., Janetzko,A., Flaccus,A., Hilgenberg,L., Tekotte,H., Margolis,R.K., and Margolis,R.U. (1991). Isolation and characterization of developmentally regulated chondroitin sulfate and chondroitin/keratan sulfate proteoglycans of brain identified with monoclonal antibodies. J Biol.Chem. *266*, 14785-14801.

Reiss,J.A., Sheffield,L.J., and Sutherland,G.R. (1986). Partial trisomy 3p syndrome. Clin.Genet. *30*, 50-58.

Remondes,M. and Schuman,E.M. (2003). Molecular mechanisms contributing to long-lasting synaptic plasticity at the temporoammonic-CA1 synapse. Learn.Mem. *10*, 247-252.

Rodriguez,R., Kallenbach,U., Singer,W., and Munk,M.H. (2004). Short- and long-term effects of cholinergic modulation on gamma oscillations and response synchronization in the visual cortex. J.Neurosci. *24*, 10369-10378.

Ronn,L.C., Doherty,P., Holm,A., Berezin,V., and Bock,E. (2000). Neurite outgrowth induced by a synthetic peptide ligand of neural cell adhesion molecule requires fibroblast growth factor receptor activation. J.Neurochem. *75*, 665-671.

Rose,G.M. and Dunwiddie,T.V. (1986). Induction of hippocampal long-term potentiation using physiologically patterned stimulation. Neurosci.Lett. *69*, 244-248.

Rose,S.P. (1995). Glycoproteins and memory formation. Behav.Brain Res. *66*, 73-78.

Rosenthal,A., Jouet,M., and Kenwrick,S. (1992). Aberrant splicing of neural cell adhesion molecule L1 mRNA in a family with X-linked hydrocephalus. Nat.Genet. *2*, 107-112.

Ruoslahti,E. and Pierschbacher,M.D. (1987). New perspectives in cell adhesion: RGD and integrins. Science *238*, 491-497.

Sadoul,K., Sadoul,R., Faissner,A., and Schachner,M. (1988). Biochemical characterization of different molecular forms of the neural cell adhesion molecule L1. J Neurochem. *50*, 510-521.

Saghatelyan,A.K., Nikonenko,A.G., Sun,M., Rolf,B., Putthoff,P., Kutsche,M., Bartsch,U., Dityatev,A., and Schachner,M. (2004). Reduced GABAergic transmission and number of hippocampal perisomatic inhibitory synapses in juvenile mice deficient in the neural cell adhesion molecule L1. Mol.Cell Neurosci. *26*, 191-203.

Sakimura,K., Kutsuwada,T., Ito,I., Manabe,T., Takayama,C., Kushiya,E., Yagi,T., Aizawa,S., Inoue,Y., Sugiyama,H., and . (1995). Reduced hippocampal LTP and spatial learning in mice lacking NMDA receptor epsilon 1 subunit. Nature *373*, 151-155.

Sakurai,K., Migita,O., Toru,M., and Arinami,T. (2002). An association between a missense polymorphism in the close homologue of L1 (CHL1, CALL) gene and schizophrenia. Mol.Psychiatry *7*, 412-415.

Salin,P.A., Scanziani,M., Malenka,R.C., and Nicoll,R.A. (1996). Distinct short-term plasticity at two excitatory synapses in the hippocampus. Proc.Natl.Acad.Sci.U.S.A *93*, 13304-13309.

Salton,S.R., Shelanski,M.L., and Greene,L.A. (1983). Biochemical properties of the nerve growth factor-inducible large external (NILE) glycoprotein. J.Neurosci. *3*, 2420-2430.

Sammar,M., Gulbins,E., Hilbert,K., Lang,F., and Altevogt,P. (1997). Mouse CD24 as a signaling molecule for integrin-mediated cell binding: functional and physical association with src-kinases. Biochem.Biophys.Res.Commun. *234*, 330-334.

Schachner,M. (1997). Neural recognition molecules and synaptic plasticity. Curr.Opin.Cell Biol. *9*, 627-634.

Schenk,F. and Morris,R.G. (1985). Dissociation between components of spatial memory in rats after recovery from the effects of retrohippocampal lesions. Exp.Brain Res. *58*, 11-28.

Schmid,R.S., Graff,R.D., Schaller,M.D., Chen,S., Schachner,M., Hemperly,J.J., and Maness,P.F. (1999). NCAM stimulates the Ras-MAPK pathway and CREB phosphorylation in neuronal cells. J.Neurobiol. *38*, 542-558.

Schmid,R.S., Pruitt,W.M., and Maness,P.F. (2000). A MAP kinase-signaling pathway mediates neurite outgrowth on L1 and requires Src-dependent endocytosis. J.Neurosci. *20*, 4177-4188.

Schuch,U., Lohse,M.J., and Schachner,M. (1989). Neural cell adhesion molecules influence second messenger systems. Neuron *3*, 13-20.

Schurmann G, Haspel J, Grumet M, Erickson HP (2001) Cell adhesion molecule L1 in folded (horseshoe) and extended conformations. Mol Biol Cell 12: 1765-1773.

Schuster T, Krug M, Stalder M, Hackel N, Gerardy-Schahn R, Schachner M (2001) Immunoelectron microscopic localization of the neural recognition molecules L1, NCAM, and its isoform NCAM180, the NCAM-associated polysialic acid, beta1 integrin and the extracellular matrix molecule tenascin-R in synapses of the adult rat hippocampus. J Neurobiol 49: 142-158.

Schuster,T., Krug,M., and Wenzel,J. (1990). Spinules in axospinous synapses of the rat dentate gyrus: changes in density following long-term potentiation. Brain Res. *523*, 171-174.

Scoville,J.W. and Milner,B. (1957). Loss of recent memory after bilateral hippocampal lesions. J.Nurol.Psychiatry *20*, 11-21.

Scoville,W.B. and Milner,B. (2000). Loss of recent memory after bilateral hippocampal lesions. 1957. J.Neuropsychiatry Clin.Neurosci. *12*, 103-113.

Seeburg,P.H. (1993). The TINS/TiPS Lecture. The molecular biology of mammalian glutamate receptor channels. Trends Neurosci. *16*, 359-365.

Seidenman,K.J., Steinberg,J.P., Huganir,R., and Malinow,R. (2003). Glutamate receptor subunit 2 Serine 880 phosphorylation modulates synaptic transmission and mediates plasticity in CA1 pyramidal cells. J.Neurosci. *23*, 9220-9228.

Seilheimer,B., Persohn,E., and Schachner,M. (1989). Antibodies to the L1 adhesion molecule inhibit Schwann cell ensheathment of neurons in vitro. J.Cell Biol. *109*, 3095-3103.

Shinoe,T., Matsui,M., Taketo,M.M., and Manabe,T. (2005). Modulation of synaptic plasticity by physiological activation of M1 muscarinic acetylcholine receptors in the mouse hippocampus. J.Neurosci. *25*, 11194-11200.

Skibbens,R.V. (2004). Chl1p, a DNA helicase-like protein in budding yeast, functions in sister-chromatid cohesion. Genetics *166*, 33-42.

Son,H. and Carpenter,D.O. (1996). Interactions among paired-pulse facilitation and post-tetanic and long-term potentiation in the mossy fiber-CA3 pathway in rat hippocampus. Synapse *23*, 302-311.

Spencer,F., Gerring,S.L., Connelly,C., and Hieter,P. (1990). Mitotic chromosome transmission fidelity mutants in Saccharomyces cerevisiae. Genetics *124*, 237-249.

Squire,L.R. (1992). Memory and the hippocampus: a synthesis from findings with rats, monkeys, and humans. Psychol.Rev. *99*, 195-231.

Squire,L.R. and Alvarez,P. (1995). Retrograde amnesia and memory consolidation: a neurobiological perspective. Curr.Opin.Neurobiol. *5*, 169-177.

Staatz,W.D., Fok,K.F., Zutter,M.M., Adams,S.P., Rodriguez,B.A., and Santoro,S.A. (1991). Identification of a tetrapeptide recognition sequence for the alpha 2 beta 1 integrin in collagen. J.Biol.Chem. *266*, 7363-7367.

Staubli,U., Chun,D., and Lynch,G. (1998). Time-dependent reversal of long-term potentiation by an integrin antagonist. J.Neurosci. *18*, 3460-3469.

Takeda,Y., Asou,H., Murakami,Y., Miura,M., Kobayashi,M., and Uyemura,K. (1996). A nonneuronal isoform of cell adhesion molecule L1: tissue-specific expression and functional analysis. J.Neurochem. *66*, 2338-2349.

Tang,L., Hung,C.P., and Schuman,E.M. (1998). A role for the cadherin family of cell adhesion molecules in hippocampal long-term potentiation. Neuron *20*, 1165-1175.

Tang,Y.P., Shimizu,E., Dube,G.R., Rampon,C., Kerchner,G.A., Zhuo,M., Liu,G., and Tsien,J.Z. (1999). Genetic enhancement of learning and memory in mice. Nature *401*, 63-69.

Thiery,J.P., Brackenbury,R., Rutishauser,U., and Edelman,G.M. (1977). Adhesion among neural cells of the chick embryo. II. Purification and characterization of a cell adhesion molecule from neural retina. J.Biol.Chem. *252*, 6841-6845.

Toledo-Morrell,L. and Morrell,F. (1985). Electrophysiological markers of aging and memory loss in rats. Ann.N.Y.Acad.Sci. *444*, 296-311.

Tong,G., Malenka,R.C., and Nicoll,R.A. (1996). Long-term potentiation in cultures of single hippocampal granule cells: a presynaptic form of plasticity. Neuron *16*, 1147-1157.

Tsien,J.Z., Chen,D.F., Gerber,D., Tom,C., Mercer,E.H., Anderson,D.J., Mayford,M., Kandel,E.R., and Tonegawa,S. (1996a). Subregion- and cell type-restricted gene knockout in mouse brain. Cell *87*, 1317-1326.

Tsien,J.Z., Huerta,P.T., and Tonegawa,S. (1996b). The essential role of hippocampal CA1 NMDA receptor-dependent synaptic plasticity in spatial memory. Cell *87*, 1327-1338.

Tsukamoto,M., Yasui,T., Yamada,M.K., Nishiyama,N., Matsuki,N., and Ikegaya,Y. (2003). Mossy fibre synaptic NMDA receptors trigger non-Hebbian long-term potentiation at entorhino-CA3 synapses in the rat. J.Physiol *546*, 665-675.

Urban,N.N. and Barrionuevo,G. (1996). Induction of hebbian and non-hebbian mossy fiber long-term potentiation by distinct patterns of high-frequency stimulation. J.Neurosci. *16*, 4293-4299.

van Groen,T. and Wyss,J.M. (1992). Connections of the retrosplenial dysgranular cortex in the rat. J.Comp Neurol. *315*, 200-216.

Vits,L., Van Camp,G., Coucke,P., Fransen,E., De Boulle,K., Reyniers,E., Korn,B., Poustka,A., Wilson,G., Schrander-Stumpel,C., and . (1994). MASA syndrome is due to mutations in the neural cell adhesion gene L1CAM. Nat.Genet *7*, 408-413.

Vogt,K.E. and Regehr,W.G. (2001). Cholinergic modulation of excitatory synaptic transmission in the CA3 area of the hippocampus. J.Neurosci. *21*, 75-83.

Watanabe,M., Inoue,Y., Sakimura,K., and Mishina,M. (1992). Developmental changes in distribution of NMDA receptor channel subunit mRNAs. Neuroreport *3*, 1138-1140.

Wei,M.H., Karavanova,I., Ivanov,S.V., Popescu,N.C., Keck,C.L., Pack,S., Eisen,J.A., and Lerman,M.I. (1998). In silico-initiated cloning and molecular characterization of a novel human member of the L1 gene family of neural cell adhesion molecules. Hum.Genet. *103*, 355-364.

Weiler,K.S., Szeto,L., and Broach,J.R. (1995). Mutations affecting donor preference during mating type interconversion in Saccharomyces cerevisiae. Genetics *139*, 1495-1510.

Williams,S. and Johnston,D. (1988). Muscarinic depression of long-term potentiation in CA3 hippocampal neurons. Science *242*, 84-87.

Williams,S. and Johnston,D. (1989). Long-term potentiation of hippocampal mossy fiber synapses is blocked by postsynaptic injection of calcium chelators. Neuron *3*, 583-588.

Williams,E.J., Mittal,B., Walsh,F.S., and Doherty,P. (1995). A Ca2+/calmodulin kinase inhibitor, KN-62, inhibits neurite outgrowth stimulated by CAMs and FGF. Mol.Cell Neurosci. *6*, 69-79.

Winson,J. and Dahl,D. (1986). Long-term potentiation in dentate gyrus: induction by asynchronous volleys in separate afferents. Science *234*, 985-988.

Witter,M.P. (1993). Organization of the entorhinal-hippocampal system: a review of current anatomical data. Hippocampus *3 Spec No*, 33-44.

Witter,M.P., Groenewegen,H.J., Lopes da Silva,F.H., and Lohman,A.H. (1989). Functional organization of the extrinsic and intrinsic circuitry of the parahippocampal region. Prog.Neurobiol. *33*, 161-253.

Wong,E.V., Schaefer,A.W., Landreth,G., and Lemmon,V. (1996a). Casein kinase II phosphorylates the neural cell adhesion molecule L1. J.Neurochem. *66*, 779-786.

Wong,E.V., Schaefer,A.W., Landreth,G., and Lemmon,V. (1996b). Involvement of p90rsk in neurite outgrowth mediated by the cell adhesion molecule L1. J.Biol.Chem. *271*, 18217-18223.

Wood,P., Moya,F., Eldridge,C., Owens,G., Ranscht,B., Schachner,M., Bunge,M., and Bunge,R. (1990a). Studies of the initiation of myelination by Schwann cells. Ann.N.Y.Acad.Sci. *605*, 1-14.

Wood,P.M., Schachner,M., and Bunge,R.P. (1990b). Inhibition of Schwann cell myelination in vitro by antibody to the L1 adhesion molecule. J.Neurosci. *10*, 3635-3645.

Wu,X., Mogford,J.E., Platts,S.H., Davis,G.E., Meininger,G.A., and Davis,M.J. (1998). Modulation of calcium current in arteriolar smooth muscle by alphav beta3 and alpha5 beta1 integrin ligands. J.Cell Biol. *143*, 241-252.

Yamazaki,Y., Jia,Y., Hamaue,N., and Sumikawa,K. (2005). Nicotine-induced switch in the nicotinic cholinergic mechanisms of facilitation of long-term potentiation induction. Eur.J.Neurosci. *22*, 845-860.

Yeckel,M.F. and Berger,T.W. (1990). Feedforward excitation of the hippocampus by afferents from the entorhinal cortex: redefinition of the role of the trisynaptic pathway. Proc.Natl.Acad.Sci.U.S.A *87*, 5832-5836.

Yuan,X.B., Jin,M., Xu,X., Song,Y.Q., Wu,C.P., Poo,M.M., and Duan,S. (2003). Signalling and crosstalk of Rho GTPases in mediating axon guidance. Nat.Cell Biol. *5*, 38-45.

Zalutsky,R.A. and Nicoll,R.A. (1990). Comparison of two forms of long-term potentiation in single hippocampal neurons. Science *248*, 1619-1624.

Zhang,Y., Roslan,R., Lang,D., Schachner,M., Lieberman,A.R., and Anderson,P.N. (2000). Expression of CHL1 and L1 by neurons and glia following sciatic nerve and dorsal root injury. Mol.Cell Neurosci. *16*, 71-86.

Zhao,X. and Siu,C.H. (1995). Colocalization of the homophilic binding site and the neuritogenic activity of the cell adhesion molecule L1 to its second Ig-like domain. J.Biol.Chem. *270*, 29413-29421.

Zhao,X., Yip,P.M., and Siu,C.H. (1998). Identification of a homophilic binding site in immunoglobulin-like domain 2 of the cell adhesion molecule L1. J.Neurochem. *71*, 960-971.

Zisch,A.H. and Pasquale,E.B. (1997). The Eph family: a multitude of receptors that mediate cell recognition signals. Cell Tissue Res. *290*, 217-226.

Zisch,A.H., Stallcup,W.B., Chong,L.D., Dahlin-Huppe,K., Voshol,J., Schachner,M., and Pasquale,E.B. (1997). Tyrosine phosphorylation of L1 family adhesion molecules: implication of the Eph kinase Cek5. J.Neurosci.Res. *47*, 655-665.

X. Acknowledgements

This study has been performed in the Institute for Biosynthesis of Neuronal Structures of the Center for Molecular Neurobiology (ZMNH) at the University of Hamburg. I would like to thank Prof. Melitta Schachner for providing facilities for this research, fruitful discussions and for support and guidance during these years.

I am especially grateful to Dr. Alexander Dityatev for excellent supervision, fascinating ideas, patience, and time spent supporting me in science and life.

I also would like to say thanks to all members of electrophysiology group, to Dr. Olena Bukalo, for her permanent support, interesting discussions and patience; to Julia Langer for preparing Ca^{2+} channel transfected cells, helping me to deal with all documents in German, being my best friend and supporting me in science and life; to Luminita Stoenica for her friendship and support in work and life; to Martin Hammond, Tiberiu Stan, Oleg Senkov and Gaga Kochlamazashvili for their friendly attitude and interesting scientific discussions. I would like to express my special gratefulness to Galina Dityateva for her permanently smiling face, encouragement, exciting books and maternal attitude.

Many thanks to all colleagues from ZMNH for their friendship and moral support. Thanks to Fabio Morellini and Irina Leshchinska for providing me with L1 conditional and CHL1 constitutive knockout mice and their corresponding wild types. Additional thanks to Fabio and Birgit Kähler for behavioral analysis, and to Andrey Irintchev and Barbara Thilo for morphological data on CHL1 knockout mice.

By all means I should acknowledge German people and Germany for hospitality and giving me an opportunity to do science of such quality.

Thanks to my lecturers from Tbilisi State University, and to supervisor of my Diploma work - Dr. Tengis Gloveli for introducing me to the miracle world of science; also to my school teacher of biology, who pushed me to become a biologist; to my Georgian friends and relatives who always remembered, loved and believed in me; to George Soros for financial support while my studies at the Tbilisi State University.

Many thanks to my parents for being the best parents in the world, supporting me in everything, and sharing all my emotions in spite of such a long distance. Special thanks to my Mom for teaching me how to think and learn, always showing the best ways in life and dedicating her life to me.

And last but not least, many thanks to God that made all this come true.

Institute of Psychiatry

at The Maudsley

Department of Neurology

De Crespigny Park
Denmark Hill
London SE5 8AF

KING'S College LONDON
Founded 1829

University of London

12th April 2006

Bestätigung der Korrektheit der Englischen Sprache in der Dissertation von Eka Lepsveridze mit dem Thema ‚Synaptic transmission and plasticity in major excitatory hippocampal synapses of L1 conditional and CHL1 constitutive knockout mice *(Mus musculus)*'

Hiermit bestätige ich, Martin Hammond, die Korrektheit der englischen Sprache in Wort und Schrift.

Martin Hammond